THE ROLE OF NOVEL HISTONE POST-TRANSLATIONAL MODIFICATIONS IN TRANSCRIPTION

DISSERTATION DER
FAKULTÄT FÜR BIOLOGIE DER
LUDWIG-MAXIMILIANS-UNIVERSITÄT MÜNCHEN

Lara Zorro Shahidian

Munich, 2020

The work for this thesis was carried out at the Helmholtz Zentrum München under the supervision of Prof. Dr. Robert Schneider.

Date of submission: February 4th, 2020.

Date of examination: June 16th, 2020.

First referee: Prof. Dr. Robert Schneider

Second referee: Prof. Dr. Heinrich Leonhardt

Statutory Declaration

I, hereby, declare that I have authored this thesis independently and without any unauthorized help. Additionally, I declare that I have not previously taken a doctoral examination without success and that this dissertation was neither fully nor partially presented to another examination board.

Lara Shahidian

Publications

Published

Campagne, A, Lee, MK, Zielinski, D, Michaud, A, Le Corre, S, Dingli, F, Chen, H, Shahidian, LZ, Vassilev, I, Servant, N, Loew, D, Pasmant, E, Postel-Vinay, S, Wassef, M and Margueron, R (2019). BAP1 complex promotes transcription by opposing PRC1-mediated H2A ubiquitylation. Nature Communication; 10(1):348.

Kebede, A, Nieborak, A, Shahidian, LZ, Le Gras, S, Richter, F, Gómez, DA, Baltissen, MP, Meszaros, G, Magliarelli, HF, Taudt, A, Margueron, R, Colomé-Tatché, M, Ricci, R, Daujat, S, Vermeulen, M, Mittler, G and Schneider, R (2017). Histone propionylation is a mark of active chromatin. Nature Structural & Molecular Biology; 24(12):1048-1056.

Submittted

Shahidian, LZ, Haas, M, Mourão, A, Geerlo, A, Le Gras, S, Margueron, R, Michaelis, J, Daujat, S and Schneider, R. Succinylation of H3K122 destabilizes the nucleosome and enhances transcription.

Table of contents

1. Summary

Histone post-translational modifications (PTMs) are important players in chromatin regulation. While the majority of studies on histone modifications is centered on those located on the histone tails, here we focused on different modifications on the globular domain of histone H3. In this work, we aimed to study the poorly understood H3K122succ, characterize the role this modification plays in transcription and explore a possible synergistic effect between the acetylations of lysine 56, 64 and 122 on H3.

In the first part of this work, we show that H3K122succ is enriched on active promoters and is associated with active gene transcription. We identified p300/CBP as the succinyltransferases responsible for its establishment and SIRT5 as a novel desuccinylase capable of removing H3K122succ. We demonstrate that, *in vitro*, chromatin enriched by H3K122succ transcribes more efficiently than unmodified chromatin, revealing that H3K122succ is not simply correlated with active transcription, but can directly stimulate it. Moreover, we show that H3K122succ destabilizes the nucleosome structure, leading to increased DNA accessibility.

In the second part of this thesis, we compared the effects of H3K56ac, H3K64ac, H3K122ac and combinations of these acetylations in transcription. Our results confirm that all three acetylations, previously shown to be associated with active regulatory regions, stimulate transcription *in vitro*. In addition, combinations of these modifications lead to higher transcription. Furthermore, we identify sharp promoters as a subset of promoters regulated by these modifications. Our data suggests that the combinations of H3K56ac,

H3K64ac and H3K122ac have an increased effect on genes regulated by sharp promoters comparing to the single H3 globular domain acetylations.

2. Zusammenfassung

Histon-posttranslationale Modifikationen spielen eine wichtige Rolle in der Chromatinregulierung. Während sich die Mehrheit der Studien auf N-terminale Histonmodifikationen konzentrieren, haben wir uns in dieser Dissertation auf verschiedene Modifikationen innerhalb der globulären Domäne von Histon H3 fokussiert. Das Ziel dieser Arbeit war es die bisher weniger erforschte Modifikation H3K122succ zu untersuchen und die Rolle dieser Modifikation bei der Transkription zu charakterisieren. Desweiteren untersuchen wir einen möglichen synergistischen Effekt auf die Transkription zwischen den H3 Acetylierungen von Lysin 56, 64 und 122.

Im ersten Teil dieser Arbeit zeigen wir, dass H3K122succ an aktiven Promotoren angereichert ist und mit der aktiven Gentranskription assoziiert ist. Wir identifizierten p300/CBP als verantwortliche Succinyltransferasen für H3K122succ und SIRT5 als eine neuartige Desuccinylase, die in der Lage ist, H3K122succ zu entfernen. Wir zeigen, dass mit H3K122succ angereichertes Chromatin in vitro effizienter transkribiert wird als unmodifiziertes Chromatin. Dies zeigt, dass H3K22succ nicht nur mit der aktiven Transkription korreliert, sondern diese auch direkt stimulieren kann. Darüber hinaus demonstrieren wir, dass H3K122succ die Nukleosomenstruktur destabilisiert, was zu einer erhöhten Zugänglichkeit der DNA führt.

Im zweiten Teil dieser Arbeit haben wir die Wirkungen von H3K56ac, H3K64ac, H3K122ac und Kombinationen dieser Acetylierungen auf die Transkription verglichen. Unsere Ergebnisse bestätigen, dass alle drei Acetylierungen von denen zuvor gezeigt wurde, dass sie mit aktiven regulatorischen Regionen assoziiert sind, die Transkription in vitro stimulieren. Darüber hinaus führen Kombinationen dieser Modifikationen zu einer höheren Transkription. Des

Weiteren identifizieren wir „sharp promoters“ als eine Untergruppe von Promotoren, die durch diese Modifikationen reguliert werden. Unsere Daten legen nahe, dass die Kombinationen von H3K56ac, H3K64ac und H3K122ac einen erhöhten Effekt auf die Transkriptionlevel von Genen haben, die durch „sharp promoters“ reguliert werden, verglichen mit den einzelnen Acetylierungen der globulären H3-Domäne.

3. Introduction

3.1 Epigenetics

The term “epigenetics” was first employed by Conrad H. Waddington in 1942 to describe “the branch of biology which studies the causal interactions between genes and their products, which bring the phenotype into being”[1]. Since then, several additional definitions have been suggested. Although, the exact definition of “epigenetics” is still under discussion, it is commonly accepted that epigenetics refers to the study of heritable changes in gene expression that are not the result of changes of the DNA sequence[2]. Among the best studied “epigenetic factors” are covalent modifications of DNA bases, histone variants and PTMs of histones amino acids.

3.2 Chromatin organization

The nuclear DNA in eukaryotic cells follows a well-structured organization, which not only allows the long DNA molecules to fit in the small 1-10 μm-diameter nucleus, it also safeguards easy accessibility to any part of the DNA sequence. This accessibility is of crucial importance to numerous cell processes, such as transcription[3], DNA replication[4] and DNA repair[5].

The basic unit of chromatin, the nucleosome, consists of 2 copies of each core histone (H2A, H2B, H3 and H4), organized in a histone octamer, wrapped by 147 base pairs (bp) of DNA[6]. The organization of higher order chromatin structures comprises several levels including: the 10 nm chromatin structure - also known as “beads on a string” – where the nucleosomes are spaced by 10 to 80 bp of linker DNA; 300 and 700 nm chromatids and on the highest level the mitotic chromosome structure[7,8] (figure 3.1).

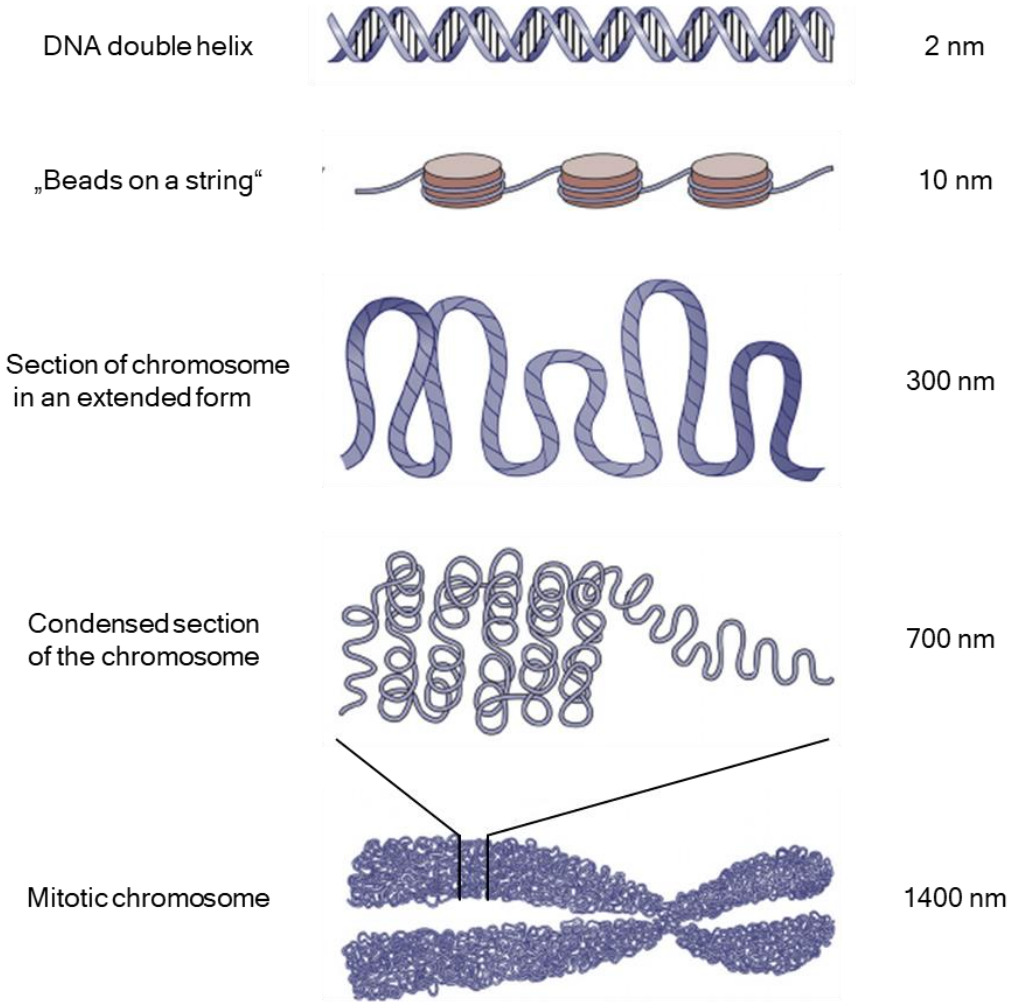

Figure 3.1 Chromatin organization

The nucleosomal DNA is organized into different levels of compaction ranging from the 2 nm-diameter naked DNA to the 1400 nm-diameter mitotic chromosome. Adapted from Jansen *et al.*, 2011.

3.3 Histone structure and nucleosome formation

Histones are among the most evolutionarily conserved proteins in eukaryotes. Histones are small, highly positively charged proteins that share a common structure composed of two domains: the histone tails and the fold domain[9].

All core histones contain N-terminal tails and, in addition, H2A has a C-terminal tail. The histone tails are flexible structures that protrude from the nucleosome core structure[10]. They are known to interact with the nucleosomal DNA, the linker DNA and, in case of the H4 tail, with the acidic patch, a negatively charged anchor region formed by residues from H2A and H2B[11], of neighboring

nucleosomes. The N-terminal tail of H4 is thought to play an important role in the formation of higher order chromatin structures whereas the N-terminal tail of H2B has been shown to be necessary for chromosome condensation[9]. The removal of the histone tails results in an increased accessibility to the nucleosomal DNA.

The histone fold domains, also known as the histone globular domains, are essential for the formation of the nucleosome. Although the fold is not conserved at the sequence level between histones, its structure is. The globular domain is composed of 3 α-helices (α1, α2 and α3) connected by 2 short β-loops (L1 and L2). The loops mediate the heterodimerization of H2A-H2B and H3-H4 as following: the L1 loop of one histone aligns with the L2 loop of the other, in what is referred to as the handshake motif[12]. Two H3-H4 dimers dimerize through a four-helix bundle at the dyad axis, forming $(H3\text{-}H4)_2$ tetramers[13] (figure 3.2A).

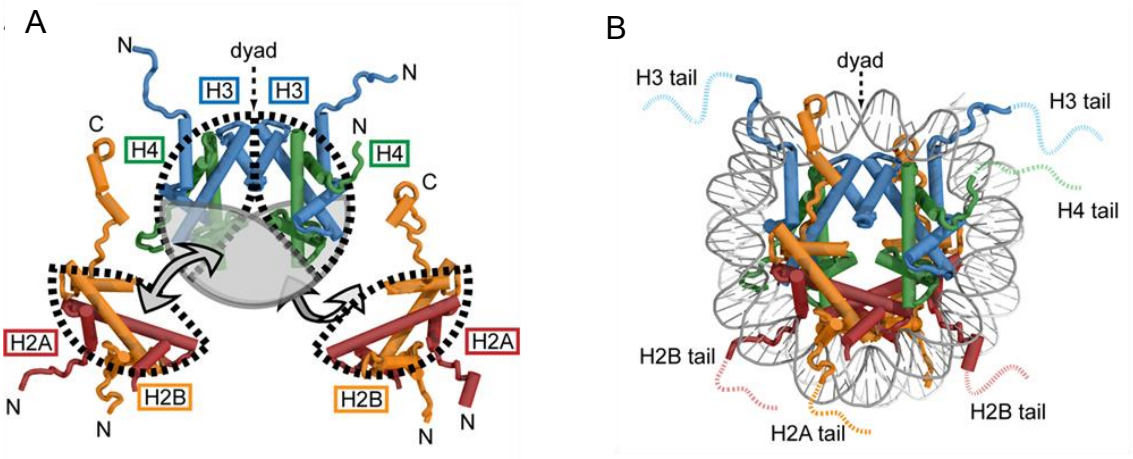

Figure 3.2 - Nucleosome structure

A Representation of the dimerization of H2A-H2B dimers and H3-H4 tetramers during octamer formation. **B** Nucleosome structure. Adapted from Bowman *et al.*, 2015.

In the nucleosome (figure 3.2B), an $(H3\text{-}H4)_2$ tetramer is centered at the dyad axis, surround on each side by a H2A-H2B heterodimer, which dock at the DNA entry and exit sites[14,15]. The protein complex composed by a $(H3\text{-}H4)_2$ tetramer and two H2A-H2B heterodimers is known as the histone octamer.

3.4 Histone variants

One way how chromatin structure and function are regulated is through histone variants. For the exception of H4 which only has one, all core histones in metazoans have multiple variants[16]. The variants of the same histone vary not only in sequence, but also in genomic location and regulation. Histones can be classified into two general groups: canonical and replacement histones.

The main feature that distinguishes canonical from replacement histones regards the fact that the expression of canonical histones is cell cycle dependent, in other words they are mainly expressed and incorporated into chromatin during S phase, when the DNA undergoes replication. This is important as they will be necessary to assemble the newly synthesized chromatin. To facilitate the large need of histones during this phase, there are several gene copies for each canonical histone in the genome. Canonical histone genes lack introns and have a stem loop structure at the 3' end of their mRNAs. The canonical histones are often referred to as simply H2A, H2B, H3 and H4[16,17].

Replacement histones, unlike canonical histones, are expressed throughout the cell cycle. They are only biallelic and often contain introns. Replacement histones are sometimes poly-adenylated at the 3' end of their mRNAs and can be subjected to alternative splicing[17].

Among the core histones, H2A has the largest number of replacement histones, including macroH2A, H2A.B, H2A.Z and H2A.X. Some of them are conserved through evolution, like H2A.Z, while others are specific to vertebrates or mammals like macroH2A and H2A.B. MacroH2A, the largest of all H2A variants, is enriched at the inactive mammalian X-chromosome, and is associated with gene silencing. Both H2A.Z and H2A.X are constitutively expressed and found throughout the genome[1617], with H2A.Z being particularly enriched at intergenic regions[18].

H2B has significantly less replacement histones that H2A. The few that have been studied seem to have very specialized roles and can be found in specific locations[18]. As an example, TH2B, a testis-specific histone, replaces H2B during meiosis and is the main H2B in round and elongating spermatids[19].

Only recently, a variant for H4 was found: H4G. Histone H4G is expressed in several human cell lines, but it is overexpressed in particular tumor-stages of breast cancer patients. Initial data on this variant suggests H4G induces ribosomal DNA (rDNA) transcription in breast cancer tissues[20].

3.4.1 H3 variants

Histone H3 has two canonical forms: H3.1 and H3.2, which differ on a single nucleotide located in the globular domain (figure 3.3). H3.1 and H3.2 are usually referred to as H3. While H3.2 is present in all metazoans, H3.1 only exists in mammals. Besides H3.1 and H3.2, in mammals several H3 replacement histones have been identified: H3.3, cenH3 (CENP-A in humans) and H3T (H3t in humans). Additionally, there are two primate-specific replacement histones: H3.X and H3.Y.

H3.3 has a very high sequence homology with the canonical H3, differing in only four nucleotides - one in the N-terminal tail and three in the globular domain - comparing to H3.2 (figure 3.3)[21].

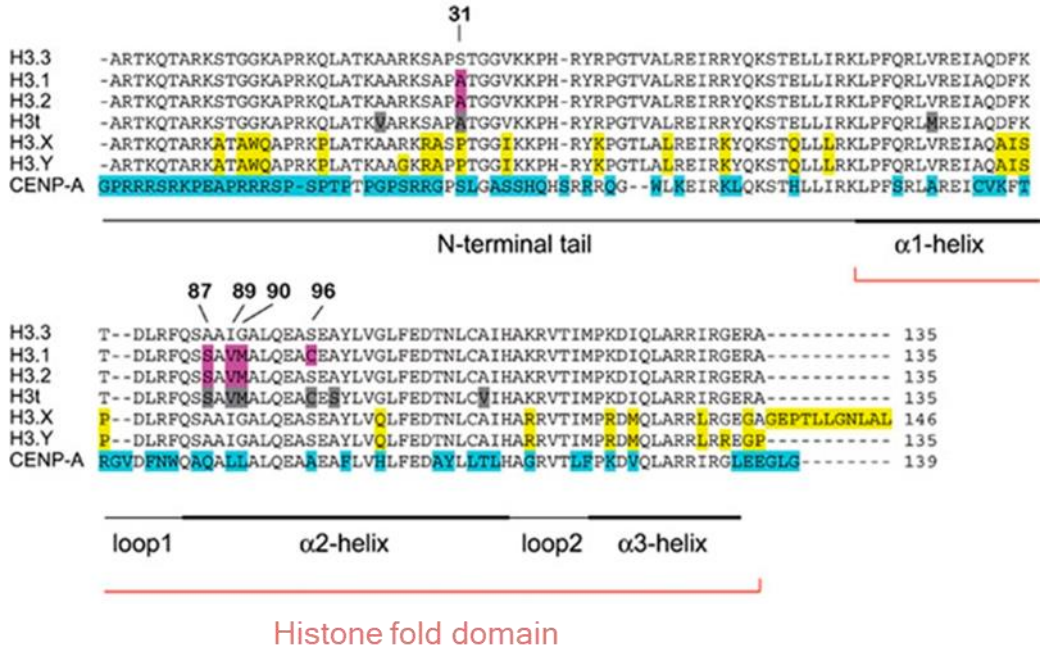

Figure 3.3 - Sequence alignment of human H3 variants.
The amino acid sequences of the human H3 variants were aligned and compared to H3.3. The differences in sequenced are highlighted as following: H3.1 and H3.2 in purple, H3t in gray, H3.X and H3.Y in yellow and CENP-A in blue. The different amino acids position between H3.3 and the canonical H3 are indicated. Modified from Szenker *et al.,* 2011.

H3t is a testis specific replacement histone that evolved from H3.3. It has been shown that this histone is necessary for spermatogenesis. Nucleosomes containing H3t form an open chromatin structure[22].The current knowledge on H3.X and H3.Y is very limited as they were identified relatively recently. [23].

CENP-A is a histone replacement that can be found at centromeres. This variant replaces canonical H3 in a significant proportion of centromeric nucleosomes[24]. CENP-A plays a central role in the assembly of kinetochores and centromere function[25].

3.5 Histone modifications

Histone modifications are reversible chemical alterations of the histone proteins[26]. The first modification identified on histones was lysine acetylation in the early 1960s[27]. Since then a multitude of PTMs at different sites have been identified[28–30] and numerous studies have focused in attempting to understand how these modifications are regulated and how to they influence chromatin structure and function[31].

In general, histone PTMs can be classified into two groups: histone tail modifications and globular domain modifications. Histone tail modifications were the first ones to be studied as they are significantly more abundant. Since the histone tails protrude from the nucleosome core and can interact with other nucleosomes, it was initially assumed that modifications on the tails could affect inter-nucleosome interactions and consequently affect chromatin structure. It is now known that most histone tail modifications act via recruiting or repelling specific binding proteins (or complexes).

Globular domain PTMs, are often less abundant and their identification has only been possible with the advancement of mass-spectrometry (MS) techniques. Interestingly, the majority of the PTMs at the globular domain are located on the lateral surface of the histone octamer[32,33], at positions where the histone octamer and the nucleosomal DNA are in direct or water-mediated contact, suggesting that they play an important role regulating nucleosome structure or stability[34,35]. Studies on different globular domain modifications have shown that these modifications can indeed affect the stability of the nucleosome by affecting intra-nuclear interactions or the interactions between the histone octamers and the nucleosomal DNA[36–38].

A “histone code” has been proposed, in which the combination of different N-tail modifications determines the binding of specific “reader proteins” to chromatin, regulating downstream effects[39]. According to the histone code hypothesis, the different combinations of tail modifications serve as a code that regulates the chromatin environment controlling *e.g.* gene expression. Since it was proposed, many studies have challenged the concept of a histone code. On one hand, the identification of reader proteins containing more than one chromatin binding domain, such as multiple bromodomains (BD) which recognize acetylation[40], supports the idea that the binding of such proteins is dependent on the co-existence of multiple modification[39,41]. On the other hand, evidence that histone PTMs can directly, without an intermediate reader protein, modulate chromatin structure opposes the idea of an rather indirect, reader mediated code[42].

3.6 Histone lysine acylations

Acylations are PTMs on lysine residues that result from the addition of an acyl group, from an acyl-CoA donor, to the ε-amino group of the lysine side chain. Acylations alter the overall positive charge of the lysine side chain, resulting in a decreased affinity towards DNA[30]. The first acylation to have been identified, and most extensively studied, was lysine acetylation (figure 3.4B), which we will discuss in the next chapter. In addition to acetylation, in recent years a wide array of short-chain histone lysine acylations have been identified by MS-based approaches, including lysine propionylation, butyrylation, crotonylation, malonylation and succinylation (figure 3.4C-G)[28,29,31,43]. The addition of the different acyl groups to the lysine residue has different effects on the lysine: while acetylation, propionylation, butyrylation and crotonylation result in the neutralization of the positively charged lysine side chain, malonylation and

succinylation lead to a complete reverse of charge from positive to negative[30,44-46].

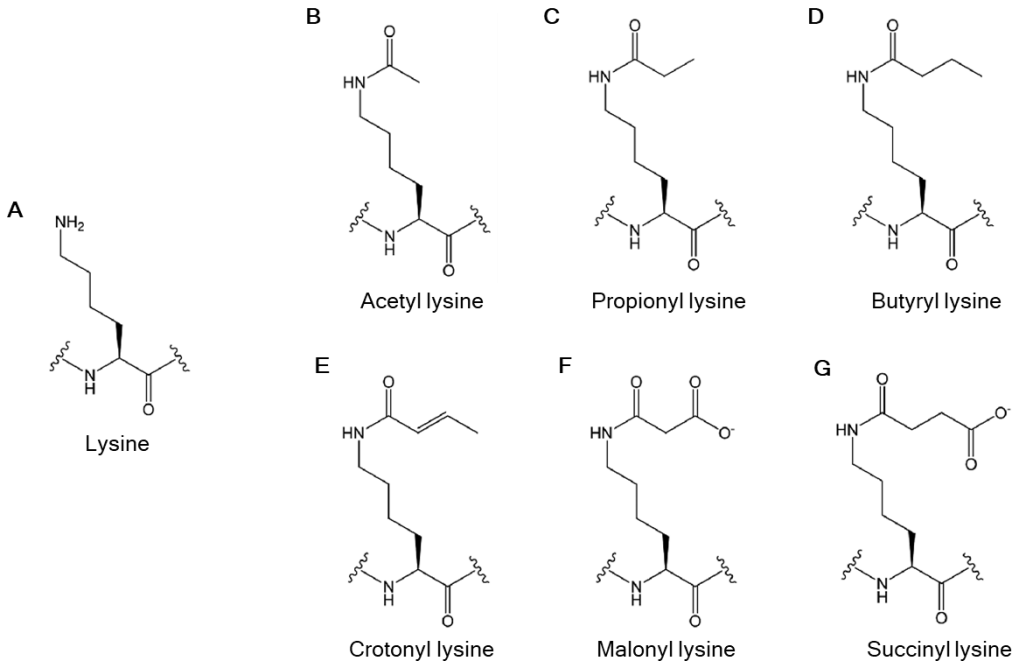

Figure 3.4 - Lysine acylations

Chemical structure of the lysine residue carrying to modifications (**A**) and different acylations: acetylation (**B**), propionylation (**C**), butyrylation (**D**), crotonylation (**E**), malonylation (**F**) and succinylation (**G**). Modified from Lee, 2013[47].

Acylations have become the topic of great interest due to the possibility that they might link epigenetics and cellular metabolism[48]. The acyl-CoA required for the formation of these marks are intermediates of metabolic pathways, such as the tricarboxylic acid (TCA) cycle. It has been suggested that acylation levels are closely related to the availability of the metabolic intermediates they derive from[49]. While it has been shown that, to a certain degree, acylations can be established non-enzymatically, their enzymatic deposition is a far more efficient process. All identified acyl-transferases are enzymes that have been previously described as acetyl-transferases. Evidence suggests that the preference for one specific acylation over another depends on the specific affinity the enzymes have towards specific acyl-CoA donors, and on their availability[50,51].

3.6.1 Lysine acetylation

Histone lysine acetylation is an abundant histone mark which neutralizes the positive charge of the ε-amino group of the lysine side chain (figure 3.4B). This results in the weakening of the interactions between the histones and the negatively charged phosphate group of the DNA (tails and globular domain) or the acidic patch of neighboring nucleosomes (in the case of the H4 tail), leading to the exposure of the underlying DNA[52,53]. Additionally lysine acetylation in the histones tails can be specifically bound by BD containing proteins[54,55].

In the course of this project, I focused on the study of three acetylations located on the lateral surface of the histone octamer, at lysines 56, 64 and 122 of histone H3 (H3K56ac, H3K64ac and H3K122ac).

There are two main groups of enzymes that regulate histone acetylation: histone acetyl-transferases (HATs) and histone deacetylases (HDACs).

Table 3.1 - Mammalian type A HAT subfamilies

Mammalian Type A HAT sub-families	Examples
GNAT	KAT2A, KAT2B
MYST	MOF, MOZ, MORF, HBO1, TIP60
Orphan	p300/CBP, TAFII

HATs are a group of enzymes that use acetyl-CoA (ac-CoA) and can catalyze the transfer of the acetyl group to the ε-amino group of the lysine side chain. They can be divided into two main classes: type A and type B. Type B HATs are highly conserved and can be mainly found in the cytoplasm, where they acetylate free histones, prior to their deposit in the chromatin[56,57]. Type A HATs, are a larger and more diversified group of enzymes, which can be subdivided

into three sub-families according to their sequence and structure (table 3.1)[58]. HATs, in the majority of the cases, do not present specificity towards single lysine residues, instead they can acetylate multiple sites[59].

HDACs remove the acetyl group from lysine residues, restoring their positive charge. While HATs are predominantly associated with transcription activation, HDACs are generally associated with transcriptional repression. HDACs have relatively low substrate specificity and a single enzyme can deacetylate several sites. HDACs can be classified into four classes: I, II, III and IV[60].

Class I is composed of enzymes related to the yeast scRpd3 and its members are exclusively found in the nucleus. HDACs class II is composed of enzymes similar to the yeast enzymes Hda1 and can be found both in the nucleus and cytoplasm. HDAC11 is the only member of class IV and little is known about this enzyme[61]. Class III, commonly referred to as sirtuins, differs from the rest as they require a specific co-factor, NAD^{+}[27]. Sirtuins can be found in the nucleus, cytosol and/or mitochondria[60].

Table 3.2 - Human HDAC classes

HDAC classes	Membranes of the class
Class I	HDAC 1-3 and 8
Class II	HDAC 4-7 and 9-10
Class III	Sirtuins 1-7
Class IV	HDAC11

3.6.2 Lysine succinylation

Lysine succinylation was described for the first time in 2011[62] and soon after the first histone lysine succinylations were identified (figure 3.5)[63]. Interesting the majority of the residues that can be succinylated are located on the globular

domain of the core histones, suggesting this modification could directly regulate chromatin function.

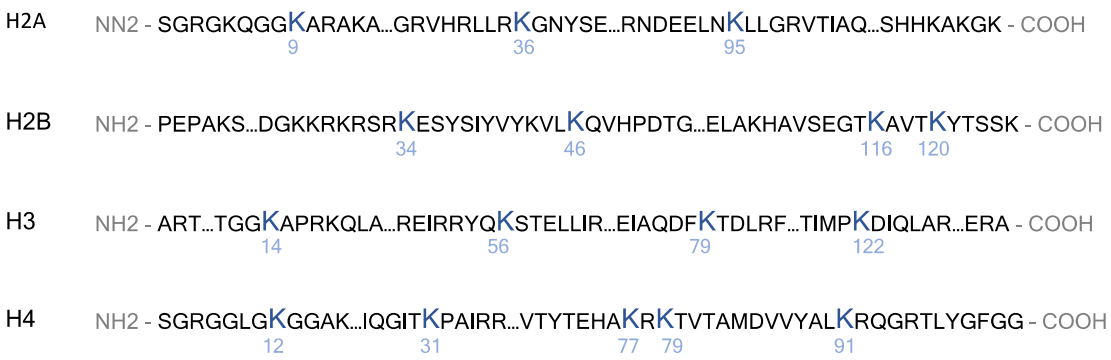

Figure 3.5 – Known lysine succinylation sites on human core histones.
Lysines known to be succinylated are highlighted in blue.

Regarding the removal of this mark, it has been reported that sirtuins can have desuccinylase activity. Sirtuin 5 (SIRT5), a HDAC with very limited deacetylase activity, has been shown to have a preference towards negatively charged acylations, such as malonylation and succinylation[64]. SIRT5 is mainly found in the mitochondria, but can be found in smaller amounts in the cytosol and nucleus[65]. Sirtuin 7 (SIRT7), has been shown *in vitro* and *in vivo* to have desuccinylase activity in the nucleus[66].

3.7 Epigenetic regulation during transcription

The organization of the DNA into chromatin constitutes a physical obstacle to gene transcription, as RNA polymerase II (RNA pol II) is prevented from accessing the DNA. Several mechanisms work simultaneously to regulate transcription. In an initial step, chromatin structure decondenses, resulting on the exposure of specific DNA regulatory regions, such as promoters and enhancers, to DNA binding factors. Specific epigenetic factors mark these regulatory regions (table 3.3) and, directly or through binding proteins, lead to

the reduction of the nucleosome occupancy. Transcription factors and RNA pol II bind the chromatin to form the pre-initiation complex (PIC). Once transcription is initiated, new histone PTMs are established guaranteeing the DNA stays accessible while necessary (table 3.3).

Table 3.3 – Summary of main histone PTMs signaling for active and inactive chromatin regions

Chromatin state	Location	Signature marks
Active	Promoters	H3K4me3[67]; H3K9ac[68]; H3K14ac[68]
	Gene body	H3K36me3[69]
	Enhancers	H3K4me1[70]; H3K27ac[71]
Inactive	Promoters	H3K27me2/3[72]
	Enhancers	H3K27me3[73]

3.8 H3K56ac

The acetylation of lysine 56 on histone H3 was the first histone globular domain modification to be extensively characterized[74]. Lysine 56 is located near the entry and exit sites of the nucleosomal DNA, a region of the nucleosome where the DNA is weakly bound to the histone octamer (figure 3.6)[26]. Acetylation of H3K56 increases DNA breathing, a condition in which the DNA transiently unwraps from the histone octamer starting at the DNA entry and exit sites[75].

The majority of studies on this PTM were carried out in budding yeast, where it was initially identified. In yeast, Rtt109, together with the histone chaperon Asf establishes H3K56ac. Rtt109 can only acetylate free histones and as a result, H3K56ac is mainly established during S phase and largely disappears during G2/M phases[76]. Newly synthesized H3 histones are marked by this modification, which is necessary for nucleosome formation both during DNA replication and repair[77]. In addition to this role, H3K56ac is enriched at the highly dynamic

promoter nucleosomes, where it enhances nucleosome turnover. H3K56ac stimulated DNA breathing [42], is believed to result in increased transcription. The deacetylation of H3K56 in yeast is mediated by two members of the sirtuin family, Hst3 and Hst4[78].

In mammals, H3K56ac is a low abundant PTM (with an approximate abundancy of 28 %[79] in yeast and 1 %[80] in mammals), and there is no specific HAT for this site. Three different enzymes can establish H3K56ac: p300, CBP and GCN5[81]. Similarly, to yeast, in mammals sirtuins are responsible for the removal of this mark[77]. H3K56ac in mammals is not an S phase specific mark, and newly synthesized H3 are not marked by it[77]. Instead, H3K56ac has been shown to play a role in DNA damage response (its levels decrease upon DNA damage)[77,82], pluripotency[83] and transcription[78].

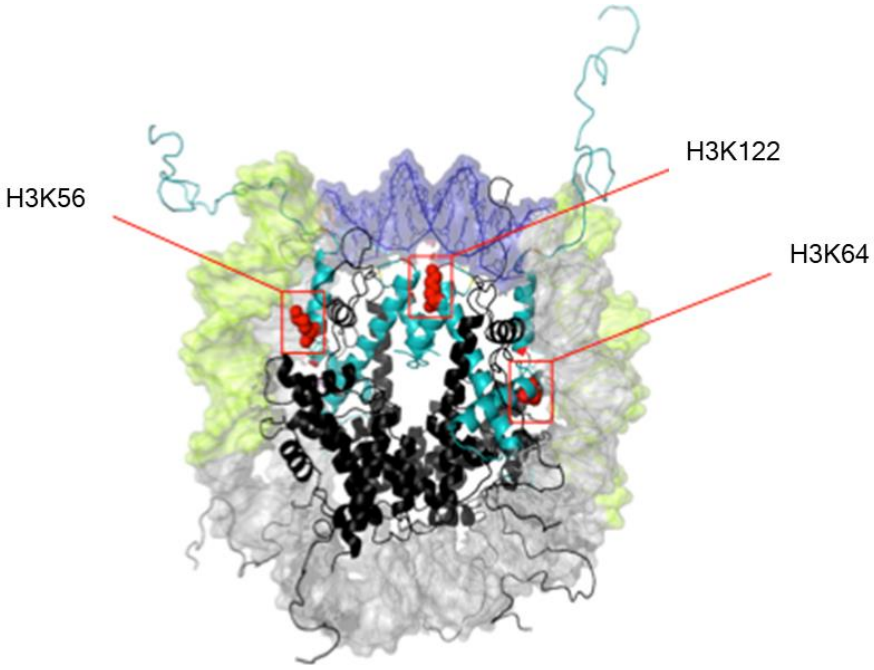

Figure 3.6 – Ribbon structure of the nucleosome.
Lysines 56, 64 and 122 on histone H3 are highlighted in red. The nucleosomal DNA is indicated as following: entry and exit sites in green, dyad axis in purple and the remaining nucleosomal DNA is in grey.

3.9 H3K64ac

Lysine 64 on histone H3 is the first amino acid of the α1 helix. It is positioned on the lateral surface of the histone octamer and is in water-mediated contact with the nucleosomal DNA[84]. Like H3K56, it is located in proximity to the entry and exit sites of the nucleosomal DNA (figure 3.6) although further in the nucleosome[6].

H3K64ac is an active chromatin specific PTM, which is enriched at active transcriptional start sites (TSS) and enhancers[37]. It has been shown that H3K64ac disrupts the nucleosome stability, facilitating histone eviction[37]. In addition to its genomic localization, time course studies suggested that H3K64ac at promoter and enhancers is involved in gene regulation[37,85]. p300/CBP are the main enzymes responsible for the establishment of this mark, but no eraser has been identified[37].

3.10 H3K122ac

Lysine 122 on histone H3 is located near the nucleosome dyad axis (figure 3.6), the nucleosome region which coordinates the most internal segment of the nucleosomal DNA. It is at the dyad axis that the DNA and the histone octamer have the strongest interactions[26,86]. H3K122 is in water-mediated contact with the nucleosomal DNA[84], and it has been shown that the substitution of lysine 122 by an acetylation mimic (H3K122Q) leads to the destabilization of this contact[87]. p300/CBP[36], as well as bromodomain protein 4 (BRD4), have been shown to acetylate H3K122[88]. No binder or eraser for H3K122ac have, so far, been identified.

H3K122ac is enriched at active promoter and enhancers. Regarding its role at the promoter, H3K122ac can be detected early during gene activation and *in vitro*, this single modification can stimulate transcription by itself[89]. H3K122ac has been used to identify a new class of active enhancers, which are characterized by the co-presence of H3K4me1 with H3K64ac and/or H3K122ac and the absence of H3K27ac[85].

3.11 H3K122succ

H3K122 succinylation has been identified recently[29], however our understanding on the function and regulation of H3K122succ is still very limited. In an initial study on this PTM, it was shown that H3K122succ is regulated by SIRT7. SIRT7 can remove H3K122succ from chromatin in response to DNA break, leading to chromatin compaction[66]. Failure to desuccinylate H3K122 is associated with impaired homologous recombination and non-homologous end-join repair. [66].

4. Aims

The organization of the DNA into chromatin plays a crucial role in the regulation of all DNA dependent processes, including transcription. Among the known factors controlling DNA organization are histone modifications. These histone modifications can act both indirectly - by attracting or repelling specific chromatin-binding proteins - or directly - by modulating the intra- and inter-nucleosome interactions or histone-DNA interactions[90].

With the recent advancement of MS techniques, novel, less abundant, globular domain histone PTMs have been identified. Interestingly, many of these modifications are acylations (including acetylation and succinylation), whose acyl-donor groups are intermediates of different metabolic pathways, suggesting that these modifications could link metabolism with chromatin organization[29]. However, currently very little is known about the function of many of these acylations in the globular domain.

In the first part of my thesis, my aim was to unravel the function of a novel histone modification, H3K122succ, in transcription. This modifications was of particular interest since lysine 122, located on the nucleosome dyad axis, forms a water-mediated salt bridge with the DNA backbone[6]. Acetylation of this residue disrupts this interaction leading to destabilization of the nucleosome and has been shown to stimulate transcription *in vitro*[85,89]. I hypothesized that the succinylation of this residue, due to the reverse of charge it imposes on the lysine's side chain[28] could lead to a possibly higher destabilization of the nucleosome and, likewise, affect transcription.

For the second part of the project my aim was to explore possible synergistic effect between three described H3 globular domain acetylations: H3K56ac, H3K64ac and H3K122ac. These acetylations had previously been studied by

our lab and others, to different extents, individually. The available data suggests they share genomic locations and might co-occur. All these three core acetylations have been associated with active regulatory regions in mammals[42,81,89,91]. I set out to investigate synergistic functions of these modifications using both *in vitro* and *in vitro* techniques.

5. Results

5.1 Part 1 - H3K122succ

5.1.1 Antibody purification and validation

In order to be able to study the succinylation of H3K122, it was crucial to raise and carefully characterize antibodies that specifically recognize H3K122succ. This was necessary since the only commercially available H3K122succ targeting antibody failed to pass the validation process, as it clearly recognized several other H3 PTMs in peptide immunoblot (figure 5.1A). We, therefore, immunized 14 rabbits with H3K122succ peptides and double affinity-purified antibodies from their serum. Out of 14 immunizations, we successfully purified antibodies from 3 rabbit sera. The first characterization step was a peptide immunoblot which confirmed the antibodies did not recognize a selection of other known PTMs (figure 5.1B-D). Next, we tested these antibodies in immunoblot on unmodified (un), H3K122succ and H3K122R recombinant octamers (rOctamers; figure 5.1E). The antibodies only detected the H3 band when H3K122 was succinylated (lane 1) and did not recognize the unmodified nor H3K122R mutant.

Next, we tested the antibodies' specificity in peptide competition, for which the antibodies were pre-incubated with peptides before being added to the nitrocellulose membranes onto which the histones had been transferred to. All antibodies recognized specifically H3 and this signal was only competed away by the H3K122succ peptide (figure 5.1F).

Due to the high abundance of histone tail PTMs, to exclude that the antibody signal was caused by the recognition of modifications at the H3 N-terminal tail, chromatin was limited digested by trypsin in order to cleave the histone tails off (figure 5.1G). While on the undigested chromatin a single H3 band can be

recognized, in the sample that undergone partial trypsin digestion two bands can be observed, corresponding to the full length and the tail-less H3.

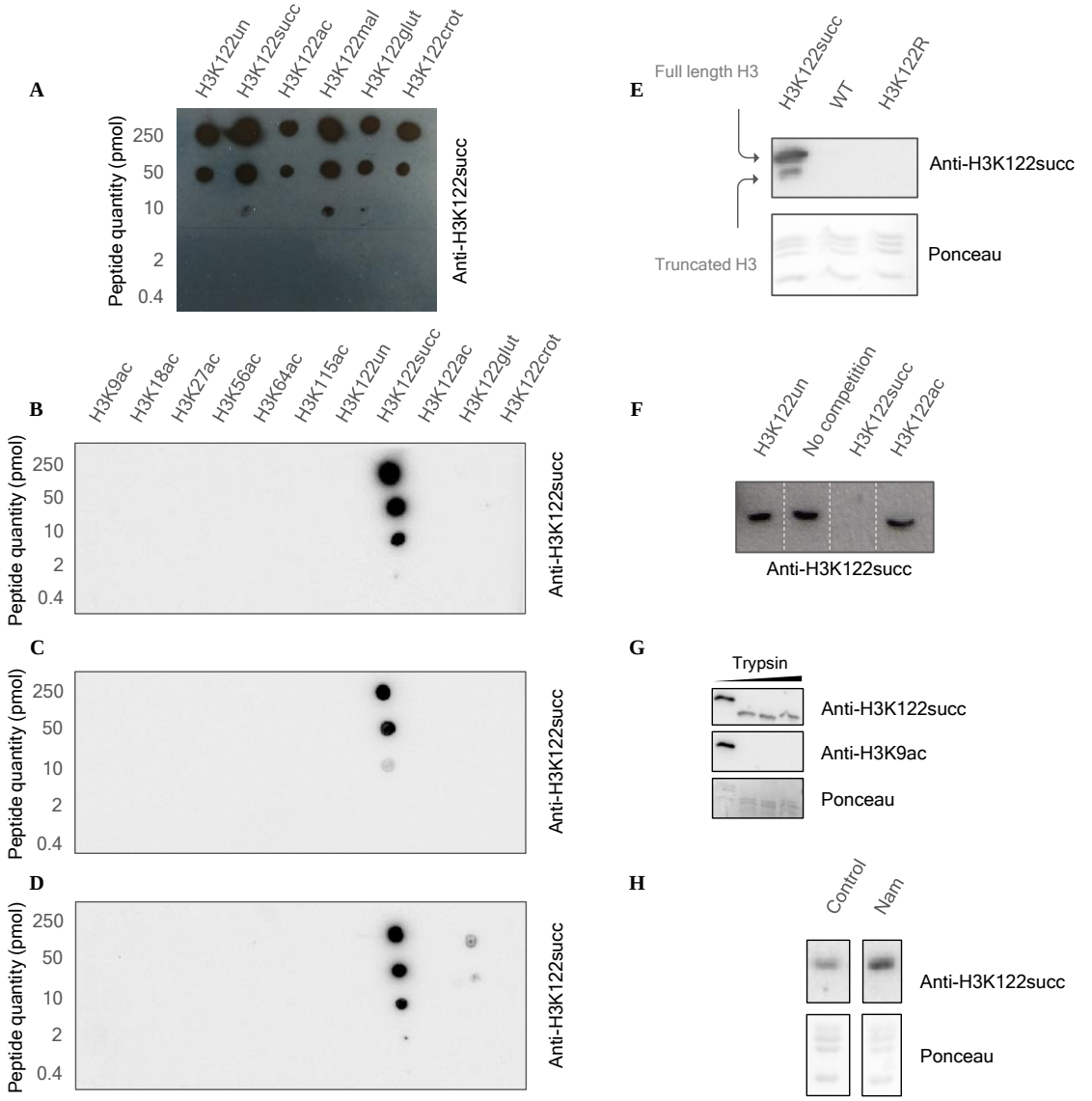

Figure 5.1 - Anti-H3K122succ antibody validation

A Peptide dotblot array probed with the commercially available anti-H3K122succ antibody. **B-D** Peptide dotblot arrays probed with anti-H3K122succ antibodies #1, #2 and #3. Peptides with indicated modifications were dotted on membranes. **E** Immunoblotting analysis showing that only H3K122succ-carrying rOctamers are recognized by the anti-H3K122succ antibody. Ponceau staining of histones is shown as a loading control. **F** Peptide competition of H3K122succ immunoblot. H3K122succ antibody was pre-adsorbed with the indicated peptides. Only in the presence of the H3K122succ peptide was the signal competed away. **G** MNase digested chromatin (10 µg) was incubated at 26 °C for 10 minutes in the absence or presence of different quantities of trypsin (250, 500 and 1000 ng). The levels of H3K122succ were assessed by immunoblot. Ponceau staining of histones is shown as a loading control. **H** Immunoblot on native acid extracted histones from MCF7 that were incubated O/N with 20 mM of Nam. Ponceau staining of histones is shown as a loading control.

It has been reported that sirtuins can desuccinylate histones[66]. Therefore, we treated MCF7 cells overnight (O/N) with nicotinamide (Nam) a sirtuin inhibitor and asked if this increases the H3K122succ signal (figure 5.1H). Indeed, the immunoblot signal on H3 from Nam treated samples was stronger than the untreated control samples. Altogether these results confirmed the quality of the antibody, validating it as a reliable tool to study H3K122succ.

5.1.2 Distribution of H3K122succ on histone variants

As mentioned in the introduction chapter, H3 has several variants in mammals[18]. The main somatic variants are the canonical H3 and H3.3. In general, canonical H3 is found throughout chromatin, while H3.3 is enriched at active sites with a high turnover of nucleosomes, such as promoters and enhancers[92]. In order to understand if H3K122succ was enriched at specific H3 variants we compared H3K122succ levels on H3.1 and H3.3. For this, we collected histone acid extracts from HEK293 cells ectopically expressing H3.1 or H3.2 carrying a HA/FLAG-tag and probed on immunoblot for H3K122succ (figure 5.2). Our results revealed that H3K122succ is enriched on H3.3 when compared to H3.1.

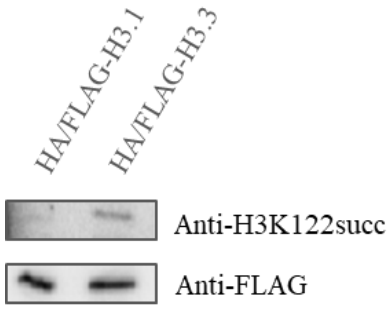

Figure 5.2 - H3K122succ is enriched on H3.3 compared to H3.1

Histones were acid extracted from approximately $20x10^6$ HEK293 cells ectopically expressing H3.1 or H3.3 carrying an HA/FLAG-tag. The levels of H3K122succ were assessed by immunoblotting. Anti-FLAG blot is shown as a loading control.

5.1.3 Distribution of H3K122succ in chromatin

In order to gain a comprehensive understanding of the genomic distribution of H3K122succ, we performed chromatin immunoprecipitation followed by massive DNA parallel sequencing (ChIP-seq) in MCF7 cells. The analysis of the data was performed by Stephanie Le Gras at the Institut de Génétique et de Biologie Moléculaire et Cellulaire (Strasbourg, France). All three validated anti-H3K122succ antibodies were used for this experiment. The peaks from the three anti-H3K122succ samples were compared using TODO1 and the results revealed there is a very high-overlap between them (figure 5.3A).

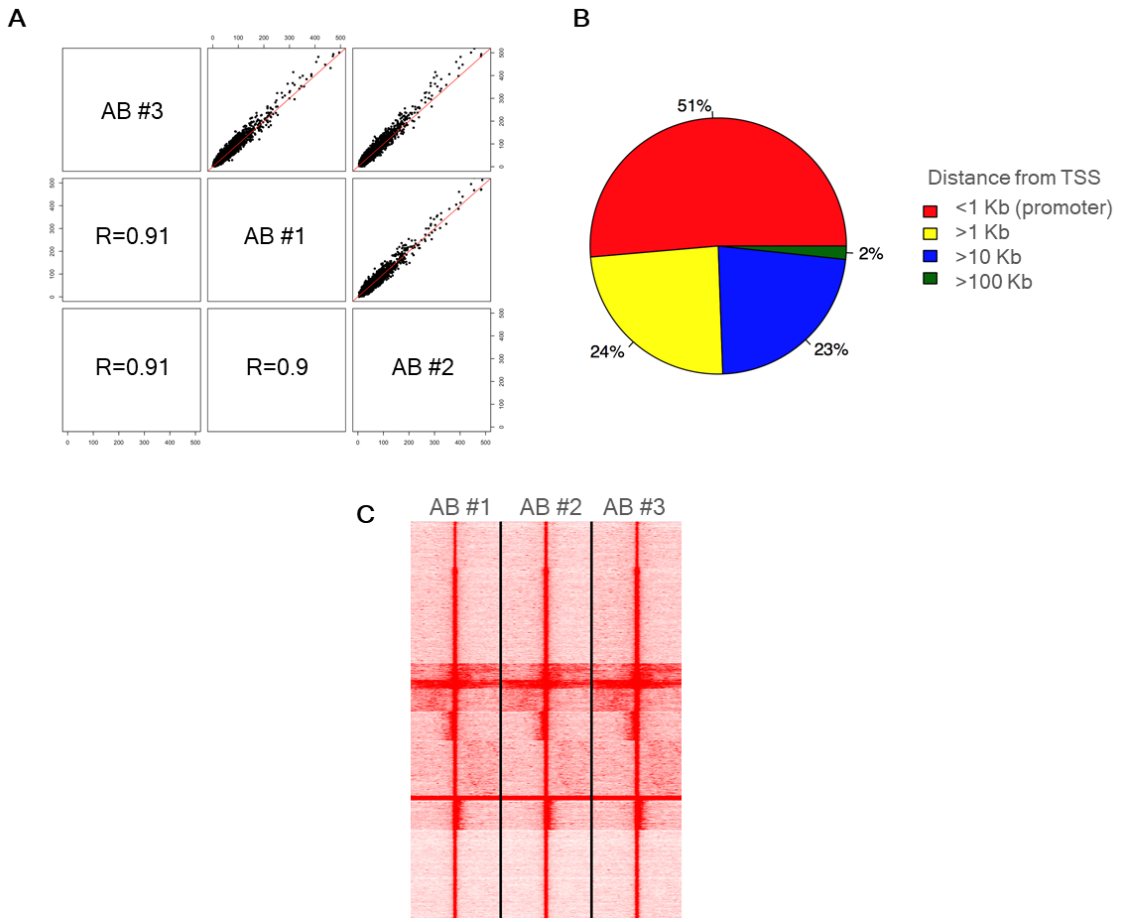

Figure 5.3 - ChIP-seq results show H3K122succ is enriched at the TSS

A Scatter plot showing the peak correlation between purified anti-H3K122succ antibodies 1-3. **B** Pie chart displaying the relative distance of the H3K122succ peaks relative of the TSS. Peaks were annotated with HOMER and Ensembl database v94 (for human genome hg38). **C** Heatmap comparing the H3K122succ peaks from the three samples. The peaks were aligned to the TSS (± 5000 bp). **D** Average profile at the region surrounding the TSS for each anti-H3K122succ sample.

To characterize the genomic distribution of H3K122succ the peaks were annotated using HOMER and the Ensembl database v94. Approximately 50 % of all peaks are located in the proximity of TSSs, suggesting an enrichment of H3K122succ at promoter regions (figure 5.3B). Next we plotted all H3K122succ peaks in a ± 5 kb window around the TSS. Interestingly, the results revealed a single peak overlapping the TSS, in a region often referred to nucleosome-free region (NFR) where the nucleosome occupancy is decreased[93] (figure 5.3C).

5.1.3.1 H3K122succ is associated with open chromatin

To further understand the distribution of H3K122succ in the genome, we compared the H3K122succ peaks with formaldehyde-assisted isolation of regulatory elements sequencing (FAIRE-seq) and DNase I hypersensitive sites sequencing (DNase-seq) datasets on MCF7 (figure 5.4). These two methods assess chromatin accessibility.

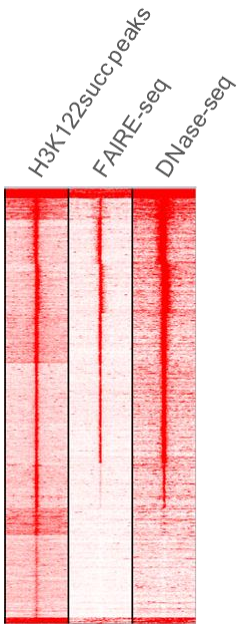

Figure 5.4 – H3K122succ is associated with open chromatin regions
Heatmap comparing all H3K122succ peaks with FAIRE-seq and DNase-seq datasets.

In short, FAIRE-seq relies on the different biochemical properties between protein-bound (compact) and protein-free (open) DNA to separate them[94], while DNase-seq is based on the premises that open chromatin regions are more susceptible to cleavage by DNase I[95]. As shown in figure 5.4, H3K122succ peaks have a clear overlap with both FAIRE-seq and DNase-seq, suggesting H3K122succ is associated with open chromatin regions as expected for an active chromatin mark.

5.1.3.2 H3K122succ correlates with active transcription

The data suggest a correlation between H3K122succ and an active transcription state. To further explore this, we compared the levels of H3K122succ with gene expression levels. For this we clustered all genes into four groups according to their steady-state mRNA levels: Q1 corresponds to the 25 % least expressed genes and Q4 to the 25 % highest expressed genes (figure 5.5A). The results revealed that H3K122succ is particularly enriched on highly expressed genes and that enrichment levels correlate with gene expression.

Next, we compared the levels of H3K122succ and H3K4me3 (a mark for active TSS) in all TSS (figure 5.5B), revealing a strong correlation between H3K122succ and H3K4me3 enrichments at active genes. Plotting the enrichments overs transcribed TSS demonstrates that H3K122succ peaks co-localize not only with H3K4me3 peaks but also H3K122ac and H3K9ac peaks.

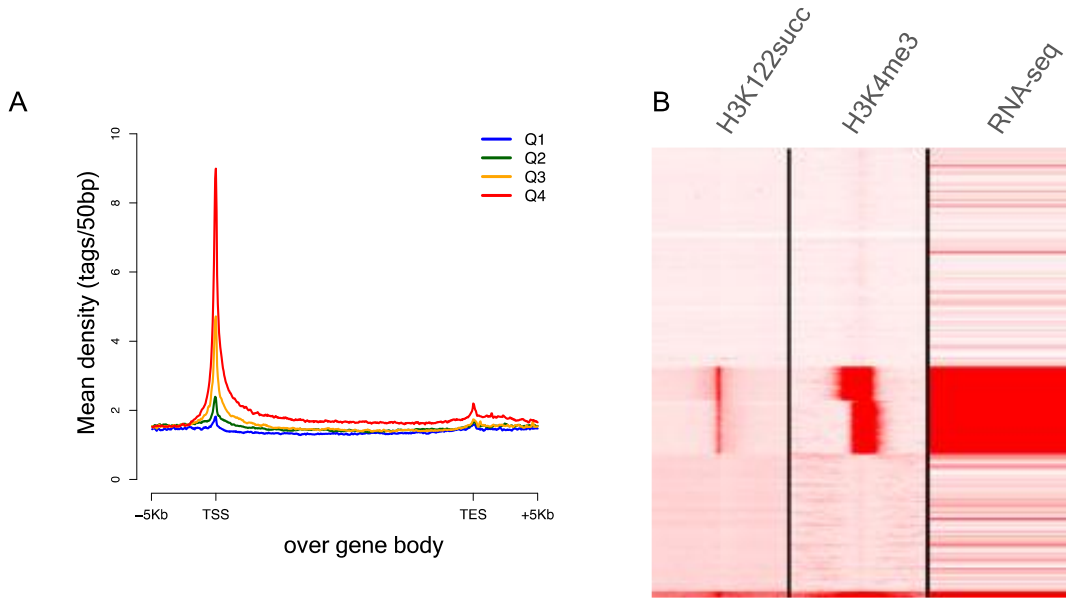

Figure 5.5 - H3K122succ is associated with known active histone marks and to active transcription
A Metagene plot displaying the distribution of H3K122succ around the TSS according to its quartile of expression. **B** Heatmap showing the proportion of TSS regions with H3K122succ, H3K4me3 and the corresponding mRNA expression.

5.1.4 p300/CBP is a succinyltransferase for H3K122

As mentioned in the introduction chapter, it has been shown that HATs can act as succinyltransferases[96]. In order to identify the enzyme(s) responsible for the establishment of H3K122succ a selection of HATs known to act as succinyltransferases was considered, including KAT2B, p300 and CBP.

5.1.4.1 Knockdown of candidate succinyltransferases

To identify the succinyltransferase(s) responsible for the succinylation of lysine 122 on histone H3, we depleted selected of HATs from MCF7 cells by short interfering RNA (siRNA) and quantified the relative of the levels of H3K122succ through immunoblotting.

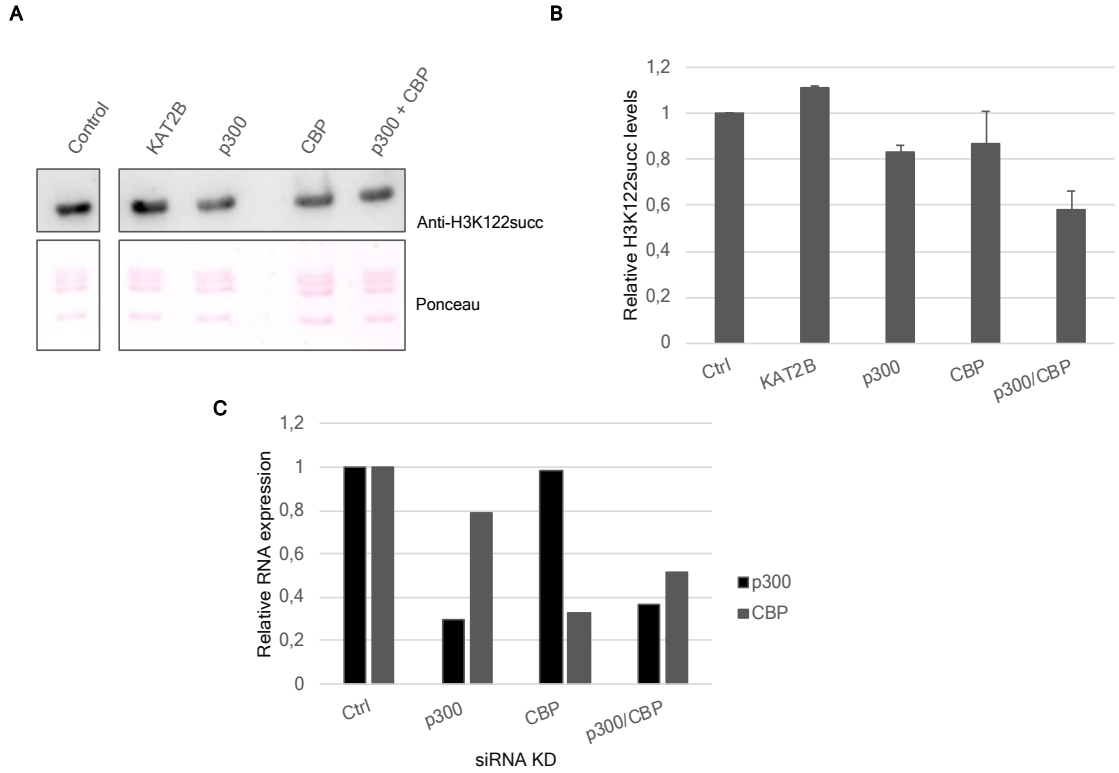

Figure 5.6 - The double knockdown of p300/CBP leads to the decrease in the levels of H3K122succ
A Representative immunoblot displaying the levels of H3K122succ upon siRNA depletion of various HAT enzymes. Ponceau staining of histones is shown as a loading control. **B** Histone acetyltransferases (pCAF, p300 and/or CBP) were depleted from MCF7 cells by siRNA. The bar graph shows the average ± standard deviation (STD) of H3K122succ levels, relative to the scramble siRNA control, of two biological replicates. **C** The levels of RNA expression of p300 and CBP upon siRNA KD were measured by qPCR.

While the knockdown of KAT2B did not lead to a decrease of H3K122succ, the individual depletion of p300 and CBP led to a slight decrease in the levels of this modification (figure 5.6A-B). Since p300 and CBP share a high sequence homology[97], in order to exclude that the relatively small effects of the individual depletion of these enzymes were not due to compensation by the other, a double knockdown of p300/CBP was performed. As it is shown in figure 5.6B, the double depletion of p300 and CBP led to a higher decrease in the H3K122succ levels (approximately 55 % comparing to the siRNA control). We compared the p300 and CBP mRNA levels upon the individual and double knockdown of these enzymes. The results revealed that upon KD, over 35 % of

the mRNA levels of p300 and approximately 50 % of the mRNA levels of CBP were kept, possibly explaining why no stronger effects on the H3K122succ levels were observed (figure 5.6C).

5.1.4.2 *In vitro* succinyltransferase assay on short peptides

To confirm that the paralogues p300 and CBP can indeed establish H3K122succ, we performed succinyltransferase assays on peptides spanning the region around lysine 122 on histone H3. For this we expressed and purified full length p300 in Sf9 cells (more details on section 8.2.22). We incubated H3 peptides with increasing amount of p300 in the presence of [^{14}C]suc-CoA and quantified the radioactivity incorporated by liquid scintillation counting (figure 5.7). In agreement with the results from the knockdown results, the *in vitro* succinyltransferase assays confirmed p300 as an enzyme that can establish H3K122succ.

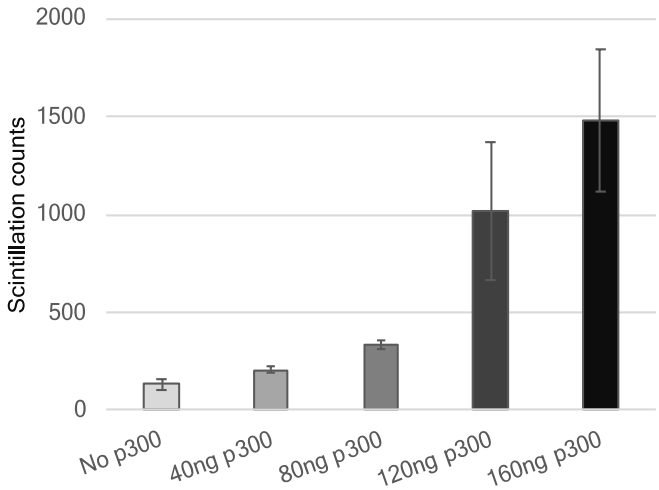

Figure 5.7 - *In vitro* succinyltransferase assay on peptides

In vitro succinyltransferase assay on peptides spanning H3K122. Samples were incubated overnight with different concentrations of p300 (0 to 160 ng) in the presence of [^{14}C]suc-CoA. The radioactivity incorporated in the peptides was quantified by liquid scintillation counting. The bar graph displays average and STD of two independent replicates

5.1.4.3 *In vitro* succinyltransferase assay on recombinant octamers

To further support the evidence that p300/CBP can act as succinyltransferases for H3K122succ, we carried out a second type of *in vitro* succinyltransferase assays on recombinant wild type histone octamers as substrates. For this assay, recombinant octamers were incubated O/N at 30 °C, with p300 in absence of any co-enzyme or suc-CoA and immunoblotting was used to determine H3K122succ levels (figure 5.8).

As shown in figure 5.8, the results demonstrated that p300 is a succinyltransferase for H3K122succ.

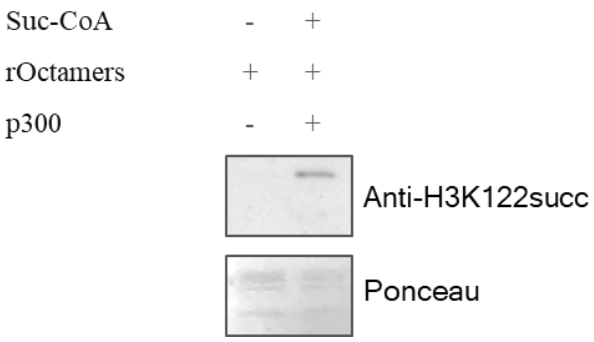

Figure 5.8 - p300 can establish H3K122succ on octamers *in vitro*

In vitro succinyltransferase assay, on recombinant unmodified histone octamers as substrate. After incubation with p300 and suc-CoA, the levels of H3K122succ were assessed by immunoblot. Ponceau staining of histones is shown as a loading control.

5.1.5 Sirtuin 5 can remove H3K122succ

Sirtuins have been shown to act as deacylases, in particular SIRT5 and SIRT7 have shown to act a desuccinylases[66,98]. For SIRT7, but not for SIRT5, it been reported that it can specifically remove H3K122succ[98]. To address the possible involvement of SIRT5 in the removal of H3K122succ, *in vitro* and *in vivo* assays were designed to address this question.

5.1.5.1 *In vitro* desuccinylase assay

To explore a potential role of SIRT5 in the removal of H3K122succ, we performed *in vitro* desuccinylase assays on H3K122succ peptides using recombinant SIRT5 and SIRT7 (figure 5.9). As expected, we found that SIRT7 can desuccinylate H3K122succ. Additionally, the results revealed that SIRT5 can also desuccinylate H3K122succ *in vitro*.

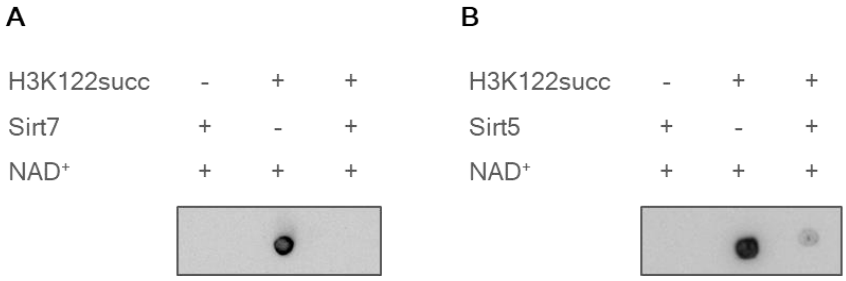

Figure 5.9 - SIRT5 can desuccinylate H3K122succ *in vitro*

A-B *In vitro* desuccinylase assay on H3K122succ peptides. Unmodified H3K122 peptide was used as control. Peptides were probed with H3K122succ antibody after incubation with sirtuins. Note that only in the co-presence of SIRT7 or SIRT5 and NAD^+, the levels of H3K122succ decreased.

5.1.5.2 SIRT5 acts as a H3K122succ desuccinylase *in vivo*

To confirm the activity of SIRT5 *in vivo,* we compared the levels of H3K122succ on histones extracted from wild type (WT) and *Sirt5*-knockout (KO) mouse embryonic fibroblasts (MEFs[64]) by immunoblot (figure 5.10).

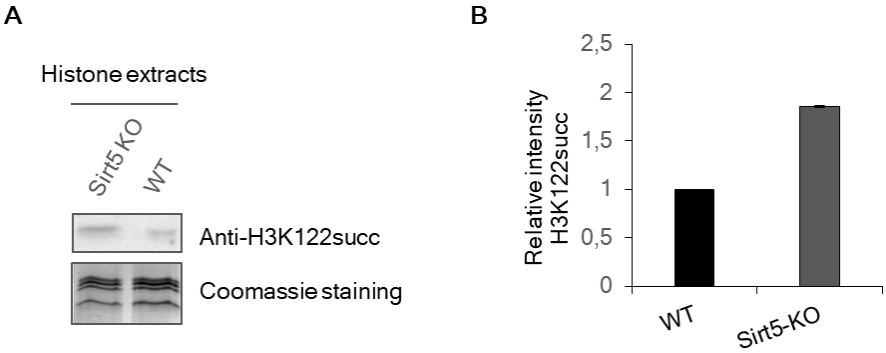

Figure 5.10 - SIRT5 acts as H3K122succ desuccinylase *in vivo*

H3K122succ levels in *Sirt5*-KO cells. Histones were acid extracted from WT and *Sirt5*-KO MEFs and levels of H3K122succ determined by immunoblot. **A** Representative immunoblot comparing the levels of

H3K122succ in WT and *Sirt5*-KO MEFS. Coomassie staining of histones is shown as a loading control. **B** Quantification of H3K122succ levels. Average and STD of two independent experiemnts are shown.

In agreement with the *in vitro* desuccinylase assays, levels of H3K122succ were higher on histones extracted from the *Sirt5*-KO MEF cell line compared to WT MEFs. These results confirm, therefore, that SIRT5 can act as H3K122succ desuccinylases.

5.1.6 Reconstitution of recombinant chromatin

To investigate the effect of H3K122succ on transcription in a well-controlled setup, we decided to perform *in vitro* transcription on chromatinized templates with unmodified H3 or site-specifically succinylated at H3K122.

5.1.6.1 Reconstitution of WT and H3K122succ histone octamers

Tag-less WT H2A, H2B and H4 were expressed on *E. coli* and purified from inclusion bodies as described in section 8.2.14. H3K122succ and WT H3 were generated by protein synthesis (Almac, UK). To assemble recombinant octamers, we mixed the core histones in equal molar amounts and processed them as described in section 8.2.15. Two types of histone octamers were assembled, one unmodified on H3 and another carrying fully succinylated H3 at lysine 122. After assembly, the octamers were successfully separated with a Superdex200 increase gel filtration column (figure 5.11).

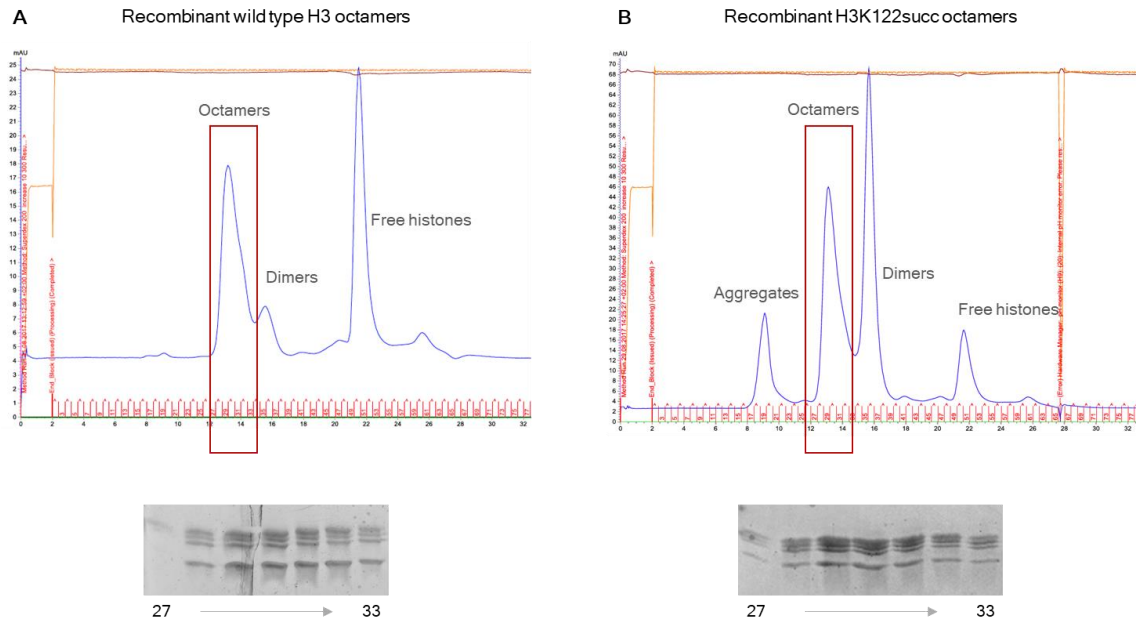

Figure 5.11 - Purification of histone octamers by gel filtration

Recombinant histones core histone including wild type H3 or H3K122succ were refolded as described in the methods section, concentrated and loaded on a Superdex200 increase gel filtration column. The upper panels show the UV elution profile from the Superdex200 increase column for histones refolded with **A** WT H3 or **B** H3K122succ. The peak fractions were analyzed by SDS-PAGE and coomassie stained (bottom panels). The fractions containing all four histones in stochiometric amounts (28-31) were pooled, concentrated to 2 mg/ mL and stored at -20 °C in refolding buffer with 50 % glycerol.

5.1.7 *In vitro* transcription

The *in vitro* transcription assay is an elegant experiment designed to recapitulate all major steps of eukaryotic transcription in a cell free assay. It is composed of three main steps: chromatin assembly, sucrose gradient purification and the *in vitro* transcription assay *per se* (figure 5.12).

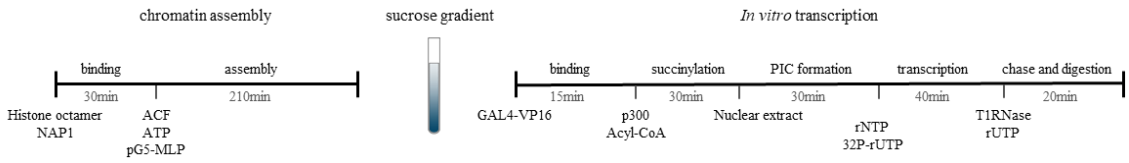

Figure 5.12 - *In vitro* transcription assay summary

Schematic representation of the *in vitro* transcription assay: chromatin assembly, density selection by sucrose gradient and *in vitro* transcription. For details see section 8.2.24.

The assay requires several components including a DNA template (which can consist of free or chromatinized DNA) containing a promoter and a transcription activator binding site; a transcriptional activator protein; a source of Pol II, transcription factors and mediator complex and ribonucleotide tri-phosphates (rNTP). For the purpose of this thesis, we used as DNA template the previously described pG5-MLP[99], an approximately 5 Kb plasmid containing a viral promoter (major late promoter, MLP), downstream of five GAL4-binding domains (where the activator protein will bind) and upstream of a 380 bp G-less cassette, which will serve as a template for the transcript.

Figure 5.13 - Regulatory region of PG5-MLP

Schematic representation of the regulatory region of the DNA template used on the *in vitro* transcription assays. The template includes five GAL5-binding domain, one major late promoter and an approximately 380bp G-less cassette.

The use of a transcriptional activator is required for assays using chromatinized templates, as chromatin inhibits transcription. For that purpose, we used recombinant viral VP16, fused to GAL4 (GAL4-VP16). HeLa nuclear extracts, prepared as described in methods 8.2.23, were used as a source of Pol II, transcription factors and mediator complex. Adding radiolabeled rUTP-32P in the rNTP mix, allows the quantification of the transcript amount produced in each assay. The purity of all components was checked on SDS-page followed by coomassie staining (figure 5.14).

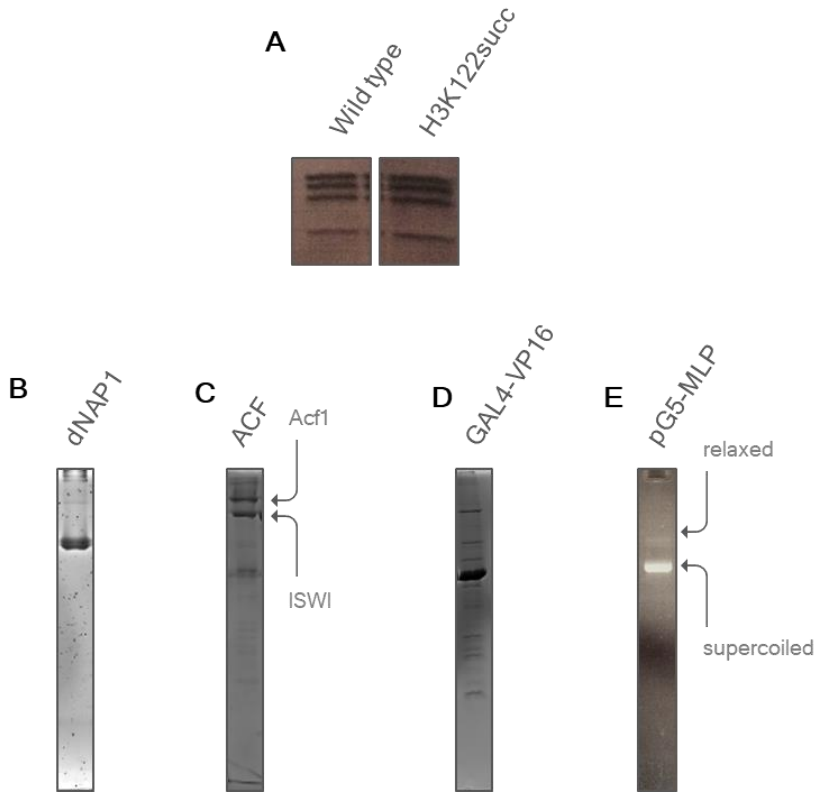

Figure 5.14 - Purity control of the reagents used for the *in vitro* transcription
SDS-PAGE and coomassie staining of **A** WT and H3K122succ histone octamers, **B** NAP1, **C** ACF and **D** GAL4-VP16. **E** Agarose gel electrophoresis of pG5-MLP plasmid.

5.1.7.1 Chromatin assembly

The reconstitution of chromatin can be accomplished through gradient salt dialysis (from high to low concentrations of salt) of histone octamers and DNA or through ATP-dependent assembly by a histone chaperone and a chromatin remodeling complex. While chromatin assembly by salt dialysis results in random distribution of nucleosomes, ATP-dependent assembly results in the periodically distribution of nucleosomes. Since the latter resembles chromatin structure *in vivo*, we chose it for the *in vitro* transcription assays. Histone chaperone nucleosome assembly protein (NAP1) and chromatin remodeler ACF were expressed in Sf9 cells infected with baculovirus and purified as described in the methods chapter. For each chromatin assembly, we tested different ratios of histone octamers to DNA (0.9:1, 1:1 and 1.1:1).

Chromatin assembly efficiency was assessed by MNase mapping (methods 8.2.19) followed by agarose gel electrophoresis and ethidium bromide (EtBr) staining (figure 5.15). Preliminary assays showed that for both WT and H3K122succ chromatin, a histone octamer to DNA ratio of 1:1 led to the best resolved MNase mapping and was thus chosen for the assembly.

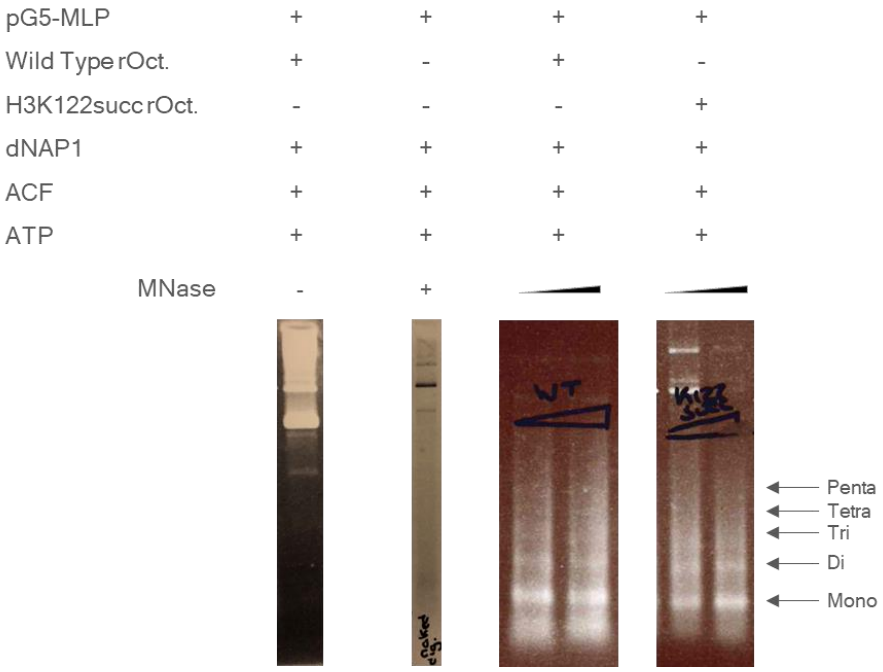

Figure 5.15 - Chromatin assembly by NAP1 and ACF

Agarose gel electrophoresis, followed by ethidium bromide staining of MNase digested assembled chromatin. On the left lane, no MNase was added to the incubation as a digestion control. On the second left, no histone octamers were added to assembly reaction.

5.1.7.2 Sucrose gradient

After assembly, we fractionated the chromatin by sucrose gradient centrifugation. The migration of chromatin through the gradient is dependent on the speed and length of the centrifugation, as well as the density of the chromatin. Under similar conditions, chromatin will migrate through the gradient according to its compaction. The selection of the same fractions, allows therefore, an increase in the homogeneity of different batches of chromatin assembly (figure 5.16).

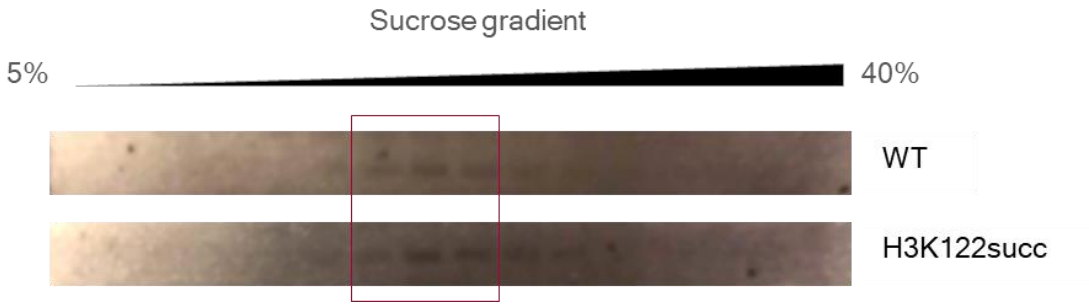

Figure 5.16 - Sucrose gradient purification of recombinant chromatin

Sucrose gradient centrifugation of WT (top) and H3K122succ (bottom) chromatin. The red box marks fractions 6-8, that were pooled together and dialyzed in BC50 prior to *in vitro* transcription assays.

5.1.7.3 *In vitro* transcription assays on chromatin

In vitro transcription assays were performed in collaboration with Raphael Margueron at the Institut Curie (Paris, France), where we performed initial assays before establishing them in the laboratory of Robert Schneider.

5.1.7.3.1 Suc-CoA stimulates transcription *in vitro*

First to understands if suc-CoA can stimulate transcription (as ac-CoA does), performed *in vitro* transcription assays on unmodified chromatin in the presence of suc-CoA and compared the results to the levels of transcription in the absence of co-enzymes or in the presence of ac-CoA (figure 5.17).

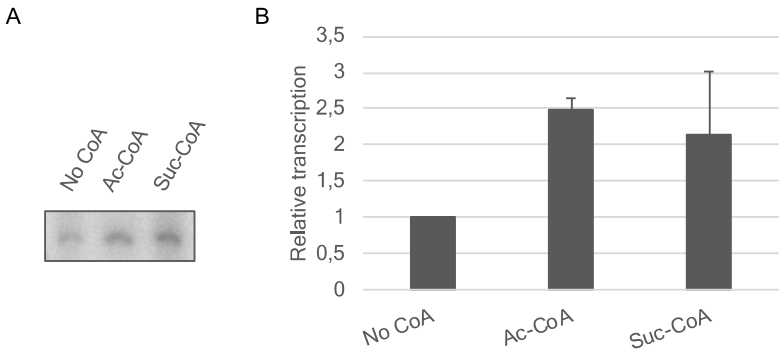

Figure 5.17 - Suc-CoA can stimulate transcription *in vitro*

A *In vitro* transcription in the presence of GAL4-VP16 and p300 in the absence of co-enzymes, presence of ac-CoA and suc-CoA. Shown is a representative audioradiogram. **B** Quantification of *in vitro* transcription reactions as in A. Expression relative to no CoA is plotted. Average and STD of two independent experiments are shown.

The results shown in figure 5.17, suggest that suc-CoA can stimulate transcription, to a similar degree to ac-CoA.

5.1.7.3.2 H3K122succ increases transcription *in vitro*

In order to study the impact of H3K122succ on transcription, we performed *in vitro* transcription assays on WT and H3K122succ chromatin. Remarkably, the presence of H3K122succ stimulated transcription (compared to unmodified chromatin) by approximately 1.6-fold (figure 5.18).

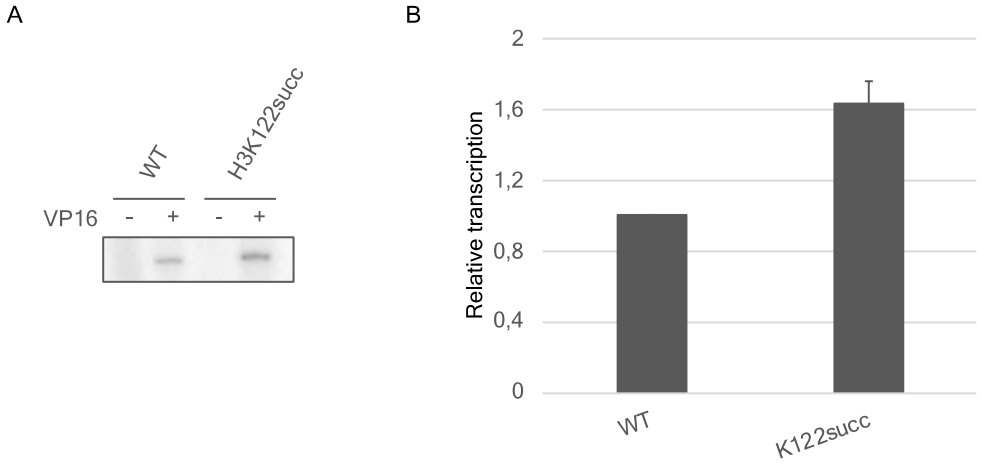

Figure 5.18 - H3K122succ increases transcription *in vitro*

A *In vitro* transcription on unmodified chromatin or H3K122suc chromatin. Shown is a representative audioradiogram. **B** Quantification of reactions. Expression relative to transcription on unmodified chromatin is plotted. Average and STD of two independent experiments are shown.

5.1.8 H3K122succ affects nucleosome stability *in vitro*

In order to gain insight in a potential mechanism how H3K122suc might simulate transcription we asked next whether H3K122succ affects nucleosome stability. For this we performed single molecule Fluorescence Resonance Energy Transfer (smFRET) assays. These assays were carried out by Mariska Haas from Dr. Jens Michaelis' laboratory at Ulm University (Ulm, Germany).

Mono-nucleosomes were assembled (from WT and H3K122succ octamers) by salt dialysis onto a modified MMTV-A DNA positioning sequence[100], carrying two fluorescent dyes at positions F48 and R28. This method allows the comparison of the kinetics of nucleosome salt-induced disruption of WT and H3K122succ nucleosomes (figure 5.19A).

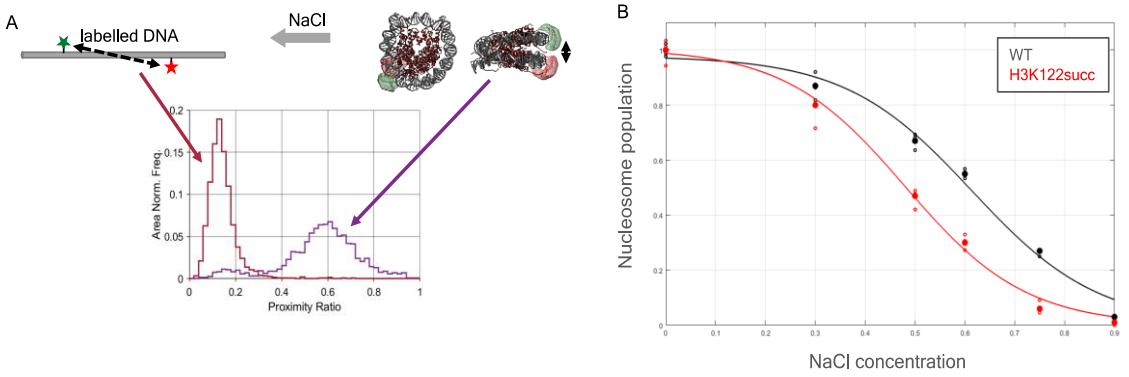

Figure 5.19 - H3K122succ contributes to the destabilization of nucleosomes

A Schematic representation of the smFRET assays. **B** Mean fraction of bursts in the nucleosome population (proximity ratio >0.35) of WT (black) and H3K122succ (red) plotted against different NaCl concentrations. Three measurements were performed for each salt concentration. The data were fitted to $f(x) = A2 + \frac{A1-A2}{1+e^{(x-x0)/dx}}$ where A2 was restricted to a minimum of zero.

The results revealed that under low salt concentrations (below 0.3M) unmodified and H3K122succ nucleosomes showed a similar stability. However, nucleosomes carrying H3K122succ were more sensitive to destabilization upon increased salt concentrations (from 0.3M; figure 5.19B). This assay demonstrates that H3K122succ can indeed destabilize nucleosomes and reveals a potential mechanism how H3K122suc can stimulate transcription.

5.2 Part 2 – Histone H3 core domain acetylations

In the second part of my thesis I wanted to investigate if multiple lateral surface modifications are acting synergistically. For this I focused on the acetylations of H3K56, H3K64 and H3K122, since all are found at TSS of active genes.

5.2.1 *In vitro* transcription on recombinant chromatin

To understand the potential synergistic role of H3K56ac, K64ac and K122ac in transcription, we performed *in vitro* transcription assays, as described on section 8.2.24. For these assays, we expressed and purified wild type and site-specifically modified recombinant histones from *E. coli*. For the expression of acetylated histones, an amber suppression system was used.

5.2.1.1 Optimization of the amber suppression system

Several variations of amber suppression systems have been described[42,101,102]. In general, these approaches rely on two essential components: a modified protein coding sequence, in which the codon where the modified amino acid to be inserted is substituted by an amber codon (TAG), and an evolved orthogonal transfer RNA (tRNA)/aminoacyl tRNA synthetase pair (figure 5.20). The amber codon is the least frequent STOP codon in *E. coli*[103]. In amber suppression systems, during translation this codon is recognized by the modified tRNA leading to the incorporation of an acetyl-lysine (AcK) by the aminoacyl tRNA synthetase[101].

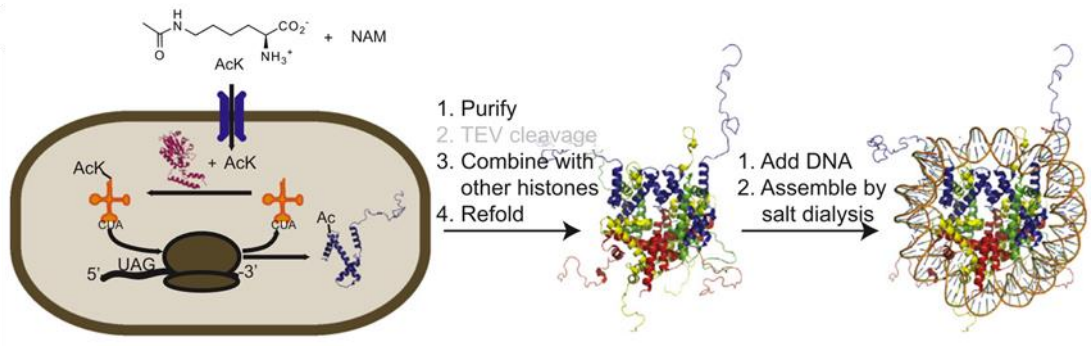

Figure 5.20 - Amber suppression system

Schematic representation of the recombinant expression of site-specifically modified histones in *E. coli* strain BL2. Bacteria transformed with the plasmid(s) carrying the components of this amber suppression system are supplemented with Nam and acetyl-lysine. Histone expression is induced with IPTG. After being expressed, histones are purified and mixed with other core histones to assemble octamers and later nucleosomes. Adapted from Neumann *et al.*, 2009.

While this method has been successfully used to express histones fully acetylated at a single site, it presented serious limitations for the expression of multiple-site acetylated proteins. During translation two parallel mechanisms compete with each other. The first one, is naturally occurring and regards the recognition of the amber codon by release factor 1 (RF1), which recognizes UAG as a STOP codon and promotes the release of the nascent peptide[104,105]. The second mechanism, consists on the already described amber suppression system. We estimate that in the initial amber suppression systems 1:50 of all expressed proteins is full length and includes the intended modification. The remaining 49:50 consist of truncated proteins at the corresponding site of the amber codon. Considering this rate, for the expression of a protein carrying three acetyl-lysines, approximately 1:125000 expressed proteins would be full length, making it inadequate for this purpose.

In a first attempt to improve the efficiency of the system, we compared different *E. coli* strains: BL21, JX33[106] and C321.ΔA[107]. The latter two strains carry a KO of RF1 in order to decrease the levels of histone truncation during translation[108]. In addition, C321.ΔA has all naturally occurring amber codons substituted into ochre codons (UAA). As expected, the amounts of full-length modified histones produced in these strains increased, however both strains presented significant growth defects (data not shown) which hindered their use and prompted us to search for alternative improvements where we could use the BL21 strain.

It has been reported that the overexpression of the C-terminal domain of L11 (L11C) - a small, highly conserved ribosomal protein that is involved in RF1-mediated peptide release – leads to high amber suppression, with nearly regular protein translation efficiency and normal growth rate[109]. Thus, we tried overexpressing L11C. Additionally, we mutated the tRNA sequence to optimize

the incorporation of acetyl-lysine[110] and substituted the promoter of the tRNA synthetase from a GlnRS promoter to a Trc promoter, a change that has been reported to increase the expression of the tRNA synthetase and consequently the efficiency of the system[111].

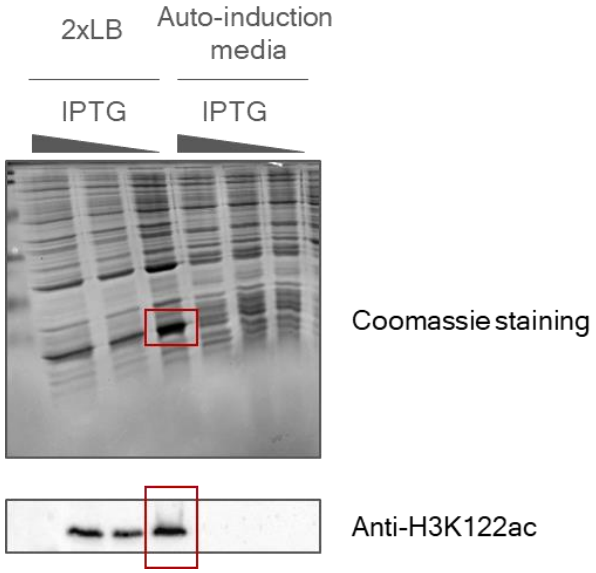

Figure 5.21 - Optimization of the amber suppression system

Total protein extract after H3K122ac expression under different conditions was loaded on an SDS-PAGE gel and coomassie stained (top panel) or immunoblotted against anti-H3K122ac (bottom panel). Red boxes indicate the highest expression of the modified H3.

To test this optimized amber suppression system and to determine the optimal growth conditions, we applied it first for the expression of single acetylated H3 histones at lysine 122. Different media and IPTG concentrations were tested. As shown on figure 5.21, we were able to express H3K122ac protein at relatively high levels when using the system in BL21 cultured in twice concentrated lysogeny broth (2x LB), with an optimal yield when protein expression was induced at a low IPTG concentration (0.05 mM) O/N at 20 °C.

5.2.1.2 Expression and purification of acetylated histones

Having now the tools to produce site-specifically acetylated histones, we expressed tag-less H3 histones carry the following lysine acetylations:

H3K56ac, H3K64ac, H3K122ac, H3K56acK64ac, H3K56acK122ac, H3K64acK122ac and H3K56acK64acK122ac. After the expression of each histone, we controlled by immunoblotting that the expressed H3 histones carried the intended acetylations (figure 5.22).

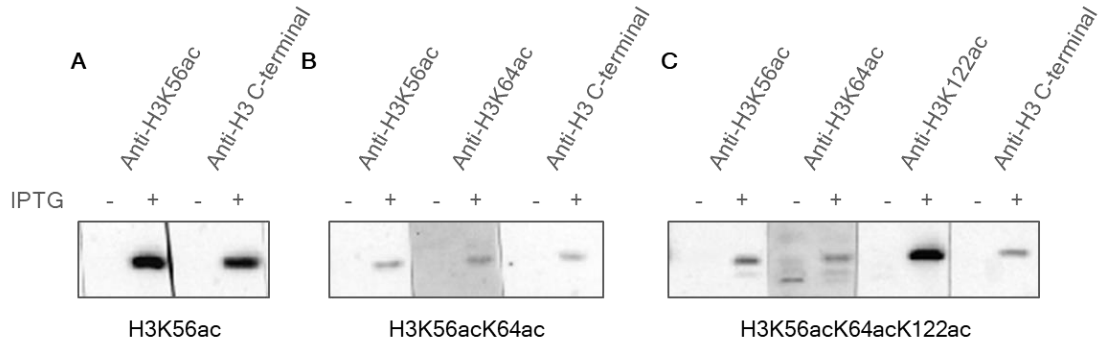

Figure 5.22 - Expression of single, double and triple-acetylated H3

Immunoblots controlling for the expression of representative single, double and triple-acetylated histone H3. Expressed histones were blotted with antibodies against the specific acetylations to control for the correct insertion of acetyl-lysine and with anti-H3 C-terminal antibody to control for the full-length histone. **A** Single-acetylated H3: H3K56ac. **B** Double acetylated-H3: H3K56acK64ac. **C** Triple-acetylated H3: H3K56acK64acK122ac.

After expression of the modified histones, we purified them from inclusion bodies as described in section 8.2.14. We used two chromatography columns, a cation exchange and a gel filtration column, to separate the acetylated full-length histones from the truncated ones. It was, however, not possible to separate the H3 truncated lysine 122 from full-length H3, since their elution profiles from both columns were very similar. Additionally, due to the nature of the system, in order to express sufficient quantities of each modified histone, large volumes of BL21 were cultured (2 L of culture yield approximately 9mg of WT H3; 5L of culture yield 1-2 mg of mono-acetylated H3; 10 L of culture and yield approximately 1 mg of double-acetylated H3 and 20 L of culture yield approximately 1 mg of triple-acetylated H3), which interfered with the

purification of the modified histones due to the relative higher abundance of DNA and contaminating proteins in the inclusion bodies (figure 5.23).

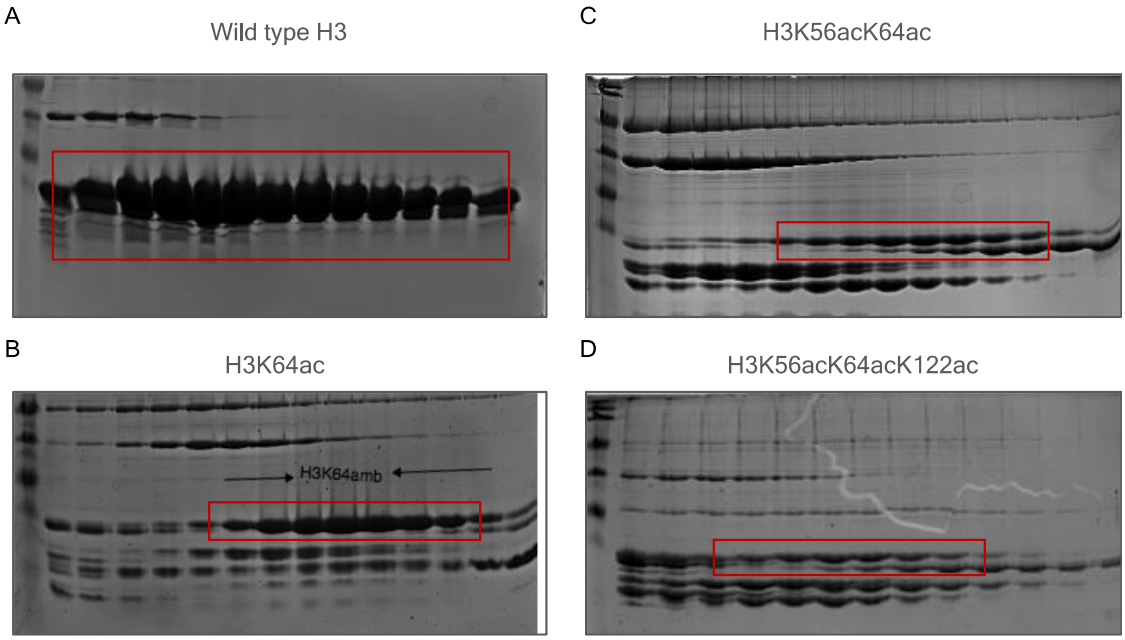

Figure 5.23 - Expression and purification of acetylated H3 histones

H3 histones were extracted from inclusion bodies as described in 8.2.14. Extracted histones were purified on a gel filtration and on a cation exchange chromatography column. The eluted fractions from the cation exchange chromatography column of **A** WT, **B** H3K64ac, **C** H3K56acK64ac and **D** H3K56acK64acK122ac were loaded on an SDS-PAGE gel and coomassie stained. The red boxes indicate the correct H3 bands.

Since it has been described that the α3 helix of H3 is necessary for octamer/nucleosome formation[112], H3 truncated at *e.g.* K122 is not able to form octamers. Therefore, the octamer reconstitution provided an additional step to separate the unwanted truncated histones, from the full-length ones.

5.2.1.3 Reconstitution of modified histone octamers

To assemble the differently acetylated histone octamers, equimolar quantities of each core histone were mixed as described in section 8.2.15. After assembly, the histone octamers were purified on a Superdex200 increase gel filtration column. As shown in the chromatograms bellow (figure 5.24), the efficiency of

the octamer reconstitution decreased proportionally to the increase in the number of acetylation sites. This could be due to a combination of several factors, including: the higher concentration of protein contaminants, higher proportion of truncated histones or simply due to the presence of higher amount of core acetylations in H3.

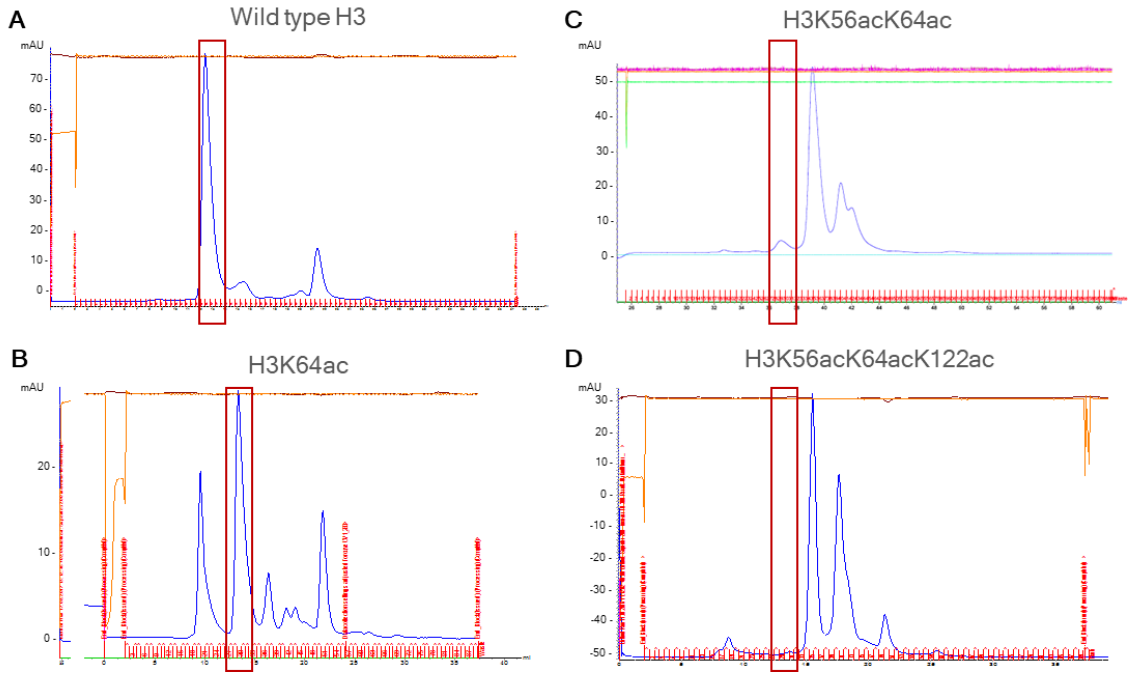

Figure 5.24 - Purification of acetylated histone octamers by gel filtration

Recombinant histones were refolded as described in 8.2.15, concentrated and purified on a Superdex 200 increase gel filtration column. Displayed are representative chromatograms displaying the UV elution profile of **A** WT H3, **B** single acetylated H3 (H3K64ac), **C** double acetylated H3 (H3K56acK64ac) and **D** the triple acetylated H3 (H3K56acK64acK122ac).

Despite the relatively low efficiency, we succeeded in assembling sufficient amounts of the differently modified histone octamers (figure 5.25).

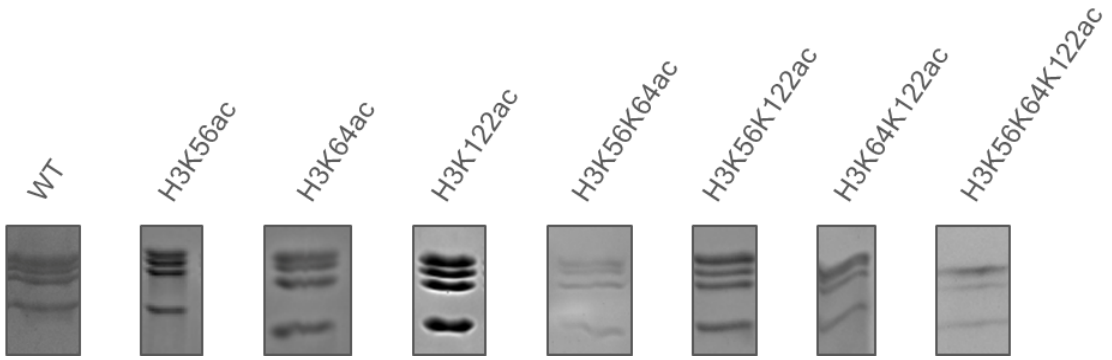

Figure 5.25 - Purified histone octamers

The purity of the recombinant histone octamers was assessed by SDS-PAGE and stained with coomassie.

5.2.1.4 Recombinant chromatin assembly for *in vitro* transcription

Next, we assembled differently modified chromatin arrays for the *in vitro* transcription assays. As mentioned on Part I of the results, for the assembly of chromatin for *in vitro* transcription we relied on the use of the histone chaperon NAP1 and the ATP-dependent chromatin remodeler ACF, which guaranteed a regular spacing between the nucleosomes.

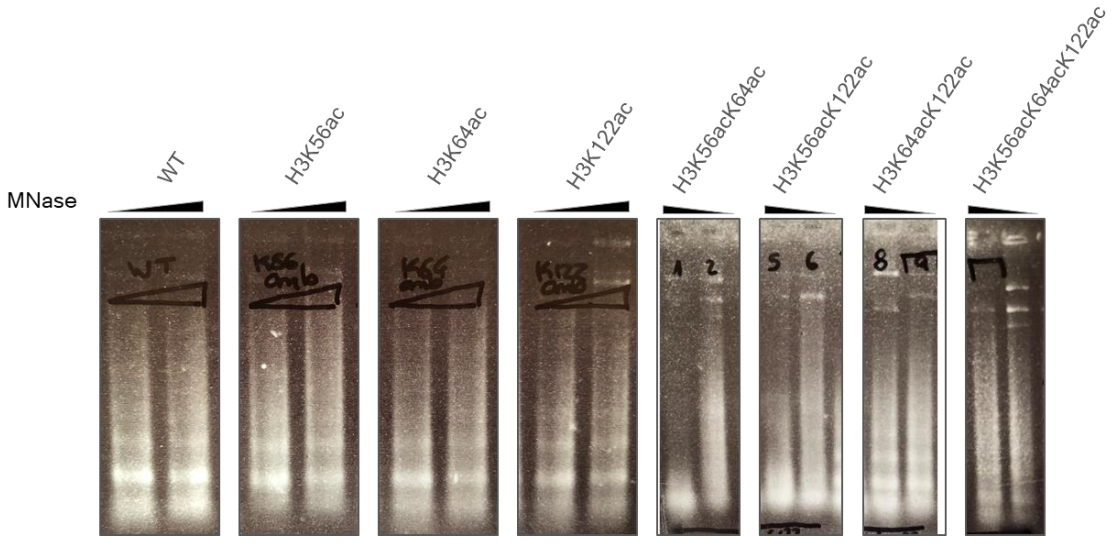

Figure 5.26 - Chromatin assembly with different octamers by NAP1 and ACF

Agarose gel electrophoresis and EtBr staining of assembled chromatin on pG5-MLP with eight different histone octamers: WT H3, H3K56ac, H3K64ac, H3K122ac, H3K56acK64ac, H3K56acK122ac, H3K64acK122ac and H3K56acK64acK122ac by NAP1 and ACF. Nucleosome positioning was assessed by of MNase digestion.

The efficiency of the assembly was assessed by partial MNase digestion (figure 5.26). As it can be observed, the efficiency of the chromatin assembly was not homogeneous, namely H3K56acK64ac and H3K56acK122ac chromatin was more sensitive to MNase digestion. In order to compensate for different chromatinizations, we purified the different types of chromatin via sucrose gradients as described on 8.2.18 and fractionated them according to their migration in the gradient. Similarly-compacted chromatin was selected by the pooling of the same fractions (figure 5.27).

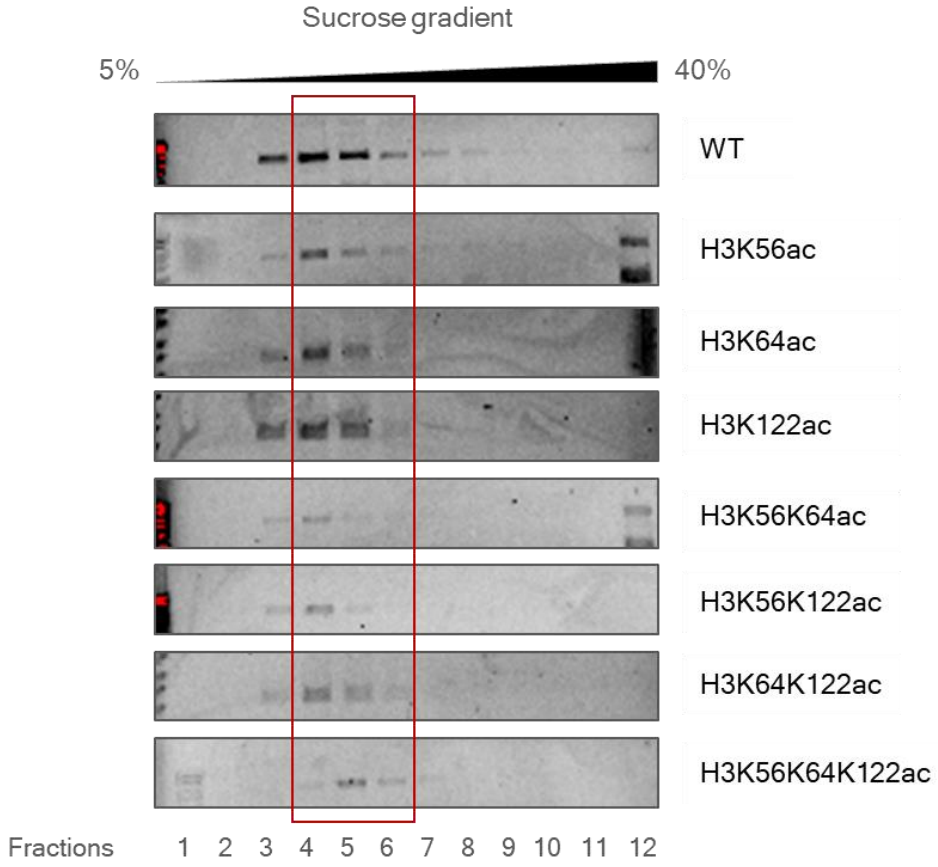

Figure 5.27 - Chromatin purification on a sucrose gradient

Sucrose gradient centrifugation of the eight chromatin assembly reactions was collected in 12 fractions of which 10 µL were analyzed by agarose gel electrophoresis and ethidium bromide staining. Fractions 4-6 were pooled together and dialyzed against BC50 buffer.

After pooling fractions 4-6 together, the samples were dialyzed against BC50 buffer O/N and then concentrated to 7.14 ng/ µL.

5.2.1.5 *In vitro* transcription assays

To investigate possible synergistic functions of the different H3 core acetylations, we next carried out *in vitro* transcription assays on WT and site-specifically acetylated chromatin. The assays were performed as previously described. Initially we tested the effect of the single acetylations on chromatin using 40 ng of p300 *per* reaction. Interestingly, all three acetylations (H3K56ac, H3K64ac and H3K122ac) mildly stimulated transcription (figure 5.28).

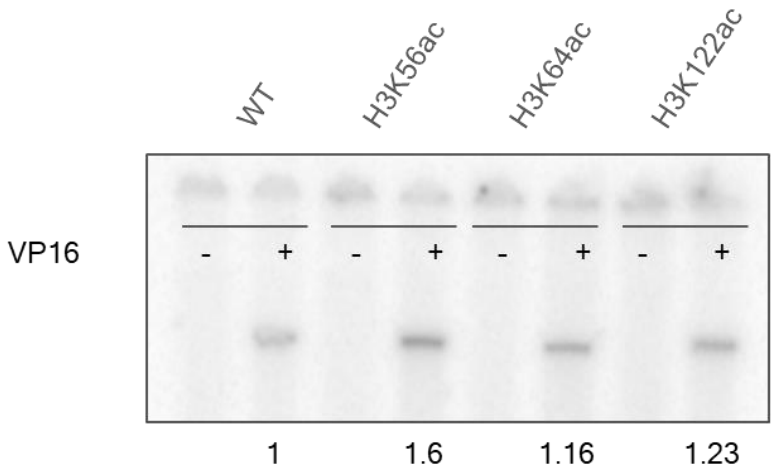

Figure 5.28 – In vitro *transcription on WT and single acetylated chromatin in the presence of 40 ng of p300.* *In vitro* transcription with 50 ng of purified chromatin in BC50. 40 ng of p300 were used and 50 ng of GAL4-VP16 were added as indicated. Autoradiogram is shown. Transcription was quantified densitometrically using ImageJ. The results indicated on the bottom of the figure are presented, as relative to WT chromatin.

We hypothesized that the mild effects we were observing were due to the high concentrations of p300 used. To test this hypothesis, we performed *in vitro* transcription assays on WT and single acetylated chromatin (H3K64ac) in the presence of decreasing amounts of p300 (data not shown). As expected, the transcript signal on the WT chromatin decreased proportionally to the decrease of p300. Interestingly, however, the level of transcription with the H3K64ac chromatin did not seem to be significantly affected by the lower amount of p300. We concluded, therefore, that by carrying out the *in vitro* transcription assays

with lower amounts of p300 the effects of the acetylations would be accentuated.

We proceeded to repeat the *in vitro* transcription assays on WT and single acetylated chromatin in the presence of 2.5 ng of p300 (figure 5.29). As we had hypothesized, the use of lower amounts of p300 in the assay, led to a significant increase on the relative effects of the single acetylations, with the acetylation of lysine 122 on histone H3 stimulating transcription by 2.84-fold.

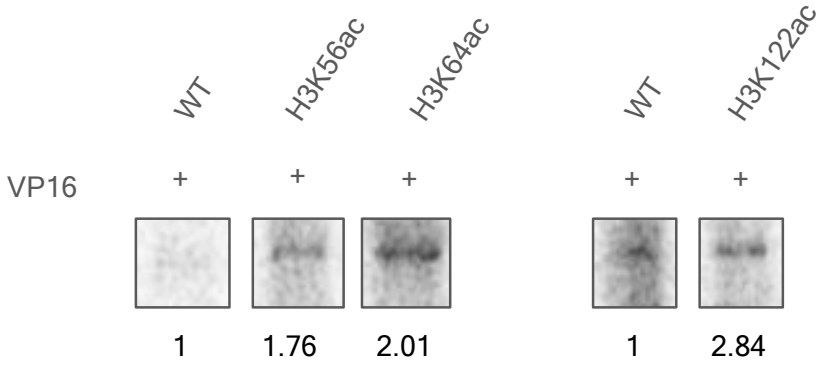

Figure 5.29 - Single core acetylations can stimulate transcription *in vitro*

In vitro transcription assays were carried out on 50 ng of chromatin, in the presence of 50 ng of GAL4-VP16 and 2.5ng of p300. Transcription was quantified densitometrically using ImageJ relative to WT chromatin.

Next, we wanted to understand how the different combinations of globular domain acetylations affected transcription. As expected, the combination of two acetylations led to a higher stimulation of transcription than the single acetylations (figure 5.30), with the two combinations carrying H3K122ac having the highest transcription levels, leading to a striking increase of approx. 4.2-fold. Interestingly, the combination of the three acetylations did not lead to a higher stimulation of transcription.

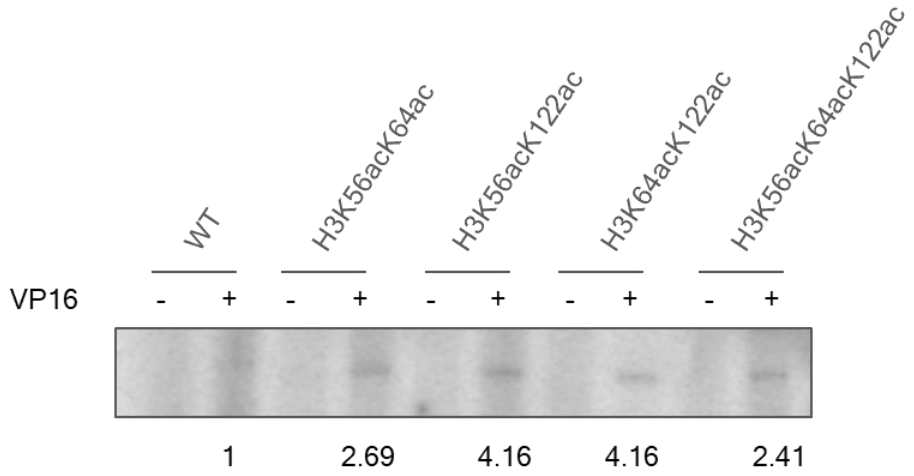

Figure 5.30 - Double and triple acetylations on H3 lead to a higher stimulation of transcription *in vitro*
In vitro transcription assay on chromatin carrying different combinations of H3 core acetylations. Assays were carried out on 50 ng of chromatin, in the presence of 50 ng of GAL4-VP16 and 2.5 ng of p300. Transcription was quantified densitometrically using ImageJ and is presented relative to WT chromatin.

Altogether, these results show that histone core acetylations stimulate transcription *in vitro* and that combinations of acetylations lead to a higher stimulation. Direct effects of H3K56ac and H3K64ac on transcription had never been shown before. Additionally, these results suggest that the effect the modifications have on transcription are site-specific hinting a specific mechanism for each modified chromatin.

5.2.2 The role of H3 core acetylations *in vivo*

In order to be able to study the role of H3K56ac, H3K64ac, H3K122ac and their combinations in transcription in an *in vivo* system, we generated a mammalian cellular system where the effects of these modifications can be investigated. This model relies on the use of amino acid substitutions to mimic unmodified and acetylated histones lysine residues. Amino acid substitutions have long been used as an approach to study protein PTMs, as certain residues due to their charge, size and tertiary structure can resemble other modified

residues[87,113]. As an example, the replacement of a lysine residue by arginine (K>R) is commonly used to mimic the unmodified lysine state, while the substitution of a lysine residue by glutamine (K>Q) is often used to mimic lysine acetylation.

Histone variant H3.3 has been shown to be enriched at the promoter and gene body of actively transcribed genes in euchromatin[92], making it a relevant variant in the study of active H3 PTMs. Additionally, H3K122ac and H3K64ac had been shown to be enriched at H3.3. In mice, H3.3 is encoded by two genes, H3f3a and H3f3b, located on chromosomes 1 and 11 respectively[114].

Table 5.1 - List of mES cells used in this study.

mES cell mutants	Mimic state
ESW26	Original cell line
H3.3B	$H3f3a^{-/-}$ $H3f3b^{-/+}$ cell line
2HA.H3.3B	WT control
2HA.H3.3K56R	Unmodified mimics
2HA.H3.3K64R	
2HA.H3.3K122R	
2HA.H3.3K56K64R	
2HA.H3.3K56K64K122R	
2HA.H3.3K56Q	Acetylation mimics
2HA.H3.3K64Q	
2HA.H3.3K122Q	
2HA.H3.3K56K64Q	
2HA.H3.3K56K64K122Q	

For the generation of our *in vivo* model, starting from the mouse embryonic stem cells (mES cell) ESW26, we deleted three of the four alleles coding for H3.3

(H3f3a$^{-/-}$H3f3b$^{-/+}$) using the Clustered Regularly Interspaced Short Palindromic (CRISPR) genome editing system (H3.3B). Next, the remaining H3.3 coding gene was replaced by a mutated H3.3 gene containing two HA tags and site-specific mutations (table 5.1). For the purpose of this work, a cell line containing a single 2HA-tagged H3.3 allele, carrying no amino acid substitution (2HA.H3.3B) will be considered our WT (non-mutated) control.

These cell lines were created by two former laboratory members Dr. Nithyha Parameswaran Kalaivani and Dr. Sylvain Daujat.

5.2.2.1 Analysis of the effect of H3.3 core acetylation on steady state transcription

In order to investigate the effects of these H3 core acetylations at the transcriptional level *in vivo*, we cultured the mES cell lines under standard 2i/LIF conditions and extracted and purified total RNA from them. Purified RNA was sequenced by next generation sequencing (RNA-seq). Data analysis was performed by Dr. Diego Rodríguez Terrones at the Helmholtz Zentrum München (Munich, Germany).

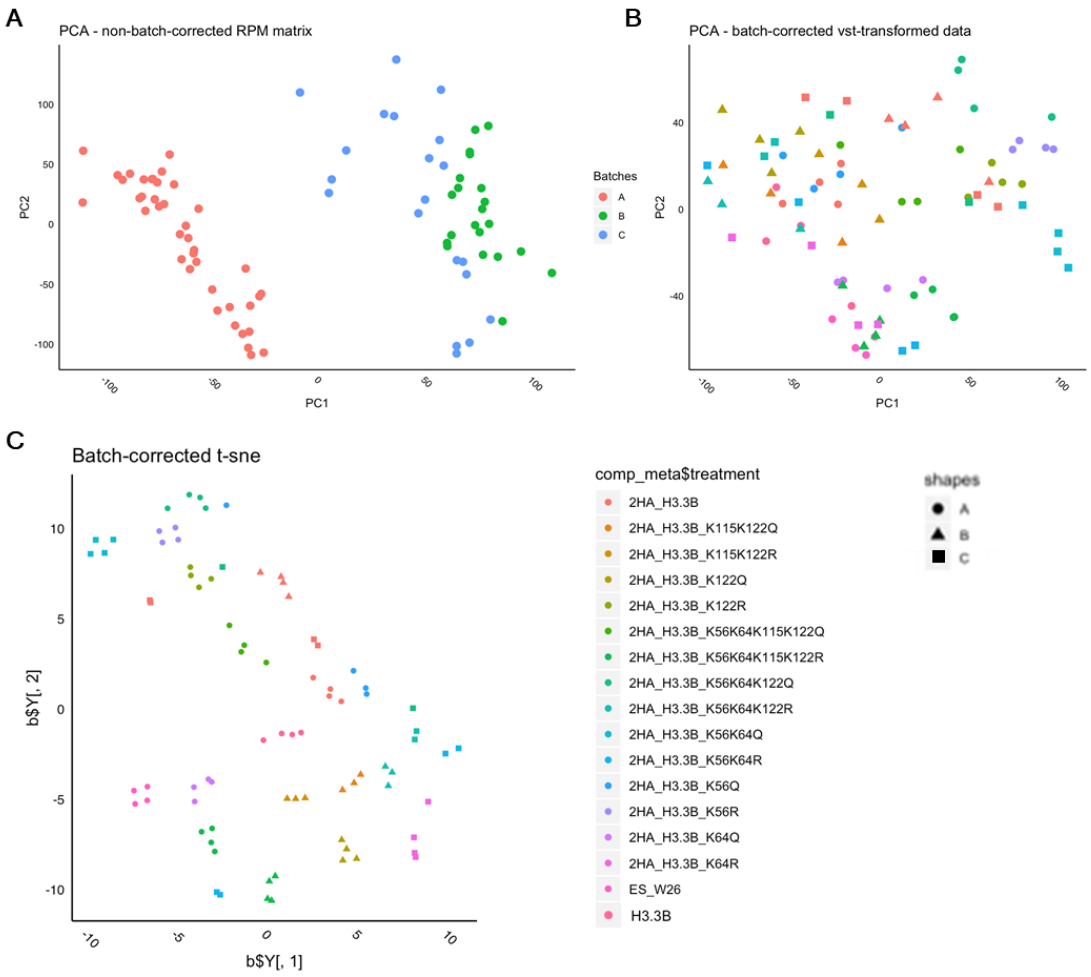

Figure 5.31 - Batch effect and batch effect correction

Total RNA was extracted and purified from mutant mES cell lines and total RNA-seq performed. **A** PCA computed on the non-batch corrected read *per* million (RPM) matrix. **B** PCA computed on the batch-corrected vst-transformed (DESeq2) data. **C** t-sne computed on the batch-corrected vst-transformed (DESeq2) matrix.

Due to experimental reasons, the samples were prepared and sequenced in three separate batches. During preliminary quality control analysis, the presence of a considerable batch effect became very apparent (figure 5.31A). We identified the main cause of this batch effect as being due to high variability in genes overlapping ribosomal RNA (rRNA) or major satellites and in small non-coding RNAs. Therefore, we removed these RNA classes from the analysis. In addition, the batches were corrected with Limma's removeBatchEffect tool. Although, these steps resulted in loss of batch-

clustering, as intended, they also led to an apparently loss of clustering among replicates on principal component analysis (PCA; figure 5.31B). We hypothesized this was normal and simply reflected the complexity of the dataset and the multitude of sample classes. In fact, upon computing the batch corrected results on t-sne, a non-linear dimensionality reduction method, the sample replicates clustered as expected together (figure 5.31C).

5.2.2.1.1 The effects of the different mutant cell lines in gene transcription

Having corrected for batch effects, we next proceeded to assess how gene expression was affected in the mES cells expressing mutated H3.3. We first assessed the number of down- and up-regulated genes in each cell line compared to the WT control (figure 5.32). Surprisingly, the cell lines carrying multiple mimics were not more affected, in terms of number of genes, than the cell lines carrying a single unmodified or acetylation mimic.

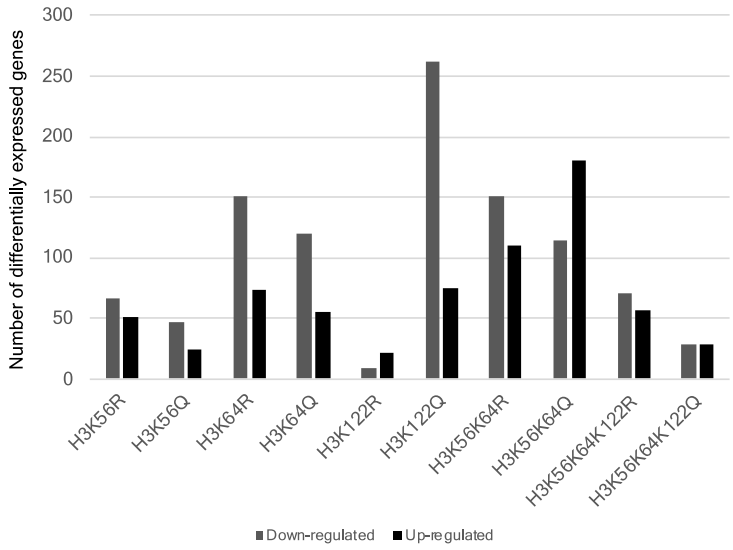

Figure 5.32 – Summary of differentially expressed genes

Differential gene expression analysis by DESeq2. Genes with a log2foldChange > +1/ -1 and an adjusted p value < 0.05 are plotted.

While differentially expressed genes were observed, we were not able to identify specific patterns regarding the number of genes affected nor specific groups of genes (e.g. GEO terms) that were up-/down-regulated in each un-modified/acetylated mimic pair, or *vice versa* (figure 5.33).

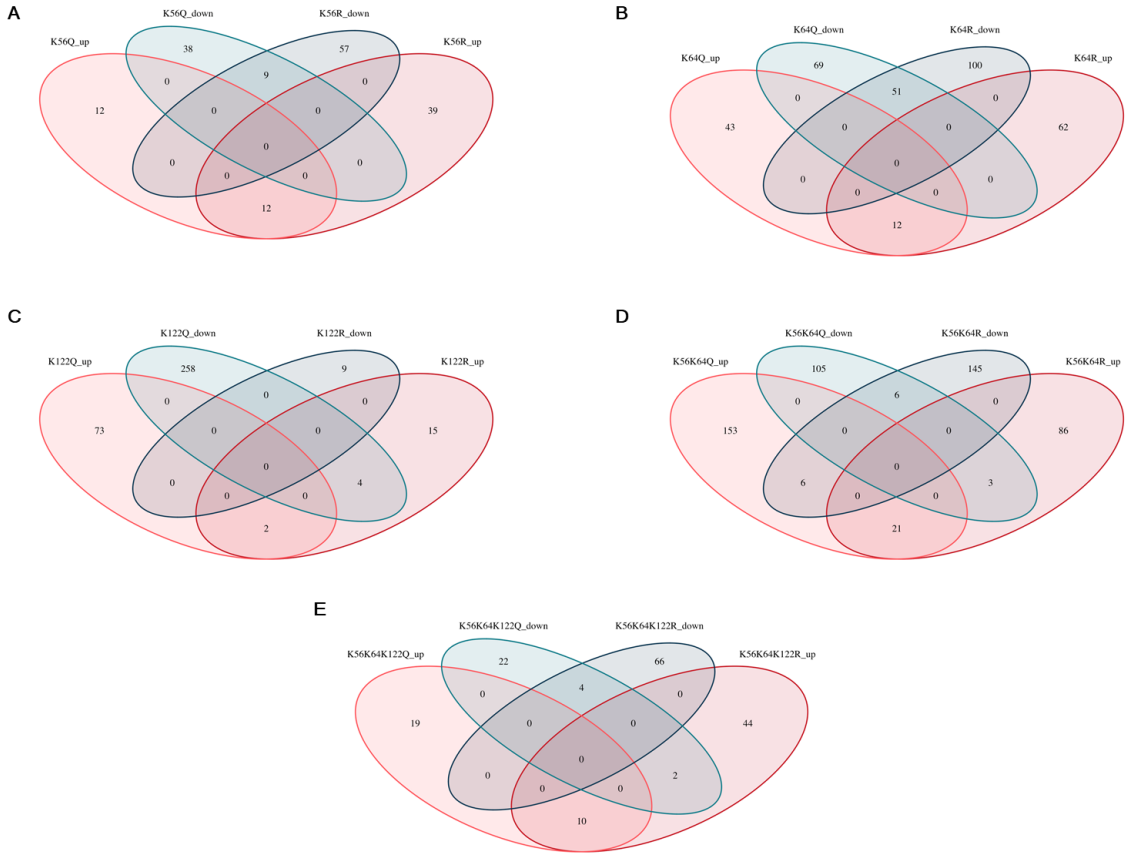

Figure 5.33 - Overlap between differentially expressed genes

Venn diagrams showing overlaps between differently expressed genes, comparing to 2HA.H3.3B, in the different mutant pairs: **A** H3K56R/Q; **B** H3K64R/Q; **C** H3K122R/Q; **D** H3K56K64R/Q and **E** H3K56K64K122R/Q.

5.2.2.1.2 The effects of the different H3.3 mutants on sharp and broad promoter genes

Mammalian gene promoters can be classified into sharp and broad depending on the spread of their TSS[115]. Sharp promoters contain a TATA box and are characterized for having a sharp and peaky TSS cluster at a strictly close distance to the TATA box[116]. Broad promoters are GC-rich and frequently

characterized by the absence of DNA methylation. It is estimated that approximately 70 % of all promoters correspond to broad promoters, making it the most common promoter type in vertebrates[117].It has been suggested that sharp and broad promoters are associated with different transcriptional regulatory elements and, therefore, regulated differently[118].

To define sharp and broad promoters we relied on a published Cap Analysis of Gene Expression (CAGE) dataset on mES cells to classify promoters into broad and sharp according to their interquartile width. Peaks of 10 or less bases were classified as sharp peaks, while peaks above 10 bases were deemed broad peaks. We compared the levels of H3.3 on sharp and broad promoters, using an available ChIP-seq dataset on mES cells (figure 5.34).

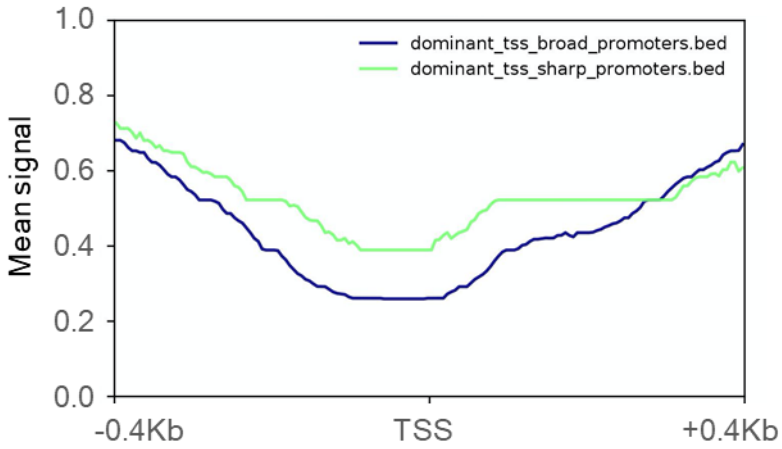

Figure 5.34 - Sharp promoters are enriched with H3.3

Metagene analysis of mES cells H3.3 ChIP-seq over broad and sharp promoters.

These results revealed that sharp promoters are comparatively enriched for H3.3, leading us to hypothesize that genes regulated by sharp and broad promoters could indeed be differently affected by the distinct modification mimics.

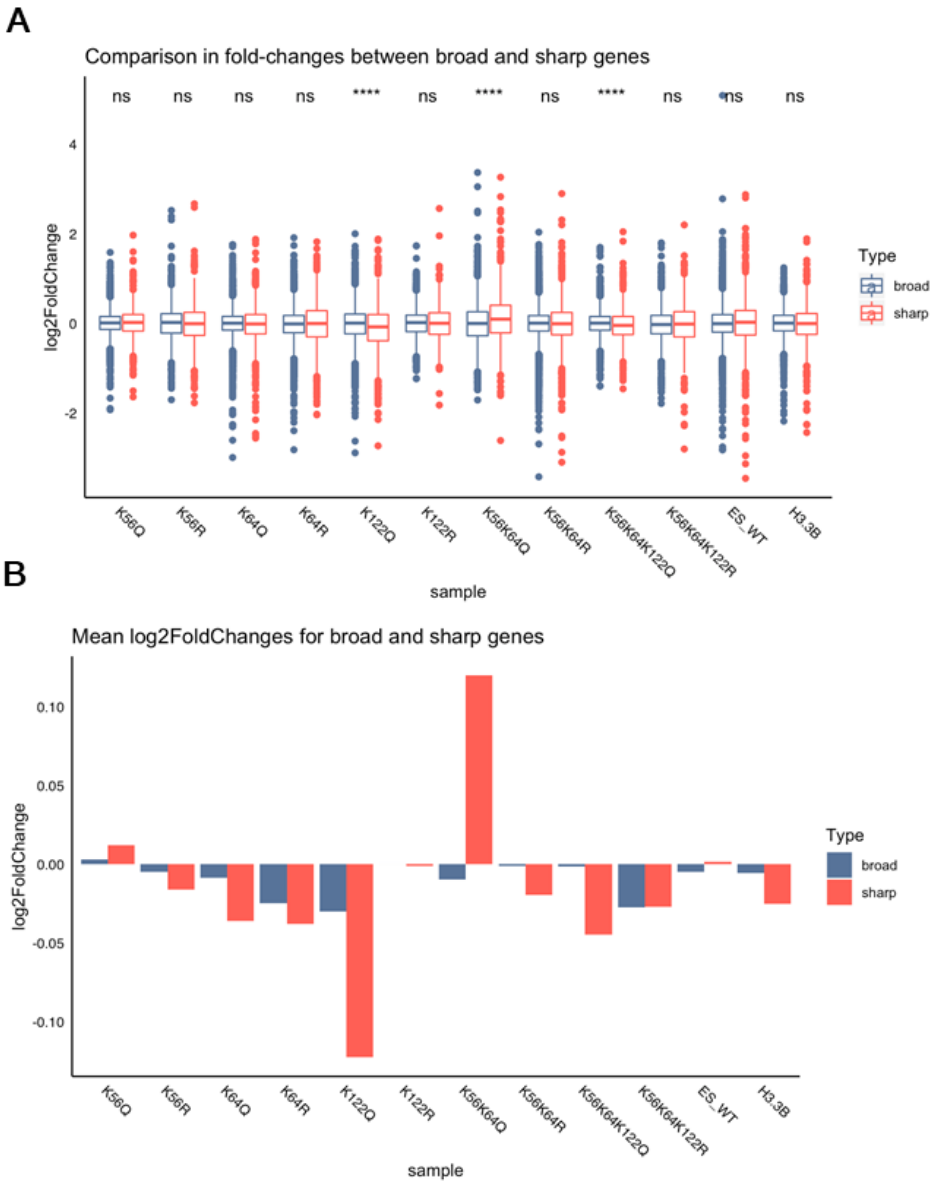

Figure 5.35 - Acetylation mimics show statistically different fold-change distributions between sharp and broad genes

A Distribution of fold-changes for sharp and broad promoter genes in the indicated mES cell mutants. **B** Mean logarithmic fold-changes for sharp and broad promoter genes in the different mES cell mutants.

We selected for each cell line the differently expressed genes compared to the control line, divided them into broad and sharp genes and we compared the differently expressed sharp and broad genes within each cell line (figure 5.35). For the classification of genes into broad and sharp, we took in consideration their major and most highly expressed promoter.

For the majority of the cell lines, genes regulated by sharp promoters were more differently expressed. In particular, acetylation mimics presented a significantly higher fold change at sharp genes. Among the single modified mimics, the 2HA.H3.3K122Q cell line displayed statistically significant differences in fold changes in the expression of sharp compared to broad genes. Moreover, the two mutants mimicking multiple acetylations also presented statistically significant differences between the two types of genes. Interestingly, while in 2HA.H3.3K122Q and 2HA.H3.3K56K64K122Q sharp genes were, in general, downregulated compared to the control cell line, we observed the opposite for the cell expressing 2HA.H3.3K56K64Q. In fact, the effect of 2HA.H3.3K56K64K122Q on sharp promoters is approximately the addition of the effects of 2HA.H3.3K122Q and 2HA.H3.3K56K64Q, supporting the idea of an additive effect of three H3 core acetylations.

Together, these results suggest that the effect of lateral surface acetylations depends on the type of promoter. Further analysis will be needed to investigate the role of functional promoter elements in more detail.

5.2.2.2 Gene induction assays

Having characterized the general effects of the different mutants on steady-state RNA expression, next we were interested in understanding how the different cell lines affected gene activation in a dynamic system. For that purpose, we set up gene induction assays and followed the activation of three immediate-early (IE) response genes (*c-Fos*, *Egr-1* and *c-Myc*), all of which are regulated by sharp promoters[119-121].

For these experiments, cells were cultured, prior to induction, for 24 hours in the absence of fetal bovine serum (FBS). Gene induction was achieved by the re-

introduction of complete media (containing FBS at a final concentration of 15 %) supplemented by 100 nM of 12-O-tetradecanoylphorbol-13-acetate (TPA). TPA is a potent tumor promoter that stimulates the protein kinase C signal transduction pathway and is extensively used in research as a strong gene activator.

5.2.2.2.1 Gene induction assays: system validation

In order to confirm the enrichment of H3.3 on the promoters of the selected IE genes and, consequently, that differences on their expression levels are due to the different mutations, we performed crosslinked ChIP assays on the WT control. The cells used for this experiment were grown under standard 2i/ LIF conditions. One antibody targeting H3.3 and two antibodies targeting the HA tag were used. The enrichment of the tagged H3.3 was evaluated by quantitative PCR (qPCR) analysis (figure 5.36). The results confirmed that the promoters of *c-Fos*, *Egr-1* and *c-Myc* are indeed enriched for the tagged H3.3.

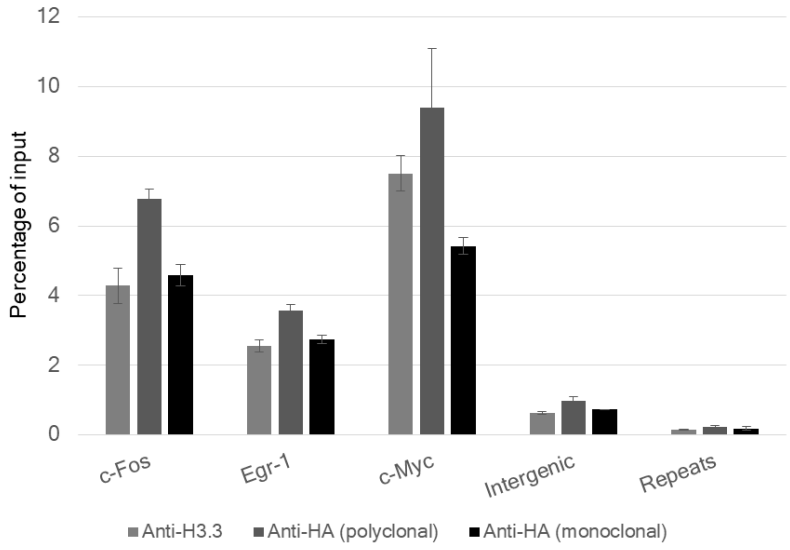

Figure 5.36 - The promoters of *c-Fos*, *Egr-1* and *c-Myc* are enriched by H3.3

Crosslinked ChIP assays were performed on chromatin extracted from the 2HA.H3.3B cell line. Three antibodies were used: an anti-H3.3, a polyclonal anti-HA and a monoclonal anti-HA. Enrichment for the tagged H3.3 at indicted gene promoters relative to input chromatin was assessed by qPCR. Two

heterochromatic regions (intergenic region chr5:79296560+79296687 and mariner repeats) were used as a negative control. Average and STD of two technical replicates are shown.

Having now shown that, under regular conditions, the promoters of the genes of interest are enriched by H3.3, next we wanted to confirm this enrichment was maintained during the induction assays. For this purpose, crosslink ChIP assays were performed on uninduced (T0), 50 minutes induced (T50) and 210 minutes induced (T210) 2HA.H3.3B cells (figure 5.37). The results revealed that not only the promoters of *c-Fos*, *Egr-1* and *c-Myc* continue to be enriched by the tagged H3.3, their enrichment increases throughout the induction.

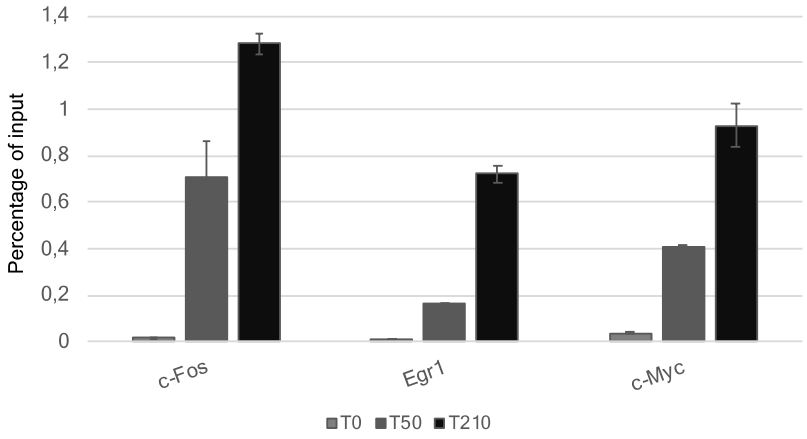

Figure 5.37 - The promoters of *c-Fos*, *Egr-1* and *c-Myc* are enriched by H3.3 during the induction assays
Crosslinked ChIP assays were performed on chromatin extracted from the 2HA.H3.3B cell line before (T0) and 50 (T50) and 210 minutes (T210) after gene induction. Immunoprecipitation was achieved using a polyclonal anti-HA antibody. Enrichment as percentage of input for the tagged H3.3 was assessed by qPCR. Average and STD of two technical replicates are shown.

Together these experiments confirm that induction of IE genes can indeed be used as a system to study the effects of H3.3 mutants on gene induction kinetics.

5.2.2.2.2 Gene induction assays on the mES cell lines

To investigate the effects that the different mimics of acetylated and unmodified lysine have during gene activation, we starved the cells from FBS for 24 hours and induced gene expression with 100 nM of TPA. Time points were collected before the induction (T0) and 20 (T20), 40 (T40), 50 (T50) and 150 minutes (T150) after induction. Each IE gene presented its own specific activation dynamics: *c-Fos* and *Egr-1* reached maximal mRNA expression around 1 hour after induction, while *c-Myc* showed a relatively slower activation dynamic.

During preliminary assays (data not shown), we noticed variations in the fold changes between experiments. To decrease these effects, we opted to carry out simultaneously the experiments on the cell line pair expressing the unmodified/acetylated mimic together with the control 2HA.H3.3B cell line. These gene expression assays are still on-going. Here we present two sets of first results: cell lines expressing the single mimic 2HA.H3.3K56R/Q and the triple mimic: 2HA.H3.3K56K64K122R/Q.

We performed TPA gene induction assays as previously described and quantified by qPCR the expression of *c-Fos*, *Egr-1* and *c-Myc* (figure 5.38). Interestingly, for all three genes the 2HA.H3.3K56Q cell line showed the highest levels of mRNA, confirming the role of H3K56 acetylation in gene activation. Likewise, for *c-Fos* and *Egr-1*, the mimic of an un-modified lysine had the lowest expression of all the three cell lines, highlighting the importance of H3K56ac during gene activation.

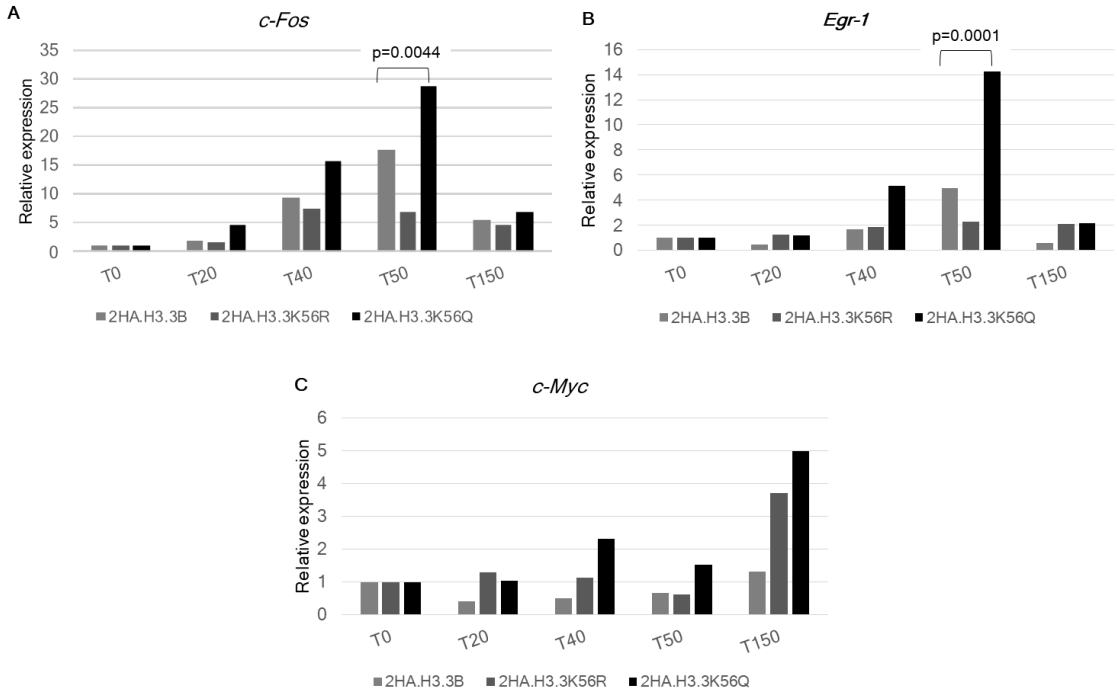

Figure 5.38 - Gene induction assays on 2HA.H3.3B and 2HA.H3.3K56R/Q pair mES cell lines

Cell lines were starved from FBS for 24hours before being induced with the re-introduction of FBS and supplementation with 100 nM of TPA. The levels of **A** *c-Fos*, **B** *Egr-1* and **C** *c-Myc* expression were quantified by qPCR. The results were normalized to the housekeeping gene *Hprt1*. Plotted is the relative expression normalized to T0. Average of two biological replicates is shown.

We repeated the experiments for the 2HA.H3.3K56K64K122R/Q pair (figure 5.39). Regarding *c-Fos*, the triple acetylation mimic expressing cell line showed the highest levels of gene activation, presenting an approximately 2-fold increase in expression compared to the control cell line and the unmodified mimic. In the case of *Egr-1*, the cell line expressing the acetylation mimic had significantly higher mRNA levels, while the unmodified mimic had the lowest. These results suggest that the acetylation of lysines 56, 64 and 122 on H3 plays a crucial role in the activation of both *c-Fos* and *Egr-1*, which was not the case for *c-Myc*, as the results revealed only slight differences between the cell lines.

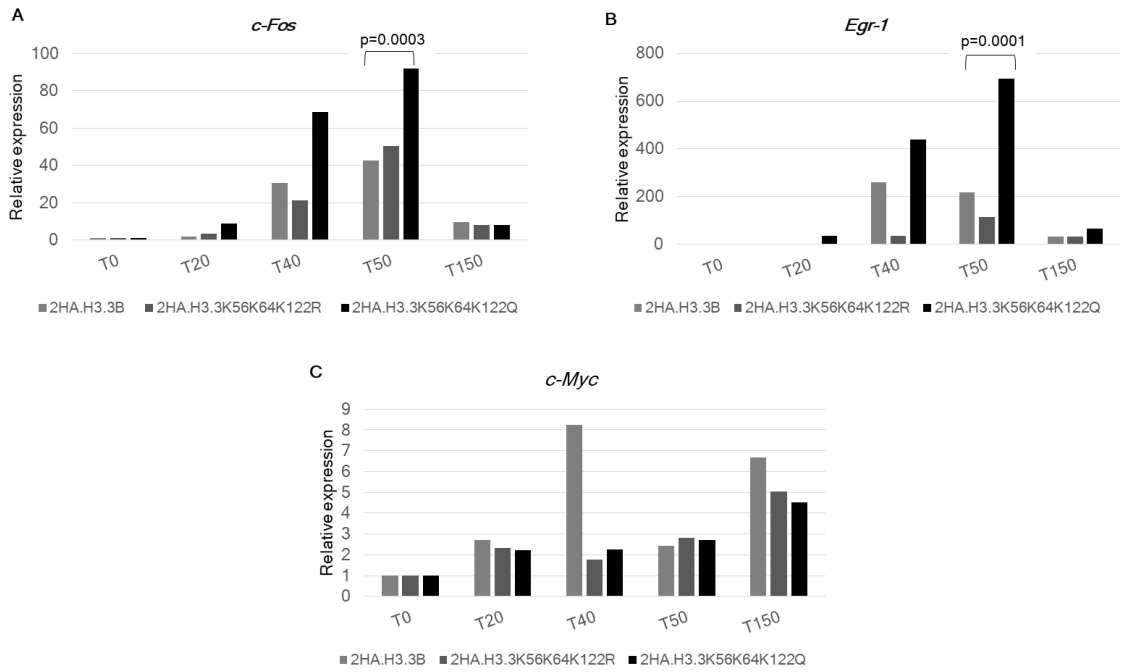

Figure 5.39 - Gene induction assays on 2HA.H3.3B and 2HA.H3.3K56K64K122R/Q pair mES cell lines
Cell lines were starved from FBS for 24hours before being induced with the re-introduction of FBS and supplementation with 100 nM of TPA. The levels of **A** *c-Fos*, **B** *Egr-1* and **C** *c-Myc* were quantified by qPCR. The results were normalized to the housekeeping gene *Hprt1*. Plotted is the relative expression normalized to T0. Average of two biological replicates is shown.

Interestingly, the triple acetylation mimic led to a relatively higher increase in the transcription of *c-Fos* (2.3- *versus* 1.6-fold) and *Egr1* (3.2- *versus* 2.8-fold) comparing to H3K56 acetylation mimic.

Altogether, the *in vivo* assays demonstrate the importance of these acetylations for correct gene expression. The RNA-seq allowed the identification of sharp genes as a subset of genes preferentially regulated by these H3 globular domain acetylations. Furthermore, the gene induction assays, revealed that these acetylations not only affect the steady state levels of gene transcription, but also modulate gene transcription activation dynamics.

6. Discussion

In the last decades many studies have been published on histone lysine acylations, mainly focused on the tails of histones. More recently acetylations in the globular domain of histones were described. These works highlight the importance of these modifications in chromatin regulation. However, despite the advancement of our comprehension on these modifications, several questions remain unanswered, including how specific histone PTMs regulate chromatin structure or influence its function and how specific combinations of such modifications influence one another.

For the purpose of this thesis, we aimed to investigate the so far poorly characterized H3K122succ and to study a possible synergism between three H3 core acetylations: H3K56ac, H3K64ac and H3K122ac.

6.1 Part 1 – H3K122succ

Although, the identification of H3K122succ was achieved almost a decade ago, only a single study characterizing its function in DNA repair had been published[66]. It remained, however, until now unclear what enzymes are setting or removing this PTM and what is its function in transcription.

6.1.1 H3K122succ associates with histone variant H3.3

H3 histone has several variants in mammals, including the canonical H3, which is distributed throughout the genome, and H3.3, a replacement histone variant that is for example associated with regulatory regions in euchromatin[92]. The enrichment of specific PTMs varies between histone variants, reflecting their specific chromatin distribution and function. H3.1, *per* instance, in enriched by

H3K9me1[122] whereas H3.3 has been shown to be enriched by H3K9ac and H3K4me3[123].

In order to have a first hint into the role of H3K122succ, we compared the levels of H3K122succ on H3.1 and H3.3. For this we relied on HEK293 cells ectopically expressing H3.1 or H3.3 carrying a HA/FLAG-tag. In both cell lines, the ectopic gene is under the control of the elongation factor 1 alpha promoter, resulting in the stable expression of the tagged H3 throughout the cell cycle. This continuous pattern of expression, mimics the normal H3.3 transcription pattern, but not the one of H3.1, which peaks during S-phase. Despite using a model that does not fully recreate the endogenous expression patterns of the two histone variants, our results, nevertheless strongly suggest that H3K122succ is enriched on H3.3 relative to H3.1, predicting that H3K122succ could be associated with active regulatory elements.

6.1.2 H3K122succ is enriched on active promoters in human MCF7 cells

Next, we mapped the distribution of H3K122succ throughout the genome in the human MCF7 cell line. The results revealed that approximately 50 % of the H3K122succ peaks locate near the TSS. These peaks presented a very particular distribution pattern, with a single H3K122succ peak centered on the TSS. As succinylation reverses the positive charge of the lysine side chain to a negative charge, it could disturb the interactions of histones with the DNA and therefore lead to the opening up of chromatin. The enrichment of H3K122succ is consistent with our previous results showing H3K122succ is enriched on the H3.3 variant. To further explore the idea of H3K122succ being associated with open chromatin regions, we compared H3K122succ to FAIRE-seq and DNase-

seq datasets. As expected, H3K122succ peaks shared a considerable overlap with open chromatin regions.

Next, to explore the association between H3K122succ and gene regulation we performed metagene analysis, which indicated H3K122succ is enriched at the TSS of active genes and tends to gradually decrease downstream of the TSS. H3K122succ accumulates at the highest quartile of expressed genes, suggesting that highly expressed genes require the establishment and maintenance of this mark to properly maintain an open chromatin environment and allow transcription.

Gene transcription is a highly complex process, which depends on the coordination of various factors, including histone PTMs[90]. A wide array of PTMs are established in a controlled and articulated manner allowing the orchestration of transcription[124,125]. Functional chromatin regions can be identified by their enrichment for histone PTMs. We found that H3K122succ enrichment co-localizes with H3K4me3, a reference mark for active promoters, in all annotated TSS.

Together, these results identify H3K122succ as an “active chromatin mark”, enriched at the TSS of active genes. They also lead us to speculate that the presence of H3K122succ could be associated with a role in enhancing DNA accessibility and nucleosome depletion, necessary for transcription.

6.1.3 p300/CBP act as H3K122 succinyltransferases

To identify the succinyltransferases responsible for the establishment of H3K122succ we used several approaches, including *in vivo* depletion of specific known HATs and *in vitro* assays. Consistently, our results identified p300/CBP as the main enzymes responsible for the establishment of H3K122succ.

p300 and CBP are two closely related HAT domain containing co-activators. They share a high structural homology[126] and can acetylate many common targets[127]. Due to their limited substrate selectivity, they can establish several histone acetylations, the majority of them located on H3 and H4[126]. Recently, p300 has been shown to establish other acylations, including lysine succinylation, propionylation and butyrylation[128,129]. However, while p300 acts as a robust acetyltransferase, it presents weaker activity on longer acyl-CoA side chains[129] suggesting a preference for ac-CoA.

The establishment of H3K122succ by p300 supports the notion of H3K122succ acting as an active mark. H3K122succ becomes the second modification, after H3K122ac, to be identified on lysine 122 of histone H3 that is established by p300/CBP. Both the acetylation and succinylation of H3K122 act as active marks of transcription and are enriched on active promoters[89]. These results tempt us to speculate that the establishment of one mark over the other on active promoter regions could be dependent on the availability of their respective acyl-donor groups, *e.g.* in specific separated chromatin domains.

6.1.4 SIRT5 and SIRT7 can desuccinylate H3K122succ

Until now, SIRT7 had been identified as the solely enzyme responsible for the removal of H3K122succ[66]. Our results, however, revealed, through *in vitro* and *in vivo* assays, that both SIRT5 and SIRT7 act as desuccinylases for H3K122succ.

It was previously reported that SIRT5 failed to remove H3K122succ from histones *in vitro* assays[66]. We, however, show that SIRT5 can consistently remove H3K122succ from peptides *in vitro* and desuccinylate H3K122succ *in vivo*. While, we cannot explain the discrepancy between our data and the data

collect previously, we are confident that the use of a *Sirt5*-KO cell line provides a more reliable method to assess enzymatic specificity *in vivo*.

SIRT7 is a nuclear protein, whereas SIRT5 is primarily a mitochondrial protein that can also be found in the cytosol and in the nucleus[130]. Both enzymes have been shown to act as desuccinylases *in vitro*[131]. SIRT5 has been previously shown to desuccinylate *in vitro* H2BK34succ[38], however to the best of our knowledge this is the first time that SIRT5 has been shown to act as a histone desuccinylase *in vivo*.

The existence of two enzymes capable of removing H3K122succ could suggest a redundancy of activity between SIRT5 and SIRT7. It is, however, feasibly to hypothesize that the removal of H3K122succ by one sirtuin over the other is associated with specific regulatory functions. Additional experiments would be necessary to address this hypothesis.

6.1.5 The role of H3K122succ in transcription

The involvement of H3K122succ in transcription regulation has been suggested by multiple indirect evidence. To directly assess its effect on transcription, we set up *in vitro* transcription assays (see figure 5.12).

6.1.5.1 Suc-CoA stimulates transcription *in vitro*

Gene transcription is largely associated with lysine acetylation[90]. While histones are the best described chromatin acetylation substrates, lysine acetylation is not restricted to them. In fact, a large variety of non-histones chromatin proteins have been shown to be acetylated by HAT enzymes, including the general transcription factor TFIIE and TFIIF[132,133]. For this reason, *in vitro* transcription

assays on chromatinized templates often include the addition of a recombinant HAT enzyme (in our case p300) together with ac-CoA.

Our results revealed that suc-CoA can stimulate transcription *in vitro* by 2-2.5-fold comparing to the no acyl-donor condition, an effect comparable to the one of ac-CoA. While these results cannot distinguish the role of histone succinylation from non-histone protein succinylation, they highlight the importance of this modification in transcription.

We had previously shown that lysine propionylation plays a role transcription activation and in a similar assay confirmed the role of this PTM in gene transcription[45]. Taken together, these two studies emphasize the importance of different acylations, besides acetylation, in biological processes such as transcription.

6.1.5.2 H3K122succ leads to increased transcription *in vitro*

In vitro transcription has been previously used to study histone lysine acetylation. Most studies relied on histone tail deletions to assess the influence acetylation of these residues have on transcription[127,134]. Multiple studies showed that H3/H4 tail acetylations are required for full p300-dependent transcriptional activation, highlighting the importance of H3/H4 tail acetylations[127,134]. More recently, a former student in our lab, Philipp Tropberger, used an amber suppression system to generate site-specifically acetylated chromatin. Interestingly, the acetylation of H3K18, a H3 tail modification enriched at active TSS, did not affect transcription *in vitro*. Whereas, the acetylation of H3K122 stimulated transcription *in vitro* by 1.6-fold comparing to recombinant WT chromatin[89].

Interestingly, both the acetylation and succinylation of H3K122 stimulate transcription *in vitro* to similar extents. H3K122 plays an important role in nucleosome stability, as this residue is in water-mediated contact with the nucleosomal DNA[6]. Acetylation of H3K122, has been shown to disrupt this contact and ultimately result on histone eviction from the nucleosome[36]. It is largely believed this is the main mechanism behind the role of H3K122ac in transcription. Since succinylation reversed the charge of the lysine's side chain, we hypothesized that, likewise, H3K122succ contributed to the destabilization of the nucleosome.

6.1.6 H3K122succ affects nucleosome stability *in vitro*

To assess the effects of H3K122succ on nucleosome stability we performed smFRET assays on WT and H3K122succ mono-nucleosomes. Our results revealed that the succinylation of H3K122 destabilizes nucleosomes, resulting in higher sensitivity to salt. Due to the position of H3K122, we speculate that the destabilization registered in these assays is due to the perturbation of the contact between the histone octamer and the DNA, resulting in chromatin opening and increased DNA accessibility to transcription factors.

H3K122succ becomes, therefore, the latest acylation in the globular domain of histones to be shown to directly modulate chromatin structure. Adding to the previously mentioned H3K122ac, H3K56ac and H3K64ac were shown to increase DNA breathing from the nucleosome and destabilize the nucleosome structure, respectively, by compromising the octamer-DNA interaction at the entry and exit sites of the nucleosomal DNA[42,91]. More recently, the succinylation of H2BK34 and the glutarylation of H4K91 have also been shown to cause nucleosomal destabilization[38,135]. Together, these studies emphasize

the importance of histone globular domain acylations in chromatin regulation via direct effects on nucleosome stability.

6.1.7 H3K122succ: Working model

Here we propose a model through which the succinylation of H3K122 contributes to the regulation of gene transcription (figure 6.1).

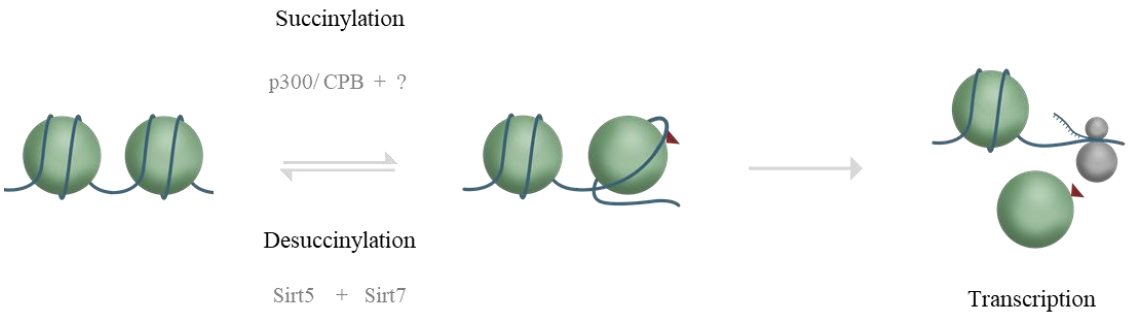

Figure 6.1 - Working model for H3K122succ
The establishment of H3K122succ by p300/CBP might favor an open chromatin state through nucleosome destabilization. Higher DNA accessibility facilitates the binding of transcriptional factors and, consequently, transcription. The desuccinylation of H3K122succ, by SIRT5 or SIRT7, results in nucleosome stabilization and chromatin compaction.

In our model, the establishment of H3K122succ by p300/CBP results in the destabilization of the nucleosome and possible displacement of the histone octamer from the DNA. Consequently, the DNA fiber is more accessible to protein binding. This process is particularly important at TSS, as it facilitates the binding of transcriptional factors resulting in transcriptional activation and maintenance of active transcription. Reversely, the desuccinylation of H3K122succ by SIRT5 or SIRT7 leads to increased chromatin stabilization and compaction, decreasing, therefore, DNA accessibility.

6.2 Part 2 – The role of histone globular domain acetylations in transcription

As our comprehension on individual histone PTMs has expanded, the existence of a crosstalk between histone modifications has become evident. One of the earliest identified examples regards H3S10phos and H3K14ac, where the phosphorylation of H3S10 stimulates the acetylation of H3K14 by GCN5[136]. Since then, several other examples of crosstalk between different epigenetic elements have been identified[137,138]. We were interested in extending this concept and investigate a possible crosstalk between histone globular domain modifications. For this purpose, we selected three H3 core acetylations (H3K56ac, H3K64ac and H3K122ac) which have been shown through different studies to share both regulatory and functional similarities.

6.2.1 H3 core globular domain acetylations stimulate transcription *in vitro*

The acetylations of H3K56, H3K64 and H3K122 have been individually correlated with active transcription in separate studies[36,37,78]. To characterize, under similar conditions, how the individual acetylations and combinations of these modifications affect transcription, we carried out *in vitro* transcription assays on differently modified chromatin.

6.2.1.1 All three globular domain acetylation stimulate transcription *in vitro*

In vitro, all three H3 globular domain acetylations led to the stimulation of transcription. Out of the single acetylated chromatin arrays, H3K122ac led to the strongest increase in transcription, followed by H3K64ac. H3K122ac is the only H3 globular domain acetylation to have been previously tested on *in vitro* transcription assays. While our results recapitulate what has been previously shown, in our system H3K122ac led to a higher stimulation of transcription

(approximately 2.8-fold in our assays *versus* the previously shown 1.6-fold[89]). We believe, supported by the evidence compiled during the validation of the *in vitro* assays, that the higher extent of the stimulation is due to differences in the assays, such as p300 concentration.

While different approaches have been used to characterize the direct effects that the acetylations of lysines 56, 64 and 122 on H3 have on the nucleosome stability, general conclusions can be taken from their comparison. H3K56ac has been shown to allow DNA-breathing from the histone octamers, increasing, therefore, DNA accessibility while maintaining the integrity of the nucleosome[42]. This is a milder effect than the one described for H3K64ac and H3K122ac, which have been shown to increase nucleosome instability and histone eviction respectively. In fact, in our assays, H3K56ac had the lowest effect on transcription. Regarding H3K64ac and H3K122ac, the use of different techniques does not allow the quantitative comparison of the effects these modifications have on the nucleosome. However, the *in vitro* transcription assays suggest that the destabilization of the histone octamer-DNA interactions at the dyad axis could have a stronger effect on nucleosome stability and, consequently, on transcription.

6.2.1.2 Combinations of H3 globular domain acetylations lead to higher stimulation of transcription *in vitro*

To explore a possible synergism in transcription between different H3 globular domain acetylations, we compared the effects of different combinations of two acetylations. Our results reveal that the two combinations including H3K122ac stimulate transcription the most, with both H3K56acK122ac and H3K64acK122ac increasing transcription by approximately 4.2-fold. These

results are consistent with the results we previously obtained, as H3K122ac-carrying chromatin led to the highest transcription increase among the individual acetylations tested.

A possible mechanism behind these results could lie on the position of these residues. While H3K56 and H3K64 are located near the entry and exit sites of the nucleosomal DNA, H3K122 is positioned near the dyad axis. Therefore, while H3K56acK64ac-carrying nucleosomes are, like their single acetylated counter parts, only destabilized at one nucleosomal region, nucleosomes containing H3K122ac, as well as, either H3K56ac and H3K64ac are destabilized at two important regions of the nucleosome.

Surprisingly, the triple acetylation of H3 at lysines 56, 64 and 122 did not lead to higher stimulation of transcription compared to the double acetylated chromatin. Additional experimental replicates would be needed to confirm these results, and if confirmed, mechanistic assays would be necessary to fully understand them, *e.g* by using different nucleosome positioning sequences.

6.2.2 The role of H3 core globular domain acetylations *in vivo*

To characterize the effects of H3K56acK64acK122ac *in vivo*, we generated mES cell lines with a single endogenous allele encoding for H3.3, which carried different mutations mimicking distinct unmodified and acetylated states. This model complemented the *in vitro* transcription assays as it provided a cellular model, allowing the characterization of these PTMs.

We created cell lines carrying either one or all three acetylation mimics, as well as their respective unmodified mimic. Additionally, a single combination of two unmodified/acetylated mimics, carrying H3K56 and H3K64, was prepared.

These two modifications were chosen as they are the only two residues known to be acetylated on H3 near the entry and exit site of the nucleosomal DNA.

6.2.2.1 H3 core globular domain acetylations regulate sharp-promoter genes *in vivo*

We performed total RNA-seq on the different mutant cell lines. While we did not affect global differences in gene expression patterns between the 2HA.H3.3 cell line and the cell lines expressing histone mutants, small, yet significant, changes were observed when we compared genes with broad and sharp TSS.

Mammalian Pol II-dependent promoters can be classified into two groups: sharp and broad promoters. Sharp promoters contain a TATA-box and are characterized for having a sharp and peaky TSS cluster at a strictly close distance to the TATA-box[116]. Broad promoters are GC-rich and frequently characterized by the absence of DNA methylation. It is estimated that approximately 70 % of all promoters correspond to broad promoters, making it the most common promoter type in vertebrates[117]. In general, sharp promoters are associated with tissue specific genes and broad promoters with constitutive expressed genes such as housekeeping genes[116]. Since the two types of promoters are associated with different types of regulation, we hypothesized that genes controlled by the two promoter types would be differently affected by the histone mimics.

Overall, the acetylation mimics presented a higher differential expression when comparing the fold changes of broad- and sharp-promoter genes. Interestingly, H3K122Q was the only cell line mimicking a single lysine acetylation that led to such significant fold changes between sharp and broad promoters. This cell line

mimics H3K122ac, the single acetylation that led to the highest increase in transcription on the *in vitro* transcription assays.

The H3K56K64Q expressing cell line also displayed significant fold change differences between broad and sharp genes, however, contrary to 2HA.H3K122Q where sharp genes were significantly downregulated, in 2HA.H3K56K64Q sharp genes were up-regulated.

The triple acetylation mimic also presented significant differences in the expression of genes with sharp and broad TSS. These results, again confirm the *in vitro* transcription assays.

Altogether, the RNA-seq results demonstrate that lateral surface acetylation can affect steady state transcription in cells also with relatively mild effects.

Taking in consideration these results, we decided to reconsider the viral promoter used in the *in vitro* transcription assays: the adenovirus major late promoter. This promoter contains a TATA-box[139], resembling a sharp promoter. It is tempting to suggest that the similarities between the *in vitro* transcription assays and the *in vivo* effects of the acetylation mimics on sharp promoter genes is, at least partially, due to regulatory similarities between the promoters and their regulation by histone globular domain acetylations.

6.2.2.2 H3 globular domain acetylations stimulate gene activation upon TPA induction

Since the effects of laterals surface acetylations on steady state transcription are relatively mild, we hypothesized that they might have a stronger effect in a dynamic gene expression system. We thus set up gene induction assays, in which we silenced and later induced the expression of genes using TPA. We selected three IE genes, which are responsive to this treatment and are all

regulated by sharp promoters. Although, these experiments are still ongoing and we cannot make conclusions regarding the extent of the effects on the different mutant, preliminary results confirm the importance of H3K56ac, H3K64ac and H3K122ac in gene activation. On the cell lines tested, the acetylation mimics were generally associated with higher mRNA expression levels upon induction, while the unmodified mimics were correlated with lower inductions. These results also suggest that the effects of the PTMs are not uniform throughout all genes, as some genes seem to be more affected than others by the mimics, *i.e.* *Egr-1* activation was highly affected by the 2HA.H3.3K56K64K122Q, which was not the case for *c-Myc*.

6.2.3 Model for the role of H3 globular domain acetylations in transcription

Histone acetylation is widely associated with open chromatin and transcriptional activation. In this study we explored the potential synergism between H3K56ac, H3K64ac and H3K122ac, which allowed us to propose, for the first time, a model for crosstalk between H3 globular domain modifications.

Individually the acetylations of H3K56, H3K64 and H3K122 are associated with open chromatin and are enriched at regulatory regions of active genes[37,89]. We propose a model in which these modifications are established at sharp promoters, increasing the accessibility of the TSS. The establishment of one or more of these acetylations will determine the overall destabilization of the nucleosome and, consequently, regulate the transcription level. Maximal transcription through maximal DNA accessibility could be obtained when the stability of the nucleosome is disrupted on different regions, such as the entry and exit sites of the nucleosomal DNA and the dyad axis (figure 6.2). Regarding the mild effect of H3K56acK64acK122ac on *in vitro* transcription, we

hypothesize it is due to the interference caused by these acetylations on chromatin assembly *in vitro*.

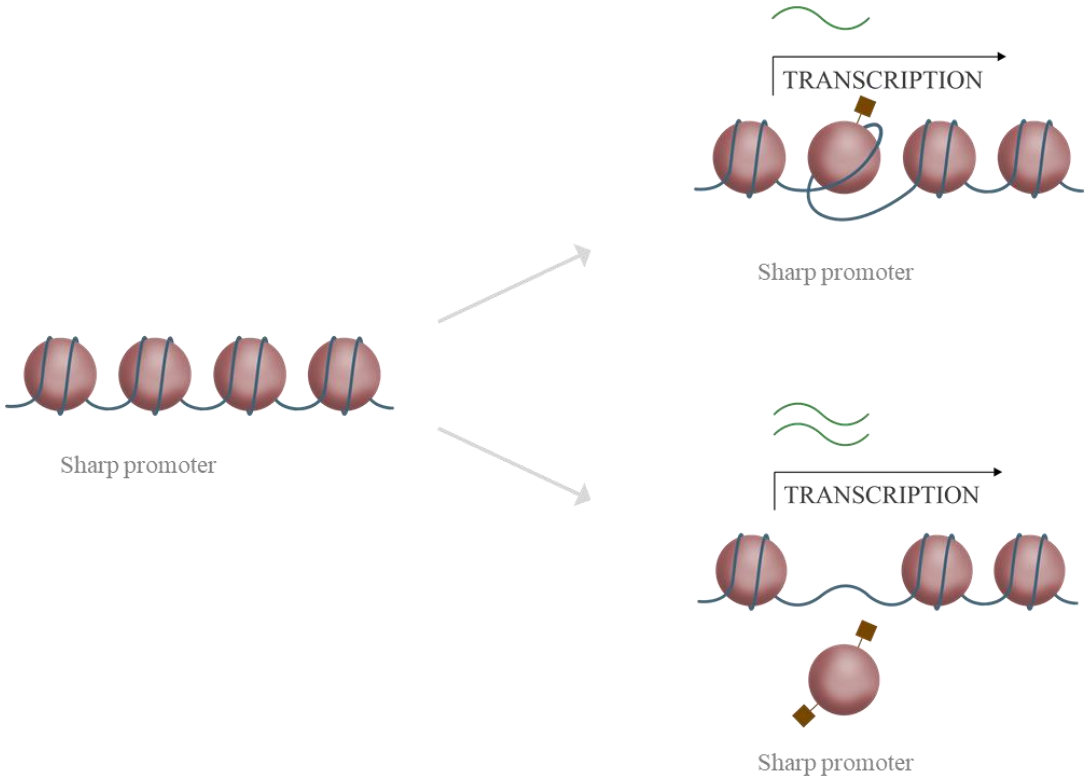

Figure 6.2 - Working model of the synergistic effects between H3 globular domain acetylations
The establishment of one acetylation at the globular domain of H3 of nucleosomes associated to sharp promoters leads to their destabilization, allowing transcription (top panel). The co-existence of more than one H3 globular domain acetylation leads to a more open chromatin structure and, therefore, higher transcription levels.

6.3 Conclusion

In the context of this thesis I carried out two projects, each tackling specific open questions. According to our results, we propose two models for the role of lateral surface acetylations and succinylation in transcription. In the first one, we suggest that H3K122succ plays a crucial role in the regulation of gene transcription, adding, therefore, a new modification to the *repertoire* of factors already known to regulate this process. In the future, it will be interesting to explore the function of H3K122succ when enriched in other regions. Our ChIP-seq data found that approximately 50 % of H3K122succ peaks are located near active TSS, it remains unanswered what are the functions of H3K122succ when it is not located at these regions (*e.g.* at enhancers). In the second project, we explored the synergism between three H3 globular domain acetylations and suggest an interplay between them in the regulation of gene transcription. Our future goal is to continue exploring the crosstalk between H3K56ac, H3K64ac and H3K122ac by systematically studying their effect on gene induction.

7. Materials

7.1 Peptides

Table 7.1 - Peptides

Peptide abbreviation	Company	Peptide sequence
H3K9ac	Genecust	TKQTAR-Kac-STGGKAGC
H3K18ac	IGBMC	GGKAPR-Kac-QLATKAGC
H3K27ac	IGBMC	ATKAAR-Kac-SAPATGC
H3K56ac	Biosynthan	IRRYQ-Kac-STELLIGGC
H3K64ac	Biosynthan	STELLIR-Kac-LPFQRLVGC
H3K115ac	IGBMC	CAIHA-Kac-RVTIMPK
H3K122un	IGBMC	CGGTIMP-K-DIQLA
H3K122succ	IGBMC	CGGVTIMP-Ksuc-DIQLA
H3K122ac	IGBMC	CGGTIMP-KAc-DIQLA
H3K122glut	IGBMC	CGGVTIMP-Kglut-DIQLAR-sre
H3K122crot	IGBMC	CGGVTIMP-Kcrot-DIQLAR-sre

7.2 Primers for ChIP-qPCR

Table 7.2 - Primers for ChIP-qPCR

Internal number	Name	5'-3' sequence
OL1548	m*c-Fos* F	CCAGATTGCTGGACAATGACCC
OL1549	m*c-Fos* R	GGAAAGGCAGAGAAGGCGAGC
OL1556	m*Egr-1* F	ATGGGAGGGCTTCACGTCACTCC
OL1557	m*Egr-1* R	AGTTCTGCGCGCTGGGATCTCTC
OL1560	m*c-Myc* F	CAGCCTTAGAGAGACGCCTG
OL1561	m*c-Myc* R	TGTGTTCTTGCCCTGCGTAT
OL439	mIntergenic F	GCTCCGGGTCCTATTCTTGT

OL440	mIntergenic R	TCTTGGTTTCCAGGAGATGC
OL605	mMariner repeats F	AGGCAGCAGAGCACAAATG
OL606	mMariner repeats R	TTGCTGTTAAGGGAATTGTGG

7.3 Primers for RT-qPCR

Table 7.3 - Primers for RT-qPCR

Internal number	Name	5'-3' sequence
OL157	m*Hprt1* F	GCTGGTGAAAAGGACCTCT
OL158	m*Hprt1* R	ACAGGACTAGAACACCTGC
OL1578	m*c-Fos* F	AGGGGCAAAGTAGAGCAGCTA
OL1579	m*c-Fos* R	CAGTCTGCTTTGTACGAGCCATGGTA
OL1588	m*Egr-1* F	TATGAGCACCTGACCACAGAG
OL1589	m*Egr-1* R	GCTGGGATAACTCGTCTCCA
OL1592	m*c-Myc* F	GCTCTCCATCCTATGTTGCGG
OL1593	m*c-Myc* R	TCCAAGTAACTCGGTCATCATC

7.4 Primers for cloning and mutagenesis

Table 7.4 - Primers for cloning and mutagenesis

Internal number	Name	5'-3' sequence
OL1153	H3K56amber F	GCCGCTACCAGTAGTCCACCGAGCT
OL1154	H3K56amber R	AGCTCGGTGGACTACTGGTAGCGGC
OL1640	H3K64amber F	TCCACCGAGCTGCTCATCCGCTAGCTG CCTTTCCAGC
OL1641	H3K64amber R	GACCAGGCGCTGGAAAGGCAGCTAGC GGATGAGCAGC
OL1142	H3K122amber F	CATCATGCCCTAGGACATCCAGC
OL1143	H3K122amber R	GCTGGATGTCCTAGGGCATGATG

OL1888	H3K56amberK64amber F	CCGCTACCAGTAGTCCACCGAGCTGCT CATCCGCTAGCTGCCTTTCC
OL1889	H3K56amberK64amber R	GGAAAGGCAGCTAGCGGATGAGCAGCT CGGTGGACTACTGGTAGCGG
OL2294	L11C F	ATAGGATCCATGACCAAGACCCC
OL2295	L11C R	GTGGATCCTACCTTAGTCCTCCA
OL2292	T7 BamHI	CTGGATCCCGCGAAATTAATAC
OL2293	Terminator BamHI	CTGGATCCCAAAAAACCCCTCA
OL2296	tRNA optimization_A F	CTAGATCTGGAAACGTGATCATGTAG
OL2297	tRNA optimization_A R	CGTTACAAGTATTACACAAAG
OL2298	tRNA optimization_B F	ATCCGTTCAGTGGGGTTAGATTCC
OL2299	tRNA optimization_B R	TTAGAGTCCATTCGATCTAC
OL2300	tRNA optimization_C F	TTAGATTCCCCACGTTTCCGCCCAACTA GTATC
OL2301	tRNA optimization_C R	CCCCACTGAACGGATTTA
OL2302	Trc F_Gibson	AGTTTTTCTAATCAGAATTGGTTAATTGG TTGTAACACTGTTGACAATTAATCATCC GGCTCGTATAATGAGGAATCCCATATGA TGGATAAAAAACCGCTGGATGTGCT
OL2303	Trc R_Gibson	AGCACATCCAGCGGTTTTTTATCCATCA TATGGGATTCCTCATTATACGAGCCGGA TGATTAATTGTCAACAGTGTTACAACCA ATTAACCAATTCTGATTAGAAAAACT
OL2304	pET447 F_Gibson	AGGAATCCCATATGATGGATAAAAAACC
OL2305	pET447 R_Gibson	CAGTGTTACAACCAATTAACCAATTCTG AT

7.5 Plasmids

Table 7.5 - Plasmids

Internal number	Vector	Origin
PL1527	pG5-MLP	Dr. Raphael Margueron
pET395	pET15b GAL4-VP16	Dr. Raphael Margueron
pET393	pAcKRS-3	Dr. Jason Chin

pET380	pCDF PylT-1 H3	Dr. Jason Chin
pET448	pAcKRS-3 with Trc promoter + L11C	Self-made
pET392	pCDF PylT-1 H3K56amber	Self-made
pET420	pCDF PylT-1 H3K64amber	Self-made
pET382	pCDF PylT-1 H3K122amber	Self-made
pET444	pCDF PylT-1 H3K56amberK64amber	Self-made
pET445	pCDF PylT-1 H3K56amberK122amber	Self-made
pET446	pCDF PylT-1 H3K64amberK122amber	Self-made
pET433	pCDF PylT-1 H3K56amberK64amberK122amber	Self-made
PL1644	pFastBac1 Acf1-FLAG	Dr Peter Becker
PL1645	pFastBac1 ISWI-FLAG	Dr Peter Becker

7.6 Antibodies

Table 7.6 - Antibodies

Internal number	Antigen	Species	Company	Catalogue number
369	H3K122succ	Rabbit	PTM Biolabs	PTM-413
	H3K122succ	Rabbit	In house	
	H3K122succ	Rabbit	In house	
	H3K122succ	Rabbit	In house	
365	H3K56ac	Rabbit	Active Motif	39281
241	H3K64ac	Rabbit	Active Motif	39545
369	H3K122ac	Rabbit	In house	PTM-413
31	H3.3	Rabbit	Abcam	Ab4263
110	HA-tag	Mouse	Roche	11583816001
112	HA-tag	Rabbit	Abcam	ab9110

7.7 Chemicals

Table 7.7 - Chemicals

Name	Source or Specification
2-[4-(2-hydroxyethyl)piperazin-1-yl]ethanesulfonic acid (HEPES)	Roth, Karlsruhe, Germany
4-(2-Aminoethyl)benzolsulfonylfluorid (AEBSF)	Sigma-Aldrich, St. Louis, USA
Acetic acid	VWR, Ismaning, Germany
Acrylamide 40 %	SERVA Electrophoresis, Heidelberg, Germany
Agarose	Roth, Karlsruhe, Germany
Ammonium sulfate	VWR, Ismaning, Germany
Ammonium chloride	Roth, Karlsruhe, Germany
Ammonium persulfate (APS)	Roth, Karlsruhe, Germany
Ampicillin (1000x stock at 50 mg/mL)	Roth, Karlsruhe, Germany
Beta-mercaptoethanol (ß-mercaptoethanol)	Roth, Karlsruhe, Germany
Bradford reagent	Roth, Karlsruhe, Germany
Bromophenol blue	Sigma-Aldrich, St. Louis, USA
Calcium chloride ($CaCl_2$)	Merck, Darmstadt, Germany
Cesium chloride (CsCl)	Sigma-Aldrich, St. Louis, USA
Charcoal activated	VWR, Ismaning, Germany
CHIR 99021	Axon Biochemicals BV, Groningen, the Netherlands
Colloidal coomassie stock	Roth, Karlsruhe, Germany
cOmplete™ EDTA-free protease inhibitor cocktail	Roche, Basel, Switzerland
Coomassie brilliant blue	Roth, Karlsruhe, Germany
Cysteine-HCl	Roth, Karlsruhe, Germany
Dextran T70	Sigma-Aldrich, St. Louis, USA
Di-potassium hydrogen phosphate (HK_2O_4P)	Roth, Karlsruhe, Germany
Di-sodium hydrogen phosphate (Na_2HPO_4)	Roth, Karlsruhe, Germany

Dimethyl sulfoxide (DMSO)	Roth, Karlsruhe, Germany
Dithiothreitol (DTT)	Applichem, Darmstadt, Germany
Dynabeads®	Thermo Fisher Scientific, Waltham, USA
Ethylenediaminetetraacetic acid (EDTA)	Roth, Karlsruhe, Germany
Ethanol (EtOH) 100 %	Roth, Karlsruhe, Germany
Ethidium bromide (EtBr)	Roth, Karlsruhe, Germany
Formaldehyde 37 %	Sigma-Aldrich, St. Louis, USA
Glycerol	Roth, Karlsruhe, Germany
Hydrochloric acid (HCl)	Roth, Karlsruhe, Germany
NP40	Sigma-Aldrich, St. Louis, USA
IGEPAL CA-630®	Sigma-Aldrich, St. Louis, USA
Imidazole	Roth, Karlsruhe, Germany
Isopropyl β-d-1-thiogalactopyranoside (IPTG)	Roth, Karlsruhe, Germany
Isoamylalcohol	Roth, Karlsruhe, Germany
Isopropanol	VWR, Ismaning, Germany
Kanamycin (1000x stock at 30 mg/mL)	Roth, Karlsruhe, Germany
Leukemia inhibitory factor (LIF)	IGBMC, Strasbourg, France
Magnesium chloride ($MgCl_2$)	Roth, Karlsruhe, Germany
Nicotinamide (Nam)	Alfa Aesar, Haverhill, USA
Nε-acetyllysine (KAc)	Bachem, Bubendorf, Switzerland
PD 0325901	Axon Biochemicals BV, Groningen, the Netherlands
Pfu polymerase	Thermo Fisher Scientific, Waltham, USA
Ponceau Red S	Sigma-Aldrich, St. Louis, USA
Potassium chloride (KCl)	Roth, Karlsruhe, Germany
Potassium di-hydrogen phosphate (KH_2PO_4)	Roth, Karlsruhe, Germany
RNase A	Applichem, Darmstadt, Germany

RNasin® Ribonuclease Inhibitors	Promega, Madison, USA
Sodium acetate (CH_3COONa)	Roth, Karlsruhe, Germany
Sodium azide (NaN_3)	Roth, Karlsruhe, Germany
Sodium bicarbonate ($NaHCO_3$)	Roth, Karlsruhe, Germany
Sodium Butyrate (NaBU)	Alfa Aesar, Haverhill, USA
Sodium chloride (NaCl)	Roth, Karlsruhe, Germany
Sodium dihydrogen phosphate (NaH_3PO_4)	Roth, Karlsruhe, Germany
Sodium dodecyl sulfate (SDS)	Roth, Karlsruhe, Germany
Sodium hydroxide (NaOH)	Roth, Karlsruhe, Germany
Sodium Thiosulfate ($Na_2S_2O_3$)	Sigma-Aldrich, St. Louis, USA
Spectinomycin (1000x stock at 50 mg/mL)	Roth, Karlsruhe, Germany
Sucrose	Roth, Karlsruhe, Germany
Tetramethylethylenediamine (TEMED)	Roth, Karlsruhe, Germany
Tricine	Roth, Karlsruhe, Germany
Tris-Base	Sigma-Aldrich, St. Louis, USA
Tris-HCl	Sigma-Aldrich, St. Louis, USA
Trition X-100	Roth, Karlsruhe, Germany
Tween-20	Sigma-Aldrich, St. Louis, USA
Urea	Sigma-Aldrich, St. Louis, USA

7.8 Buffers

Table 7.8 - Buffers

Name	Composition
1x Phosphate-Buffered Saline (PBS)	10 mM Na_2HPO_4 2 mM KH_2PO_4 2.7 mM KCl 137 mM NaCl (adjust to pH 7.2)

1x Reconstitution Buffer	10 mM Tris-HCl (pH 7.5) 0.5 mM EDTA 2 M NaCl
1x Tris-Acetate-EDTA (TAE)	40 mM Tris-Acetate 1 mM EDTA
1x Tris-Borate-EDTA (TBE)	89 mM Tris-HCl 89 mM Boric acid 2 mM EDTA (pH 8.0)
1x Tris-Buffered Saline Tween (TBST)	150 mM NaCl 50 mM Tris-HCl pH 8 0,2 % Tween-20
1x Tris-EDTA (TE)	10 mM Tris-HCl (pH 8.0) 1 mM EDTA (pH 8.0)
4x Laemmli sample loading buffer	250 mM Tris-HCl (pH 6.8) 20 % ß-mercaptoethanol 2 % SDS 0.1 % Bromphenol blue 40 % Glycerol
5X HAT buffer	25 % Glycerol 250 mM Tris-HCl (pH 8.0) 0.5 mM EDTA (pH 8.0) 740 mM NaCl 5 mM DTT
8x Phosphate buffer (GAL4-VP16 purification)	160 mM Sodium Phosphate 4 M NaCl
10x Glycine transfer buffer	247 mM Tris-HCl 1.9 M Glycine
10x SDS running buffer	247 mM Tris-HCl 1.9 M Glycine 0.5 % SDS
BC100	20 mM Tris-HCl (pH 7.9) 100 mM KCl 0.2 mM EDTA 20 % Glycerol
Buffer I (Native ChIP)	300 mM Sucrose 60 mM KCl 15 mM NaCl 5 mM $MgCl_2$ 0.1 mM EDTA (pH 8.0) 15 mM Tris-HCl (pH 7.5) 0.5 mM DTT 0.1 mM AEBSF 1x cOmplete™ EDTA-free protease inhibitor cocktail (5 mM NaBU) (5 mM Nam)
Buffer II (Native ChIP)	300 mMSucrose 60 mM KCl 15 mM NaCl 5 mM $MgCl_2$

	0.1 mM EDTA (pH 8.0) 15 mM Tris-HCl (pH 7.5) 0.5 mM DTT 0.1 mM AEBSF 0.4 % NP40 1x cOmplete™ EDTA-free protease inhibitor cocktail (5 mM NaBU) (5 mM Nam)
Buffer III (Native ChIP)	1.2 M Sucrose 60 mM KCl 15 mM NaCl 5 mM $MgCl_2$ 0.1 mM EDTA (pH 8.0) 15 mM Tris-HCl (pH 7.5) 0.5 mM DTT 0.1 mM AEBSF 1x cOmplete™ EDTA-free protease inhibitor cocktail (5 mM NaBU) (5 mM Nam)
Buffer A (Nuclear extracts preparation)	10 mM HEPES (pH 7.9) 1.5 mM $MgCl_2$ 10 mM KCl 0.5 mM DTT
Buffer B (p300 purification)	20 mM Tris-HCl (pH 7.5) 250 mM NaCl 0.1 % IGEPAL CA-630 30 mM Imidazole 1x cOmplete™ EDTA-free protease inhibitor cocktail
Buffer C (Nuclear extracts preparation)	20 mM HEPES (pH 7.9) 25 % (v/v) Glycerol 0.42 M NaCl 1.5 mM $MgCl_2$ 0.2 mM EDTA
Buffer D (Nuclear extracts preparation)	20 mM HEPES (pH 7.9) 20 % (v/v) Glycerol 0,1 M KCl 0.2 mM EDTA 0.5 mM DTT
ChIP incubation buffer (Native ChIP)	50 mM NaCl 50 mM Tris-HCl (pH 7.5) 0.1 mM AEBSF 5 mM EDTA (5 mM NaBU) (5 mM Nam)
Coomassie brilliant blue staining	2 % Coomassie brilliant blue 40 % EtOH 10 % Acetic acid
DB50 buffer	5 % glycerol 50 mM Hepes (pH 7.5) 50 mM KCl

	1 mM EDTA (pH 8.0)
DB200 buffer	5 % Glycerol 25 mM Hepes (pH 7.5) 200 mM KCl 1 mM EDTA (pH 8.0) 0,1 % NP40
Dialysis Buffer (NAP1 purification)	25 mM HEPES (pH 7.6) 1 mM EDTA 10 % (v/v) Glycerol 100 mM NaCl 0.01 % (v/v) NP40 10 mM ß -glycerophosphate 1 mM DTT 0.2 mM PMSF
Dialysis Buffer (Native ChIP)	0.2 mM EDTA (pH 8.0) 0.2 mM AEBSF 1 mM Tris-HCL (pH 7.5) (5 mM NaBU) (5 mM Nam)
Dilution Buffer (Crosslinked ChIP)	1 % Triton X-100 2 mM EDTA (pH 8.0) 150 mM NaCl 20mM Tris-HCl (pH8.0)
Elution Buffer (NAP1 purification)	50 mM Sodium phosphate (pH 7.6) 100 mM NaCl 480 mM Imidazole 15 % (v/v) Glycerol 0.01 % (v/v) NP40 10 mM ß -glycerophosphate 0.2 mM PMSF 0.5 mM benzamidine
Elution Buffer (Native ChIP)	50 mM Tris-HCl (pH 7.5) 50 mM NaCl 0.1 mM PMSF 5 mM EDTA (pH 8.0) 1 % SDS
Elution Buffer (p300 purification)	20 mM Tris-HCl (pH 7.5) 100 mM NaCl 0.1 % IGEPAL CA-630 250 mM Imidazole 10 % (v/v) Glycerol 1x cOmplete™ EDTA-free protease inhibitor cocktail
Elution Buffer (Crosslinked ChIP)	100 mM $NaHCO_3$ 1 % SDS
Final wash buffer (Crosslinked ChIP)	0.1 % SDS 0.5 % NP40 2 mM EDTA 500 mM NaCl 20 mM Tris-HCl (pH 8.0)

GAL4-VP16 storage buffer	20 mM Tris-HCl (pH 7.9) 20 % (v/v) Glycerol 100 mM KCl 1 mM DTT 0.2 mM EDTA
HEPES-EDTA-Glycerol (HEG) Buffer	25 mM HEPES (pH7.6) 0.1 mM EDTA 10 % Glycerol
Histone Wash Buffer	50 mM Tris-HCl (pH 7.5) 100 mM NaCl 1 mM EDTA (pH 8.0) 5 mM ß-mercaptoethanol (1 % Triton X-100)
Incubation buffer (Native ChIP)	50 mM Tris-HCl (pH 7.5) 75 mM NaCl 5 mM EDTA (pH 8.0) 0.1 % NP40
IPH	50 mM Tris (pH 8.0) 150 mM NaCl 0.5 % NP40 5 mM EDTA
L1 lysis buffer (Crosslinked ChIP)	50 mM Tris-HCl (pH 8.0) 2 mM EDTA (pH 8.0) 0.1 % NP40 10 % Glycerol
L2 lysis buffer (Crosslinked ChIP)	1 % SDS 10 mM EDTA 50 mM Tris-HCl (pH 8.0)
Lysis buffer (ACF purification)	20 mM Tris-HCl (pH 7.9) 500 mM NaCl 4 mM $MgCl_2$ 0.4 mM EDTA 2 mM DTT 20 mM ß-glycerophosphate 20 % (v/vl) Glycerol 0.4 mM PMSF 1 mM Benzamidine-HCl 4 µg/ mL Leupeptin 2 µg/ mL Aprotinin
Lysis buffer (NAP1 purification)	50 mM Sodium phosphate (pH 7.6) 500 mM NaCl 20 mM Imidazole 15 % (v/v) Glycerol 0.01 % (v/v) NP40 10 mM ß -glycerophosphate 0.2 mM PMSF 0.5 mM benzamidine
MNase digestion buffer (Native ChIP)	320 mM Sucrose 4 mM $MgCl_2$

	1 mM $CaCl_2$ 0.1 mM AEBSF 50 mM Tris-HCl (pH 7.5)
MNase Stop Buffer	1 % SDS 200 mM NaCl 20mM EDTA
NAP1 buffer	10 mM HEPES (pH 7.6) 1 mM KCl 1.5 mM $MgCl_2$ 0.5 mM EDTA 10 % (v/v) Glycerol 0.01 % (v/v) NP40 10 mM ß-glycerophosphate 1 mM DTT 0.2 mM PMSF
P10x	200 mM HEPES-KOH (pH 7.9) 80 mM $MgCl_2$
Ponceau S staining solution	0.5 % (w/v) Ponceau S 1 % Acetic acid
Reaction buffer (histone desuccinylation assay)	20 mM Tris-HCl (pH 7.5) 1 mM DTT
Refolding Buffer	10 mM Tris-HCl (pH 7.5) 1 mM EDTA (pH 8.0) 2 M NaCl 5 mM ß-mercaptoethanol
SAU200/600 Buffer	7 M Urea 20 mM CH_3COONa (pH 5.2) 200 mM/ 600 mM NaCl 1 mM EDTA (pH 8.0) 5 mM ß-mercaptoethanol
SDS running gel	6 to 18.7 % Acrylamide 375 mM Trip-HCl (pH 8.8) 0.1 % SDS
SDS stacking gel	5 % Acrylamide 125 mM Trip-HCl (pH 6.8) 0.1 % SDS
Sucrose gradient buffer	50 mM HEPES (pH 7.5) 50 mM KCl 1 mM EDTA (pH 8.0) 5-40 % (w/v) Sucrose
Triton extraction buffer (TEB)	0.5 % (v/v) Triton X-100 in 1x PBS 300 mM NaCl 2 mM AEBSF 1x cOmplete™ EDTA-free protease inhibitor cocktail (5 mM NaBU) (5 mM Nam)
Tubing preparation solution I	2 % (w/v) $NaHCO_3$ 1 mM EDTA (pH 8.0)
Tubing preparation solution II	1 mM EDTA (pH 8.0)

Unfolding Buffer	7 M Guanidium hydrochloride 20 mM Tris-HCl (pH 7.5) 10 mM DTT
Wash buffer (NAP1 purification)	50 mM Sodium phosphate (pH 7.6) 100 mM NaCl 20 mM Imidazole 15 % (v/v) Glycerol 0.01 % (v/v) NP40 10 mM ß-glycerophosphate 0.2 mM PMSF 0.5 mM benzamidine
Wash buffer (Crosslinked ChIP)	0.1 % SDS 0.5 % NP40 2 mM EDTA 150 mM NaCl 20 mM Tris-HCl (pH 8.0)
Wash buffer F (ACF purification)	20 mM Tris-HCl (pH 7.9) 150 mM NaCl 2 mM $MgCl_2$ 0.2 mM EDTA 1 mM DTT 10 mM ß-glycerophosphate 15 % (v/v) glycerol 0.01 % (v/v) NP40 0.2 mM PMSF 0.5 mM Benzamidine-HCl 2 µg/ mL Leupeptin 1 µg/ mL Aprotinin

7.9 Bacterial strains

Table 7.9 - Bacterial strains

Strains	Genotype	Origin
DH5alpha	F^- φ80lacZΔM15 Δ(lacZYA-argF)U169 recA1 endA1 hsdR17(r_K, m_K^+) phoA supE44 λ^- thi-1 gyrA96 relA1	Lab stock
z-competent BL-21 (DE3) – RIL strain (for protein expression), no endogenous resistance	*E.coli* B F- ompT hsdS(rB-mB-) dcm+ Tetr galλ (DE3) endA [argU ileY leuW CamR]	Stratagene
z-competent Rosetta Blue (DE3) pLysS (for protein expression),	endA1 hsdR17 (rK12-mK12) supE44 thi-1 recA1 gyrA96 relA1 lac (DE3) F'[proA+B+ lacI qZDM15::Tn10] LysSRARE	Novagen

Chloramphenicol resistant	(CamR,TetR)	
Jx33	E. coli MG1655 → MDS42 fhuACDB endA, deletion of 699 additional genes, ΔprfA::cat prfB::prfBf	Dr. Lei Wang
C321.ΔA	*E. coli* MG1655 Δ (ybhB-bioAB)::[lcl857 N(cro-ea59)::tetR-bla] ΔprfA ΔmutS::zeoR	Addgene

7.10 Mammalian cell lines

Table 7.10 - Mammalian cell lines

Name	Source or specification
MCF7	Dr. Kartiki Desai
MEFs	Dr. Yingming Zhao
MEFs *Sirt5*-KO	Dr. Yingming Zhao
Hela S3	Human cervix carcinoma derived (transformed by HPV18) immortalized
HEK293 H3.1-HA/FLAG	Stably transfected with pFP-N1H3.1
HEK293 H3.3-HA/FLAG	Stably transfected with pFP-N1 H3.3
mES cell line: ESW26	MPI Freiburg
mES cell line H3.3B	Cell lines were kindly provided by former laboratory members Dr. Nithyha Parameswaran Kalaivani and Dr. Sylvain Daujat (IGBMC, Strasbourg).
mES cell line 2HA.H3.3B	
mES cell line 2HA.H3.3K56R	
mES cell line 2HA.H3.3K64R	
mES cell line 2HA.H3.3K122R	
mES cell line 2HA.H3.3K56K64R	
mES cell line 2HA.H3.3K56K64K122R	
mES cell line 2HA.H3.3K56Q	
mES cell line 2HA.H3.3K64Q	
mES cell line 2HA.H3.3K122Q	

mES cell line 2HA.H3.3K56K64Q	
mES cell line 2HA.H3.3K56K64K122Q	

7.11 Baculovirus

Table 7.11 - Baculovirus

Protein expressed	Origin
His-p300	Dr. Raphael Margueron[140]
His-NAP1	Dr. Raphael Margueron[141]

8. Methods

8.1 Molecular biology methods

8.1.1 Polymerase Chain Reaction

For the amplification of DNA fragments from DNA templates, polymerase chain reactions (PCR) were carried out using sequence-specific oligonucleotide primers. Due to *Pfu* DNA polymerase (Agilent Technologies, USA) proofreading ability, it was the polymerase chosen for cloning, while the enhanced *Pfu* Turbo DNA polymerase (Agilent Technologies, USA) was the polymerase chosen for mutagenesis.

The components of a standard PCR reaction mix are indicated in table 8.1.

Table 8.1 - Standard PCR reaction mix

DNA template	10-100 ng
10x *Pfu* reaction buffer	5 µL
dNTPs	200 µM
Forward primer	200 nM
Reverse primer	200 nM
Polymerase *Pfu*	1 U
H2O	50 µL final volume

Table 8.2 contains the steps of a standard PCR reaction. For mutagenesis the first 2-4 cycles of the PCR were carried at a lower annealing temperature (approximately 4 °C bellow the annealing temperature used for the remaining cycles).

Table 8.2 - Standard PCR cycling parameters

Initial denaturation	95 °C	2 minutes	
Denaturation	95 °C	30 seconds	26-32 cycles
Annealing	55-60 °C	30 seconds	
Elongation	72 °C	1 minutes/ kb	
Final elongation	72 °C	5 minutes	
End	4 °C	hold	

8.1.2 Agarose gel electrophoresis

Samples were mixed with 5x DNA loading dye (Thermo Fisher Scientific, USA). Depending on the expected DNA fragment size, 0.8-2 % agarose gels in 1x TAE and 1x SYBR Safe DNA gel dye (Thermo Fisher Scientific, USA) were prepared. After size separation on gel, the results were analyzed under 254 nm UV light.

When necessary, the DNA fragment of interest was cut out of the gel and recovered employing the GenElute™ Gel Extraction Kit (Sigma-Aldrich, USA) according to the manufacturer's instructions.

8.1.3 Restriction endonucleases digestion

FastDigest restriction endonucleases (Thermo Fisher Scientific, USA) were used for restriction enzyme digestion of plasmids or DNA fragments. Plasmid DNA was simultaneously dephosphorylated with FastAP Thermosensitive Alkaline Phosphatase (Thermo Fisher Scientific, USA) according to manufacturer's instructions. After digestion, enzymes were heat inactivated accordingly.

8.1.4 Ligation

The digested DNA fragment was ligated into the digested and dephosphorylated DNA plasmid by T4 DNA ligase (Thermo Fisher Scientific, USA). In a typical reaction, DNA fragment and plasmid were mixed in a molar ratio between 3:1 to 5:1 and incubated in 1x ligase reaction buffer and 0.1 U of T4 DNA ligase O/N at 16 °C.

8.1.5 Gibson assembly® cloning

Gibson Assembly® is a restriction endonuclease digestion-independent cloning method, based on the presence of homologous overlapping ends on the DNA fragments and plasmid of interest. In short, the co-activity of three enzymes - a 5' exonuclease generates long overhangs, a polymerase fills in the gaps of the annealed single strand regions, and a DNA ligase seals the nicks of the annealed and filled-in gaps – allows the assembly of multiple DNA fragments in a short period of time[142].

A typical reaction for the ligation of two fragments is described on table 8.3.

Table 8.3 - Standard Gybson® assembly mix

DNA fragment	0.5 pmol
Linearized plasmid	0.1 pmol
Gibson Assembly® 2x Master Mix (New England Biolabs inc., USA)	10 µL
Deionized H_20	To 20 µL

The reaction mix was incubated for 15 minutes at 50 °C.

8.1.6 Heat shock transformation of *E. coli*

Competent *E. coli* were thawed on ice. *E. coli* (approximately 50 µL) were mixed with either 5 µL of ligation mixture or 20-100 ng of DNA plasmid. For the amber suppression system, 100 ng of each plasmid were mixed and added to the bacteria. Regarding the *E. coli* strain selection: DH5alpha were used for cloning and plasmid propagation, while BL21, Rosetta blue, Jx33 and C321.ΔA were used for protein expression. Bacteria were transformed by quickly applying heat shock at 42 °C for 90 seconds followed by 5 minutes on ice. Next, 1 mL of LB was added to the transformed *E. coli*, which were allowed to recover for 1 hour at 37 °C before being plated on an LB-agar plate supplemented with the appropriate antibiotics.

8.1.7 Purification of plasmid DNA from *E. coli*

Individual colonies from transformed *E. coli* were picked from LB-agar plates to inoculate LB media supplemented with the appropriate antibiotics. Plasmid DNA was purified with GenElute™ Plasmid Miniprep (Sigma-Aldrich, USA) or QIAGEN Plasmid Maxi Kit (Qiagen, Germany) according to manufacturer's instructions.

8.1.8 Cesium chloride gradient centrifugation of plasmid DNA for chromatin assembly

Chromatin assembly with NAP1 and ACF requires a very high level of DNA purity. For that purpose, after purifying the pG5-MLP plasmid with the QIAGEN Plasmid Maxi Kit (Qiagen, Germany) the plasmid was further purified on a cesium chloride (CsCl) gradient purification. CsCl forms a density gradient when

centrifuged at high g-forces, allowing the separation of intact plasmid DNA from nicked, linearized and genomic DNA and RNA.

500 µg of plasmid DNA were resuspended in 4.5 mL of TE buffer containing 4.4 g of CsCl at RT. In order to visualize the DNA, 400 µL of 1 mg/ mL EtBr in TE was added to the mix. The mix was transferred with a syringe into a Beckmann 13x51 mm polyallomer OptiSeal™ tube. All air bubbles were removed before the tubes were sealed and checked for leakage. Properly sealed tubes were fixed in a NVT90 rotor and centrifuged at 48000 rpm O/N at RT. After centrifugation, the tubes were collected and placed on a horizontal stand. The lower band, containing the supercoiled DNA, was recovered by puncturing the tube just below the band. The solution containing the supercoiled plasmid was transferred to a new tube. The EtBr was extracted by multiple washed with isopropanol saturated with CsCl. Once all remains of EtBr were removed, the plasmid DNA was precipitated with the addition of isopropanol (2x the sample volume) and centrifugation at 17000 xg for 20 minutes at 4 °C. The DNA pellet was washed with 70 % EtOH before being resuspended in 1x TE. Plasmid was aliquoted and stored at -20 °C.

8.1.9 RNA purification and Reverse Transcription from mammalian cells

Total RNA was extracted and purified from mammalian cells using the Quick-RNA Miniprep kit (Zymo Research, USA) according to the manufacturer's instructions. RNA concentration was measured on a Multiskan Go (ThermoFisher Scientific, USA). For reverse transcription 100 ng of total RNA were used *per* reaction. The RevertAid H Minus First Strand cDNA Synthesis Kit (ThermoFisher Scientific, USA) was used to synthesize complementary DNA (cDNA). A standard reverse transcription reaction is exemplified on table 8.4.

Table 8.4 - Standard reverse transcription reaction mix

5x Reaction buffer	4 µL
dNTP mix	2 µL
Oligo(dT) 18 Primer	1 µL
RiboLock RNase Inhibitor	1 µL
RevertAid H Minus Reverse Transcriptase	1 µL
RNA template	100 ng
Nuclease-free water	Up to 20 µL

The reaction components were mixed and incubated for 60 minutes at 42 °C, followed by 5 minutes at 70 °C.

8.1.10 Quantitative PCR

In order to quantify the concentration of specific DNA fragments, qPCRs were carried out. The components of a standard reaction mix are indicated in table 8.5.

Table 8.5 - Standard qPCR reaction mix

ABsolute™ Blue qPCR Mix, SYBR Green, ROX (Thermo Fisher Scientific, USA)	10 µL
Forward primer	250 nM
Reverse primer	250 nM
ChIP purified DNA or cDNA	2 µL

Table 8.6 contains the steps of a standard qPCR reaction.

Table 8.6 - Standard qPCR cycling parameters

			Acquisition	
Initial denaturation	95 °C	15 minutes	None	
Denaturation	95 °C	15 seconds	None	40 cycles
Annealing	60 °C	30 seconds	None	
Elongation	72 °C	30 seconds	Single	
Melting curve	60 °C	3 minutes	None	
	95 °C	1 second	Continuous	

8.2 Biochemical methods

8.2.1 Crosslinked ChIP

Cells were grown on 15 cm dishes until they reached 70-80 % confluency and directly crosslinked with formaldehyde (final concentration of 1 %). After 10 minutes of incubation at RT, the fixation was quenched with glycine (final concentration of 125 mM) for 5minutes on ice. The cells were washed twice with ice-cold PBS and collected by scrapping in PBS supplemented with cOmplete™ EDTA-free protease inhibitor cocktail and the appropriate HDAC inhibitors. All following steps were carried out on ice unless indicated otherwise. Cells were transferred to a new tube and centrifuged at 600 xg for 5 minutes at 4 °C. Cell pellet was resuspended in 1.2 mL/ 15 cm dish of L1 buffer with cOmplete™ EDTA-free protease inhibitor cocktail and the appropriate HDAC inhibitors and incubated on ice for 5 minutes. The samples were, then, centrifuged at 800 xg for 5 minutes at 4 °C. Pellet was resuspended in 1.2 mL/ 15 cm dish of L2 buffer with the appropriate HDAC inhibitors. Next, chromatin was fractionated by sonication of a Qsonica (80 % amplitude, 20 seconds ON, 20 seconds OFF, for a total time of 25 minutes). After sonication, the samples were transferred to 1.5

mL tubes and centrifuged at 14000 xg for 10 minutes at 4 °C. The supernatant, containing the chromatin, was transferred to a new 1.5 mL tube. Chromatin concentration was measured on a Multiskan Go (ThermoFisher Scientific, USA) and diluted with dilution buffer supplemented with the appropriate HDAC inhibitors to 150 ng/ µL. In order to control the sonication efficiency, 100 µL of diluted sample were mixed with 400 µL of L2 buffer and 20 µL of 5 M NaCl and incubated at 65 °C O/N. The remaining sample was stored on ice.

On the following day, the de-crosslinked aliquot was purified by phenol: chloroform, resuspended in 50 µL of TE buffer and analyzed by agarose gel electrophoresis (section 8.1.2).

For the pre-blocking of the beads, 500 µL of protein A agarose beads were mixed with 500 µL of protein G agarose beads (GE Healthcare, USA) in a 2 mL tube. The beads were washed three times with 1 mL of TE and incubated O/N at 4 °C with 100 µL of pre-boiled single stranded salmon sperm DNA (10 mg/ mL) and 100 µL of BSA (10 mg/ mL). On the following day, the beads were washed three times with 1mL of TE and stored as a 50 % slurry on TE.

After confirming the efficiency of the sonication, the sample was pre-cleared. For that purpose, for each immunoprecipitation (IP) 40 µg of chromatin were diluted in a total volume for 1 mL of dilution buffer supplemented with the appropriate HDAC inhibitors. The samples were incubated for 1 hour at 4 °C on a rotation wheel with 20 µL of pre-blocked agarose bead-slurry. After incubation the samples were centrifuges for 5 minutes at 1000xg and the pre-cleared supernatant transferred to new tubes. Antibodies were added to each IP and incubated O/N at 4 °C on a rotation wheel,

On the next day, 50 µL of pre-blocked bead-slurry were added to each IP and incubated for 3 hours at 4 °C on a rotation wheel. Next, the beads were washed

two times with 1 mL of washing buffer and one time in 50 % wash buffer: 50 % final wash buffer. After the last wash, the samples were resuspended in 150 µL of elution buffer and incubated for 10 minutes at RT on a rotation wheel. The samples were centrifuged for 1 minute at 4000 rpm. The supernatant was collected and this step was repeated one more time. The two supernatants were pooled together. To each sample 12 µL of 5 M NaCl and 1.56 µL of RNase A (10 mg/ mL) were added and the samples were incubated for 30 minutes at 37 °C. Next, 1 µL of proteinase K (20 mg/ mL) was added to each sample and incubated for 4-5 hours at 65 °C. DNA was purified with QIAquick PCR Purification Kit (Qiagen, Germany) according to the manufacturer's instructions.

8.2.2 Native ChIP

MCF7 ($5x10^7$-$5x10^8$ cells) were collected and washed with PBS. Cell pellet was resuspended in 4 mL of buffer I and divided into two tubes. Next, 2 mL of buffer II were added to each tube. Samples were gently mixed and incubated on ice for exactly 10 minutes. The samples were carefully layered on top of 8 mL of sucrose cushion and centrifuged in a swing-out rotor at 10000 xg for 20minutes at 4 °C. The supernatant was carefully removed and the pellets were resuspended in 1 mL of MNase digestion buffer. Chromatin was fractionated by MNase digestion (at a final concentration of 2 U/ mL) for 8-12 minutes at 37 °C. The digestion was stopped with the addition of 5 mM EDTA.

Soluble chromatin fractions were collected by centrifugation of digested chromatin at 10000 rpm for 10 minutes. The supernatant (S1) was collected, while the pellet was resuspended in the same volume of dialysis buffer and dialyzed overnight against dialysis buffer. On the next day the samples were

centrifuged as before and the supernatant was collected (S2). Both fractions underwent quality control on an agarose gel electrophoresis.

Per IP, 40 µg of digested chromatin (20 µg of S1 + 20 µg of S2) were diluted in 500 µL of ChIP incubation buffer. The input chromatin was pre-cleared by incubation with 5 µL of Dynabeads® mix (50 % protein A:50 % protein G) for 1 hour at 4 °C. The samples were then incubated O/N at 4 °C with different amounts of antibody. To each sample, 20 µL of 50 % protein A:50 % protein G Dynabeads® were added and incubated on a rotating wheel for 2-4 hours. The beads were washed three times with ChIP incubation buffer, before being eluted with 2x125 µL of elution buffer. The samples were then digested with RNase A for 30-45 minutes at 37 °C and then purified using the QIAquick PCR Purification Kit (Qiagen, Germany) according to the manufacturer's instructions.

8.2.3 Antibody purification

For the generation of anti-H3K122succ antibodies, rabbits were immunized with the H3K122succ according to the immunization protocol from BioGenes Gmbh (Germany). Specific antibodies were affinity purified from rabbit serum in a two-step purification protocol using SulfoLink™ Coupling Resin (Thermo Fisher Scientific, USA). In short 1 mL of rabbit serum was mixed with EDTA (final concentration of 5 mM) and centrifuged for 20 minutes at 10000 xg at 4 °C. The cleared supernatant was mixed with 20 µL of SulfoLink™ Coupling Resin coupled to H3K122succ peptides. The sample was incubated for 1 hour at RT on a rotation wheel. After the incubation, the beads were washed three times with 10 mL of TBS/ 5 mM EDTA. For elution of the antibodies, the beads were incubated with 100 µL of 0.1 M glycine (pH 2.5) for 5 minutes on a rotation

wheel. The sample was then centrifuged for 1 minute at 2000 xg and the supernatant was quickly transferred to a new tube on ice and neutralized with 3.5 µL of Tris-HCl (pH 9.5). The pH of the eluted antibodies was checked on a pH paper and adjusted to reach an approximate pH 8.0. The elution of the beads was repeated a total of two times. The two purified supernatants were pooled together and mixed with 20 µL of SulfoLink™ Coupling Resin coupled to H3K122glut peptides. The sample was incubated for 30 minutes at 4 °C on a rotation wheel. The beads were removed by centrifugation and the purified antibodies were dialyzed O/N at 4 °C against 1 L of PBS. After dialysis, sodium azide was added to the antibodies (at a final concentration of 0.05 %). The antibodies were stored at 4 °C.

8.2.4 SDS-PAGE electrophoresis

SDS-PAGE is an analytical method that allows the separation of proteins according to their molecular weight (MW). The percentage of acrylamide in the running gel varied between 6 and 18.7 % depending on the MW of the protein of interest. A stacking gel of 5 % polyacrylamide was overlaid on top of the running gel. The protein samples were boiled in 1x laemmli loading buffer for 5minutes at 95 °C before being loaded on the gel and electrophoresed in 1x SDS running buffer for 1-2 hours at 140-200 V depending on the percentage of the gel. After electrophoresis the proteins in the gel were either staining with coomassie brilliant blue or transferred to a nitrocellulose membrane.

8.2.5 Western Blot transfer

In order to detect specific proteins or protein PTMs by immunostaining, after SDS-PAGE electrophoresis the proteins were transferred from the SDS gel to a membrane. The transfer into membranes renders the antigen epitopes accessible for antibody recognition. The proteins were transferred from the gel to 0.45 µm pore size nitrocellulose membranes in 1x glycine transfer buffer. The exact conditions of the transfer depended on the MW and overall charge of the protein of interest. For the transfer of histones, the transfer was carried out for 20 minutes at 350 mA.

8.2.6 Immunostaining of western blots

After transfer, the nitrocellulose membranes were stained for 2-3 minutes with ponceau S in order to visualize the efficiency of the transfer and compare the relative amounts of proteins in the membrane. Nitrocellulose membranes were then blocked with 4 % BSA in 1x TBST for 1 hour at RT. After blocking, the membranes were incubated O/N at 4 °C in different amounts of antibodies in 1x TBST. On the following day, the membranes were washed three times in 1x TBST for 5 minutes each time before being incubated with the secondary antibody conjugated to horseradish peroxidase (HRP) in 4 % BSA in 1x TBST for 1 hour at RT. The membrane was washed twice with 1x TBST and once with TBS for 5 minutes each. After the last was the membrane was incubated with a Clarity or Clarity Max enhanced chemiluminescent (ECL) western blotting substrate (BioRad, USA).

8.2.7 Peptide immunoblotting

Peptide immunoblotting were carried out to test the specificity of the antibodies targeting specific histone PTMs. Serial dilutions of unmodified or differently modified chemically-synthesized peptides were spotted directly unto 0.1 µm pore size nitrocellulose membranes. Membranes were air-dried for a minimum of 30 minutes at RT, before being processed at described in 8.2.6.

8.2.8 Purification of native histones by acid extraction

Histones are proteins rich in basic amino acids and can, therefore, be purified from the majority of other nuclear proteins by acid extraction. Cells were harvested and the cell pellet was washed twice with ice-cold PBS. The cell pellet was resuspended in triton extraction buffer (TEB; final concentration of 10^7 cells/ mL). The cells were lysed for 10 minutes on ice and centrifuged for 10 minutes at 2000 rpm at 4 °C. The pellet was resuspended in TEB (half the volume used before) and centrifuged as previously described. The cell pellet was resuspended in 0.2 N of HCl (a quarter of the initial volume of TEB used) and incubated O/N at 4 °C on a rotational wheel. On the following day, the samples were centrifuged for 10 minutes at 10000 rpm at 4 °C. The supernatant containing the extracted histones was transferred to a new tube and aliquoted. The aliquots of the histone acidic extracts were stored at -20 °C.

8.2.9 Clipping of histone tails by limited trypsin digestion

Trypsin is a serine protease active on the carboxyl group of lysine and arginine residues. Under limiting digestion conditions, it is possible to selectively remove histone tails as they are rich in these two residues and are comparatively more exposed than the histone globular domains. In short, 20 µg of chromatin were

incubated with 0-5 µg of trypsin for 20 minutes at 26 °C. The reaction was stopped with the addition of laemmli loading buffer (at a final concentration of 1x).

8.2.10 Histone succinyltransferase assay

For the succinyltransferase assays on rOctamers, 1 µg of sample was incubated with 40 ng of p300 in the presence of suc-CoA O/N at 30 °C. The reaction products were separated by SDS-PAGE and analyzed by immunoblotting with an anti-H3K122succ antibody.

For the succinyltransferase assays on H3K122 peptides, the samples were incubated with p300 (0-160 ng) in the presence of [14C]suc-CoA for approximately 16 hours (O/N incubation) at 30 °C. The reactions were spotted on cellulose chromatography paper P81. Chromatography papers were washed three times with 10 % TFA before the incorporated radioactivity was measured by liquid scintillation counting.

8.2.11 Histone desuccinylation assay

For the *in vitro* desuccinylation assays, 1 µg of H3K122succ peptides were incubated with 0.5-1.8 µg of SIRT5 or SIRT7 in reaction buffer supplemented, or not, with NAD^+. After 3 hours at 37 °C, 2 µL of each reaction were spotted on 0.1 µM-pore nitrocellulose membrane and probed with an anti-H2K122succ antibody.

8.2.12 Expression of recombinant unmodified histones

Canonical WT recombinant histones – H2A, H2B, H3 and H4 – were expressed in and purified from *E. coli*. RosettaBlueTM(DE3)pLysS were transformed with

plasmid DNA and streaked out on plates containing ampicillin. A single colony was picked to inoculate 50 mL of LB supplemented with ampicillin and cultured O/N of at 37 °C. On the following day, 1 L of LB supplemented ampicillin was inoculated with 25 mL of O/N culture and grown at 37 °C until OD_{600} reached 0.4-0.5. The expression of histones was induced with IPTG (final concentration of 0.5 mM) and was continued for 3-3.5 hours at 37 °C. The bacteria were spun down at 5 minutes at 4000 xg and resuspended in 25 mL histone wash buffer without triton X-100 supplemented with cOmplete™ EDTA-free protease inhibitor cocktail. The samples were frozen at -80 °C until they were purified.

8.2.13 Expression of acetylated histones

For the expression of site-specifically acetylated histones, we optimized a previously described amber suppression system as described in section 5.2.1.1[42]. The final system used in this work consisted of four components in two separate plasmids, each containing different antibiotics resistance and origins of replication.

Acetylated H3 histones were expressed in BL21(DE3)pLysS cells. The bacteria were transformed with 100 ng of each plasmid and plated on LB-agar plates supplemented with the appropriate antibiotics (spectinomycin and kanamycin). A single colony was picked to inoculate 50 mL of LB, supplemented with spectinomycin and kanamycin, and grown O/N at 37 °C. On the following day, 2 L of pre-warmed supplemented LB were inoculated with 40 mL of O/N culture and grown at 37 °C until OD_{600} reached 0.7-0.8. Acetyl-lysine and nicotinamide were added to the culture (at final concentrations of 10 and 20 mM respectively) and the culture was transferred to 20 °C. After 30 minutes, IPTG (at a final concentration of 0.1 mM) was added to the cultures, which were incubated O/N

at 20 °C. The bacteria were spun down for 15 minutes at 4000 xg and resuspended in 25 mL histone wash buffer without triton X-100 supplemented with cOmplete™ EDTA-free protease inhibitor cocktail and Nam (final concentration of 20 mM). The samples were frozen at -80 °C until they were further purified.

8.2.14 Purification of recombinant histones

8.2.14.1 Inclusion body purification

Inclusion bodies containing WT and acetylated histones were purified following the same protocol, for the exception that during the purification of inclusion bodies containing acetylated histones all buffers were supplemented with Nam (at a final concentration of 20 mM). The frozen cell suspension was quickly thaw in a water bath at 37 °C. All further steps were carried out on ice, unless stated otherwise. Cell suspension was sonicated on a Branson sonicator for 1minute, 0.5 seconds ON and 0.5 seconds OFF, at 50 % amplitude for a total of three times. The lysate was centrifuged for 10 minutes at 17000 xg to pellet the inclusion bodies, the pellet was resuspended in histone wash buffer with 1 % triton X-100 (20 mL/ L of culture) and sonicated one time as previously described. These steps were repeated a total of four times: in the first two times the pellet was resuspended in histone wash buffer with 1 % triton X-100 and in the last two times in histone wash buffer without 1 % triton X-100. After the last wash, the inclusion body pellet was either stored at -80 °C or the histones were directly purified as described in 8.2.14.2 or 8.2.14.3.

8.2.14.2 Purification of WT histones from inclusion bodies

The inclusion body pellet was resuspended in unfolding buffer (10-20 mL/ L of culture) and unfolded for 1 hour at RT on a rotation wheel. After the incubation, the solution was centrifuged for 15 minutes at RT at 17000 xg. The supernatant was transferred to a new tube and centrifuged as before. The supernatant was dialyzed against three changes of 2 L of freshly prepared SAU200 at 4 °C, with the second dialysis step performed O/N and the first and third for 3 hours. After the last dialysis step, the precipitated material was removed by centrifugation for 20 minutes at 4 °C at 17000 xg. The cleared supernatant was loaded on a 6 mL Resource S cation exchange column (GE Healthcare, USA) pre-equilibrated with SAU200 and separated with a ÄKTA Prime FPLC in a 40 mL linear gradient from SAU200 to SAU600 – a gradient of 0 to 100 % was used for the purification of H2A, H2B and H3 and a gradient of 30 to 100 % was used for the purification of H4. Fractions of 500 µL were collected and the fractions associated with the peak were analyzed by SDS-PAGE followed by coomassie staining. The fractions containing the purified histone were pooled together and dialyzed against three changes of 2 L of distilled water supplemented with ß-mercaptoethanol (final concentration of 2 mM) at 4 °C, with the second dialysis step performed O/N and the first and third for 3 hours. Dialyzed histones were centrifuged for 20 minutes at 4 °C at 17000 xg. The concentration of the histones in the supernatant was quantified using the OD_{276} according to the equation from Luger *et al.* 1999: $\left[\frac{mg}{mL}\right] = \frac{\mathrm{OD276(sample)} - \mathrm{OD276(blank)}}{molar\ extinction\ coefficient\ (\varepsilon)} \times MW$. Molecular weight and molar extinction coefficients for each histone are listed in table 8.7. Histones were aliquoted into 1mg aliquots, lyophilized and stored at -80 °C.

Table 8.7 - Molecular weight and molar extinction coefficient of core human histones

Histone	Molecular weight	ε for cm/ M 276 nm
H2A	13960	4050
H2B	13774	6070
H3	15273	4040
H4	11236	5400

8.2.14.3 Purification of acetylated histones from inclusion bodies

For the purification of acetylated histones from inclusion bodies nicotinamide (at a final concentration of 20 mM) was added to all buffers. The inclusion body pellet was resuspended in unfolding buffer (10-20 mL/ L of culture) and unfolded for 1 hour at RT on a rotation wheel. After the incubation, the solution was centrifuged for 15 minutes at RT at 17000 xg. The supernatant was transferred to a new tube and centrifuged as before. The cleared supernatant was then filtered on a 0.45 µm pore size syringe filter. The sample were then loaded on a HiPrep 26/60 Sephacryl S-200 HR gel filtration column (GE Healthcare, USA) pre-equilibrate with freshly prepared SAU200. The sample was eluted with SAU200 buffer, while 5 mL fractions were being collected. The fractions associated with the peak were analyzed by SDS-PAGE followed by coomassie staining and the ones containing the purified histone were pooled together and loaded on a Resource S cation exchange column (GE Healthcare, USA) pre-equilibrated with SAU200. From this step onwards, the purification of the acetylated histones was carried out as previously described for the WT histones in section 8.2.14.2.

8.2.15 Refolding of histone octamers

For the refolding of histone octamers, the lyophilized core histones were resuspended in unfolding buffer, for a final concentration of 1mg/mL and incubated for 1 hour at RT on a rotation wheel. After unfolding the concentration of each core histone was measured by OD_{276} as described in table 8.7. Next, the molarity of each histone was calculated taking in consideration that 1 mg/ mL of solution corresponds to the following concentrations:

H2A 71.6 nmol/ mL

H2B 72.6 nmol/ mL

H3 65.5 nmol/ mL

H4 89 nmol/ mL

The four core histones were mixed in equimolarity and dialyzed against three changes of 2 L refolding buffer at 4 °C, in which the second dialysis was carried out O/N while the first and third were carried out for 3 hours each. After the last dialysis, the sample was centrifuged for 15 minutes at 17000 xg to remove any precipitated material. The refolded octamers were concentrated to 300-500 µL using a VivaSpin 4 ultrafiltration device (Sartorius, Germany), with a 30 kDa cutoff, before being loaded on a Superdex200 Increase HR 10/30 column (GE Healthcare, USA) connected to a Äkta Prime FPLC system pre-equilibrated with refolding buffer. Sample was eluted with refolded buffer and fractions of 400 µL were collected and analyzed on an SDS-PAGE gel. Fractions containing stochiometric amounts of all four histones were pooled together and concentrated to 2 mg/ mL. For the calculation of the sample's concentration the equation $\left[\frac{mg}{mL}\right] = \frac{\mathrm{OD276(sample)} - \mathrm{OD276(blank)}}{molar\ extinction\ coefficient\ (\varepsilon)} \times MW$ was used (the MW of human

octamers is 108515 and molar extinction coefficient is 44950. The samples were diluted to 1 mg/ mL in 50 % glycerol and stored at -20 °C.

8.2.16 NAP1 purification

NAP1 was purified from cell pellets of baculovirus-infected Sf9 insect cells expressing N-terminally His-tagged NAP1 as previously described[143]. After harvesting the cells by centrifugation, the cell pellet was washed with ice-cold PBS. All subsequent steps were performed on ice unless stated otherwise. The cell pellet was resuspended in lysis buffer (1/40 of the initial cell culture volume) and homogenized by sonication (3 series of 1 minute, with 50 % amplitude, 0.5 seconds ON and 0.5 seconds OFF). The sample was cleared by centrifugation for 10 minutes at 15000 xg at 4 °C and the supernatant was loaded on a pre-equilibrated 5 mL HisTrap HP column (GE Healthcare, USA) connected to an Äkta pure. After loading the sample, the column was washed with lysis buffer and with wash buffer. NAP1 was eluted with 42 mL of elution buffer and fractions of 500 µL were collected and analyzed on an SDS-PAGE gel. The fractions containing NAP1 were pooled together and dialyzed against two changes of 4 L of dialysis buffer, where the first dialysis was carried out O/N and the second for 2 hours and against one change of 4 L of NAP1 buffer plus 100 mM NaCl for 2 hours.

After dialysis, any precipitate was removed by centrifugation for 20 minutes at 20000 xg. The soluble protein was quantified on an 8% SDS-PAGE gel followed by coomassie staining, using BSA as a mass standard. The sample was loaded on a pre-equilibrated 6 mL Resource™ Q (GE Healthcare, USA) column connected to an Äkta pure. The column was washed with NAP1 buffer plus 200 mM NaCl and eluted with a 20 CV of a linear gradient from NAP1 buffer

supplemented with 200 mM NaCl to NAP1 buffer plus 500 mM NaCl. Fractions of 0.5 mL were collected during elution and analyzed on an 18 % SDS-PAGE gel. The fractions corresponding to the first peak contained a 14 kDa contaminant in addition to the 65 kDa NAP1 band. The 14 kDa contaminant corresponds to a NAP1 inhibitor, therefore all fraction containing any traces of this contaminant were discarded. The fraction corresponding to the second peak, which are contaminant-free, were pooled together and dialyzed against two changes of 2 L of NAP1 buffer plus 100 mM NaCl, for 2 hours each. The protein concentration was quantified by SDS-PAGE gel followed by coomassie staining, frozen in liquid nitrogen and stored at -80 °C.

8.2.17 ACF purification

ACF was purified from cell pellets of baculovirus-infected Sf9 insect cells as described[144]. Pellet was resuspended in 8 mL of lysis buffer F and Dounce homogenized using an “A” pestle (three series of ten strokes over 30 minutes, on ice). Homogenate was centrifuged for 10minutes at 11000 rpm at 4 °C. The supernatant was transferred to a new tube and mixed with 250 µL of FLAG-M2 resin and 7 mL of dilution buffer F. The slurry mix was incubated for 2-4 hours at 4 °C on a rotation wheel. After incubation the samples was centrifuged for 3 minutes at 2000 rpm at 4 °C. The supernatant was removed and the pellet resuspended in 12 mL of wash buffer F by tube inversion. The wash was repeated three additional times. For elution, the pellet was resuspended in 100 µL of wash buffer F supplemented with FLAG peptide and insulin (final concentration of 0.4 mg/ mL each). The sample was incubated for 10 minutes on ice and, then, centrifuged for the 30 seconds at maximum speed. The supernatant containing the purified ACF complex was transferred to a new tube

and elution was repeated two more times. The supernatants were pooled together and aliquoted. Aliquots were frozen in liquid nitrogen and stored at -80 °C[144].

8.2.18 Chromatin assembly by NAP1 and ACF

The assembly of the recombinant chromatin used for the *in vitro* transcription assays relied on the activity of histone chaperone NAP1 and chromatin remodeling complex ACF, which resulted in the assembly of regularly spaced chromatin arrays[145].

For a standard reaction, HEG buffer supplemented with 0.2 mM AEBSF, 2 mM NaBU, 1 mM DTT and 100 ng/ uL of BSA (the final reaction volume was 140 µL) were mixed with 7 µL of 1 M KCl and 8 to 12 µL of diluted histone octamers at 100 ng/µL. Since the histone octamer:DNA ratio is critical for efficient success of the assembly, different ratios were tested to titrate the assembly of each chromatin type ranging from 0.8:1 to 1.2:1. The reaction was mixed by gentle vortexing and 2 µL of NAP1 (at a concentration of 1.8 µg/ µL in HEG buffer) were added. The reaction was gently mixed and incubated for 30 minutes at RT. In the meantime, the ATP-regenerating system was prepared by mixing 13.5 µL HEG buffer, 90 µL 500 mM of creatine phosphate, 1.5µL of creatine phosphokinase (5 µg/ µL), 45 µL of 100 mM ATP and 30 µL 250 mM $MgCl_2$. After the incubation, the following components were added: 4 µL of ACF (at a concentration of 70 ng/ µL in HEG buffer), 16.8 µL of freshly prepared ATP-regenerating system and 10 µL of plasmid DNA (at 100 ng/ µL in HEG buffer). The reaction was briefly spun down and incubated for 3 hours at 27 °C

The efficiency of the reaction was tested by MNase digestion as described on section 8.2.19.

8.2.19 MNase digestion of *in vitro* assembled chromatin

To assess the efficiency of the chromatin assemblies, the samples were submitted to limited MNase digestion. Two chromatin assembly reactions were pooled together of which 200 µL of chromatin (corresponding to approximately 1.4 µg) were transferred to a new 1.5 mL tube and mixed with $CaCl_2$ (at a final concentration of 2 mM). The sample was split into two aliquots and each was mixed with 6 to 30 mU MNase/ µL in 5 µL of HEG buffer. The samples were quickly mixed and incubated for 10 minutes at 30 °C. The digestions were stopped by the addition of 110 µL of MNase stop buffer and were incubated for 1hour at 37 °C. The DNA was phenol:chloroform extracted and EtOH precipitated. The DNA pellet was resuspended in 15 µL of 1x DNA loading dye and electrophoresed in a 1.3 % unstained agarose gel. After separation, the gel was stained with EtBr (at a final concentration of 10 µg/ mL).

8.2.20 Sucrose gradient centrifugation of *in vitro* assembled chromatin

In order to select for similarly assembled chromatin arrays, the recombinant chromatin arrays were purified according to their density on sucrose gradients. 5mL linear sucrose gradients of 10-40 % sucrose in sucrose gradient buffer were prepared and overlaid with 400 µL of sample. The gradients were centrifuged in a SW55Ti rotor (Beckman, USA) for 3 hours at 48000 rpm at 4 °C. The run was stopped without any brake and the gradient was fractionated in 300 µL aliquots. From each fraction, 5 µL aliquots were collected and mixed with 1 % SDS and 1x DNA loading dye. The samples were analyzed on an un-stained 1.3 % agarose gel. After separation, the gel was stained with EtBr (at a final concentration of 10 µg/ mL).

8.2.21 GAL4-VP16 purification

His-tagged GAL4-VP16 was expressed in BL21. After expression *E. coli* were harvested by centrifugation for 30 minutes at 1000 xg at 4 °C. All further steps were carried out on ice or at 4 °C. The bacterial pellet was washed once with ice-cold PBS and resuspended in 5 packed cell volumes (PCV) of ice-cold 1x phosphate buffer supplemented with 20 mM of imidazole. The bacteria suspension was sonicated on a Branson sonicator for 1 minute, 0.5 seconds ON and 0.5 seconds OFF, at 50 % amplitude for a total of three times and centrifuged for 10 minutes at 12000 xg. The supernatant was transferred to a new tube and filtered on a 0.45 µm pore size syringe filter. The filtered sample was loaded on a pre-equilibrated HisTrap HP column (GE Healthcare, USA) connected to an Äkta pure. After loading the sample, the column was washed with 10 column volumes (CV) of 1x phosphate buffer supplemented with 20 mM of imidazole and the purified GAL4-VP16 was then eluted with 5 mL of 1x phosphate buffer supplemented with 500 mM of imidazole. Fractions of 500 µL were collected and analyzed on an SDS-PAGE gel. The fractions containing the purified sample were pooled together and progressively dialyzed, using a peristaltic pump, against 2 L 1x PBS over a period of 16 hours. After the first dialysis, the sample was progressively dialyzed against 2 L of GAL4-VP16 storage buffer. Any precipitate was removed by centrifugation and the sample was aliquoted and snap frozen on liquid nitrogen before stored at -80 °C.

8.2.22 p300 purification

His-tagged p300 was expressed on baculovirus-infected Sf9 insect cells. After expression the cells were harvested by centrifugation for 5 minutes at 400 xg at 4 °C. Unless stated otherwise, all steps were carried out on ice. The cell pellet

was resuspended in 2.5 mL of buffer B and Dounce homogenized with 10 strokes using an “A” pestle. The sample was incubated on ice for 15 minutes before being aliquoted into 700-800 µL aliquots and sonicated (3 series of 5 minutes, with 90 % amplitude, 30 seconds ON and 30 seconds OFF). The aliquots were pooled together and centrifuged for 15 minutes at 16000 xg at 4 °C. The clarified supernatant was loaded on a pre-equilibrated 1 mL HisTrap HP column (GE Healthcare, USA) connected to an Äkta prime. After loading, the column was washed with buffer B and eluted with 10CV of elution buffer (500 µL fraction were collected during the elution). The different fractions were analyzed on a 4-12 % SDS-PAGE gel followed by coomassie staining. The fractions containing the purified p300 were pooled together and diluted with 50 % glycerol before being aliquoted at snap frozen in liquid nitrogen. The aliquots were stored at -80 °C.

8.2.23 Nuclear extract preparation for *in vitro* transcription

The preparation of the nuclear extracts for the *in vitro* transcription assays followed a protocol from Dignam *et al*[146]. Hela S3 spinner cells were grown to a density of $5x10^5$ to $1x10^6$ cells/ mL. Cells were harvested by centrifugation for 10 minutes, at 500 xg at 4 °C. All further steps were carried out on ice or at 4°C. The cell pellet was resuspended in ice cold PBS (10 mL *per* liter of culture), transferred to a 50 mL tube and centrifuged for 10 minutes, at 500 xg at 4 °C. The cells were washed with PBS a total of two times as previously described. The cell pellet was, then, resuspended in 5 PCV of buffer A and incubated on ice for 10 minutes. The sample was centrifuged for 10 minutes at 750 xg and resuspended in 2 PCV of buffer A. The cell suspension was transferred to a Dounce homogenizer and lysed by ten gentle strokes of a tight fitted pestle. The

efficiency of the lysis was checked under the microscope and, if necessary, the Dounce homogenization was repeated until approximately 70 % of all cells were lysed. The cell lysate was centrifuged for 20 minutes at 10000 rpm. After centrifugation, the cytoplasmic supernatant was decanted and any traces of lipids were removed from the top of the tube. The nuclear pellet was centrifuged for 20 minutes at 25000 xg in order to remove any traces for residual cytoplasmic material. The nuclear pellet was, then, resuspended in buffer C (3 mL per $1x10^9$ cells) and extracted by gentle stirring with a small magnetic stirring bar for 30 minutes on ice. The nuclear extract was separated by centrifugation for 20 minutes at 25000 xg and transferred to a new tube. Next, the nuclear extract was either dialyzed against 50 volumes of buffer D for 5hours or concentrated by ammonium sulfate precipitation. For the concentration of the nuclear extracts, ammonium sulfate was slowly added to the nuclear extract (0.33 g/ mL of buffer C) over 15 minutes and stirred with a magnetic stir bar for 30 minutes on ice. The sample was centrifuged for 20 minutes at 25000 xg and resuspended in buffer D (¼ to ½ of the volume of buffer C used for the extraction). The resuspended nuclear extract was dialyzed against 50 volumes of buffer D for 5 hours. After dialysis, the nuclear extract was centrifuges for 20 minutes at 25000 xg and the clear supernatant was aliquoted and snap frozen in liquid nitrogen. The nuclear extract aliquots were stored at -80 °C.

8.2.24 *In vitro* transcription assays

For *in vitro* transcription assays, *per* reaction, 50 ng of purified chromatin in 7 µL were mixed with 6 µL of BC100 buffer, 7.2 µL of c-mix (21.45 µL of P10x, 33 µL of 20 % PEG8000, 3.3 µL of 10 mg/ mL BSA, 13.2 µL of 100 mM DTT, 6.6 µL of

187.5 mM ammonium sulfate) and pre-incubated with 50 ng of recombinant GAL4-VP16 for 15 minutes at room temperature. Next, 40 ng of recombinant p300, as well as 1 μL of a co-enzyme mix (500 nM ac-CoA or suc-CoA and 200 mM sodium butyrate) were added and incubated for 30 minutes at 30 °C. 10 μL of Hela nuclear extracts were added and the reaction was incubated for 30 minutes at 30 °C. A 3 μL mix of ribonucleotides (16.5 μL of 12 mM rATP, rGTP and rCTP, 5.5 μL rUTP-32P (Perkin BLU007H; Perkin-Elmer, USA), 4.4 μL RNasin® and 6.6 μL ddH_2O) were added and transcription was allowed for 40 minutes at 30 °C. The reaction was chased with the addition of a 6 μL rUTP-mix (600 μM rUTP and 6 U/ μL RNase T1) and incubated for 20 additional minutes. The transcribed RNA was phenol:chloroform extracted, precipitated with ethanol and analyzed on 6 % acrylamide denaturing gels[147]. A phosphor screen was used to capture the signal O/N and was then measured on an Amersham Typhoon 5 Biomolecular Imager (GE Healthcare, USA). The signal quantifications were done by ImageJ (Java).

8.3 Cell culture methods

8.3.1 Cell culturing

All cells were maintained at 37 °C in a humidified atmosphere containing 5 % CO_2. MCF7 and HEK293 were grown in low-glucose DMEM, supplemented with 10% fetal bovine serum, 2 mM L-glutamine, 100 U/ mL penicillin and 0.1 mg/ mL streptomycin. MEFs were cultured in high-glucose DMEM, supplemented with 15 % FBS, 1x pyruvate, 20 mM HEPES, 2 mM L-glutamine, 100 U/ mL penicillin and 0.1 mg/ mL streptomycin. mES cells were cultured in high-glucose DMEM, supplemented with 15 % FBS, 100 U/ mL penicillin, 0.1 mg/ mL streptomycin, 1

%, non-essential amino acids, 0.1 mM ß-mercaptoethanol, 2x LIF and 2i (final concentration of 25 ng/ mL of PD 0325901 and 75 ng/ mL of CHIR 99021)

8.3.2 siRNA transfection of mammalian cells

Depletion of HAT enzymes was achieved by RNAiMAX (Invitrogen, USA) combined with a reverse transfection protocol following the supplier's instructions. The following ON-TARGETplus SMARTpools from Dharmacon (Horizon Discovery, UK) were used: p300, L-003486-00-0010; CBP, L-003477-00-0010; pCAF, L-005055-00; scramble negative control, D-001810-10. In brief, a mixture of 10-50 nM of siRNA and lipofectamine was pre-incubated for 20 minutes at RT and mixed with MCF7 cells before plating them. Cells were grown for 72 hours.

9. Abbreviations

9.1 General abbreviations

α-KGDH	Alpha-ketoglutarate dehydrogenase
Ac	Acetylation
AcK	Acetyl-lysine
BD	Bromodomain
Bp	Base pair
BRD4	Bromodomain protein 4
CAGE	Cap Analysis of Gene Expression
ChIP	Chromatin immunoprecipitation
ChIP-seq	ChIP-massively parallel DNA sequencing
CRISPR	Clustered Regularly Interspaced Short Palindromic
CV	Column volume
DNA	Deoxyribonucleic acid
DNase-seq	DNase I hypersensitive sites sequencing
E. coli	*Escherichia coli*
ECL	Enhanced chemiluminescence
EtBr	Ethidium bromide
FAIRE-seq	Formaldehyde-assisted isolation of regulatory elements sequencing
FBS	Fetal bovine serum
FPLC	Fast protein liquid chromatography
HAT	Histone acetyl-transferase
HDAC	Histone deacetylase
HRP	Horseradish Peroxidase
IE	Immediate-early
IP	Immunoprecipitation
IPTG	Isopropyl β-d-1-thiogalactopyranoside
KD	Knockdown
KO	Knockout
L11C	C-terminal domain of L11
LB	Lysogeny broth
MEFs	Mouse embryonic fibroblasts

MLP	Major late promoter
MS	Mass-spectrometry
MW	Molecular weight
NaBU	Sodium butyrate
Nam	Nicotinamide
NAP1	Nucleosome assembly protein
NFR	Nucleosome-free region
OD	Optical density
O/N	Overnight
PCR	Polymerase chain reaction
PCA	Principal component analysis
PCV	Packed cell volume
PIC	Pre-initiation complex
PTMs	Post-translational modifications
qPCR	Quantitative PCR
rDNA	Ribosomal DNA
RF1	Release factor 1
RNA	Ribonucleic acid
RNA pol II	RNA polymerase II
RNA-seq	RNA followed by next generation sequencing
rNTPs	Ribonucleotides
rOctamers	Recombinant octamers
rRNA	Ribosomal RNA
RT	Room temperature
siRNA	Short interfering RNA
SIRT5	Sirtuin 5
SIRT7	Sirtuin 7
smFRET	Single molecule Fluorescence Resonance Energy Transfer
STD	Standard deviation
Succ	Succinylation
TCA	Tricarboxylic acid
TPA	12-O-Tetradecanoylphorbol-13-acetate
tRNA	Transfer RNA

TSS	Transcriptional start site
Un	Unmodified
WT	Wild type

9.2 Abreviations for units

p	Pico
n	Nano
µ	Micro
m	Mili
k	Kilo
xg	Times gravity
°C	Degree Celsius
A	Amperes
Da	Dalton
g	Gram
L	Liter
m	Meter
M	Molar
rpm	Rotations *per* minute
RPM	Reads *per* million
U	Units
V	Volts
v/v	Volume *per* volume
w/v	Weight *per* volume

10. Acknowledgments

I would like to express my sincere gratitude to everyone who, either directly or indirectly, supported me and my work during this PhD.

To Rob, for welcoming me as a PhD student in his lab and for all the guidance and support during this process.

To Sylvain, for his unlimited patience and wisdom. For always being there for me and for always knowing how to motivate me (and make me laugh).

To Raphael Margueron, who hosted me numerous times in his lab and helped me set up the *in vitro* transcription assays.

To Poonam, for all the scientific and non-scientific discussions. For being a true friend and role model.

To Jess, for being my PhD partner through all the ups and downs of this adventure.

To Sandra, for being the best benchie a girl could ask for.

To all former and present IFE members, who in one way or another taught me how to be a better scientist.

And finally to my family, without whom this would not have been possible. To my parents who always support me in my decisions and inspire me everyday to try my best. To my brother and sister, for helping me put things into perspective, including my PhD. To Riaz, who so patiently accompanied me in this process. Thank you for being my rock. I cannot wait to continue this journey with you.

11. References

1. Waddington, C. H. The Epigenotype. *Endeavor* **1**, 18-20 (1942).
2. Dupont, C., Armant, D. R. & Brenner, C. A. Epigenetics: definition, mechanisms and clinical perspective. *Semin. Reprod. Med.* **27**, 351-357 (2009).
3. Hübner, M. R., Eckersley-Maslin, M. A. & Spector, D. L. Chromatin organization and transcriptional regulation. *Curr. Opin. Genet. Dev.* **23**, 89-95 (2013).
4. Macalpine, D. M. & Almouzni, G. Chromatin and DNA replication. *Cold Spring Harb. Perspect. Biol.* **5**, 1-22 (2013).
5. Stadler, J. & Richly, H. Regulation of DNA repair mechanisms: how the chromatin environment regulates the DNA damage response. *Int. J. Mol. Sci.* **18**, (2017).
6. Luger, K. *et al.* Crystal structure of the nucleosome core particle at 2.8 A resolution. *Nature* **389**, 251-260 (1997).
7. Ou, H. D. *et al.* ChromEMT: visualization 3D chromatin structure and compaction n interphase and mitotic cells. *Science.* **357**, 1-32 (2017).
8. Jansen, A. & Verstrepen, K. J. Nucleosome positioning in Saccharomyces cerevisiae. *Microbiol. Mol. Biol. Rev.* **75**, 301-320 (2011).
9. Iwasaki, W. *et al.* Contribution of histone N-terminal tails to the structure and stability of. *FEBS openbio* **3**, 363-369 (2013).
10. Biswas, M., Voltz, K., Smith, J. C. & Langowski, J. Role of histone tails in structural stability of the nucleosome. *PLOS Comput. Biol.* **7**, 1-12 (2011).
11. Cucinotta, C. E., Hildreth, A. E., McShane, B. M., Shirra, M. K. & Arndt, K. M. The nucleosome acidic patch directly interacts with subunits of the Paf1 and FACT complexes and controls chromatin architecture in vivo. *Nucleic Acids Res.* **47**, 8410-8423 (2019).
12. Arents, G., Burlingame, R. W., Wangt, B., Love, W. E. & Moudrianakis, E. N. The nucleosomal core histone octamer at 3.1 A resolution: A tripartite protein assembly and a left-handed superhelix. *Protocols* **88**, 10148-10152 (1991).
13. Banks, D. D. & Gloss, L. M. Folding mechanism of the (H3 - H4) 2 histone tetramer of the core nucleosome. *Protein Sci.* **13**, 1304-1316 (2004).
14. Verreault, A. De novo nucleosome assembly: new pieces in an old puzzle. *Genes Dev.* **14**, 1430-1438 (2000).
15. Weber, C. M. & Henikoff, S. Histone variants: dynamic punctuation in transcription. *Genes Dev.* **28**, 672-682 (2014).
16. Henikoff, S. & Smith, M. M. Histone variants and epigenetics. *Cold Spring Harb. Perspect. Biol.* **7**, 1-25 (2015).
17. Giaimo, B. D., Ferrante, F., Herchenröther, A. & Hake, S. B. The histone variant H2A.Z in gene regulation. *Epigenetics Chromatin* **12**, 1-22 (2019).
18. Kamakaka, R. T. & Biggins, S. Histone variants: deviants? *Genes Dev.*

19, 295–310 (2005).

19. Wang, T., Gao, H., Li, W. & Liu, C. Essential role of histone replacement and modifications in male fertility. *Front. Genet.* **10**, 1–15 (2019).
20. Long, M. *et al.* A novel histone H4 variant H4G regulates rDNA transcription in breast cancer. *Nucleic Acids Res.* **47**, 8399–8409 (2019).
21. Szenker, E., Ray-gallet, D. & Almouzni, G. The double face of the histone variant H3 . 3. *Cell Res.* **21**, 421–434 (2011).
22. Ueda, J. *et al.* Testis-specific histone variant H3t gene is essential for entry into spermatogenesis. *Cell Rep.* **18**, 593–600 (2017).
23. Resnick, R. *et al.* DUX4-induced histone variants H3.X and H3.Y mark DUX4 target genes for expression. *Cell Rep.* **29**, 1812–1820 (2019).
24. Bui, M., Walkiewicz, M. P., Dimitriadis, E. K. & Dalal, Y. The CENP-A nucleosome. *Nucleus* **4**, 37–42 (2013).
25. Régnier, V. *et al.* CENP-A is required for accurate chromosome segregation and sustained kinetochore association of BubR1. *Mol. Cell. Biol.* **25**, 3967–3981 (2005).
26. Bowman, G. D. & Poirier, M. G. Post-translational modifications of histones that influence nucleosome dynamics. *Chem. Rev.* **115**, 2274–2295 (2015).
27. Bannister, A. J. & Kouzarides, T. Regulation of chromatin by histone modifications. *Cell Res.* **21**, 381–395 (2011).
28. Zhang, Z. *et al.* Identification of lysine succinylation as a new post-translational modification. *Nat. Chem. Biol.* **7**, 58–63 (2011).
29. Tan, M. *et al.* Identification of 67 histone marks and histone lysine crotonylation as a new type of histone modification. *Cell* **146**, 1016–1028 (2011).
30. Barnes, C. E., English, D. M. & Cowley, S. M. Acetylation and Co: an expanding repertoire of histone acylations regulates chromatin and transcription. *Essays Biochem.* **63**, 97–107 (2019).
31. Zhao, S., Zhang, X. & Li, H. Beyond histone acetylation—writing and erasing histone acylations. *Curr. Opin. Struct. Biol.* **53**, 169–177 (2018).
32. Freitas, M. A., Sklenar, A. R. & Parthun, M. R. Application of Mass Spectrometry to the Identification and Quantification of Histone Post-Translational Modifications. *J. Cell Biochem.* **92**, 691–700 (2008).
33. Cosgrove, M. S., Boeke, J. D. & Wolberger, C. Regulated nucleosome mobility and the histone code. *Nat. Struct. Mol. Biol.* **11**, 1037–1043 (2004).
34. Zhao, Y. & Garcia, B. A. Comprehensive catalog of currently documented histone modifications. *Cold Spring Harb. Perspect. Biol.* **7**, 1–22 (2015).
35. Mersfelder, E. L. & Parthun, M. R. The tale beyond the tail: histone core domain modifications and the regulation of chromatin structure. *Nucleic Acids Res.* **34**, 2653–2662 (2006).
36. Tropberger, P. *et al.* Regulation of transcription through acetylation of H3K122 on the lateral surface of the histone octamer. *Cell* **152**, 859–872

(2013).

37. Di Cerbo, V. *et al.* Acetylation of histone H3 at lysine 64 regulates nucleosome dynamics and facilitates transcription. **3**, 1–23 (2014).
38. Jing, Y. *et al.* Site-specific installation of succinyl lysine analog into histones reveals the effect of H2BK34 succinylation on nucleosome dynamics. *Cell Chem. Biol.* **25**, 166–174 (2018).
39. Jenuwein, T. & Allis, C. D. Translating the histone code. *Science.* **293**, 1074–1080 (2001).
40. Roberto, S. & Zhou, M.-M. Studies on the differentiation of dopaminergic traits in human neural progenitor cells in vitro and in vivo. *Cell Transplant.* **12**, 659–665 (2009).
41. LeRoy, G., Rickards, B. & Flint, S. J. The double bromodomain proteins Brd2 and Brd3 couple histone acetylation to transcription. *Mol. Cell* **3023**, 51–60 (2008).
42. Neumann, H. *et al.* A method for genetically installing site-specific acetylation in recombinant histones defines the effects of H3K56 acetylation. *Mol. Cell* **36**, 153–163 (2009).
43. Chen, Y. *et al.* Lysine propionylation and butyrylation are novel post-translational modifications in histones. *Mol. Cell. Proteomics* **6**, 812–819 (2007).
44. Kebede, A. F., Schneider, R. & Daujat, S. Novel types and sites of histone modifications emerge as players in the transcriptional regulation contest. *FEBS J.* **282**, 1658–1674 (2015).
45. Kebede, A. F. *et al.* Histone propionylation is a mark of active chromatin. *Nat. Struct. Mol. Biol. Biol.* **24**, 1048–1059 (2017).
46. Olsen, C. A. Expansion of the lysine acylation landscape. *Angew. Chemie - Int. Ed.* **51**, 3755–3756 (2012).
47. Lee, S. Post-translational modification of proteins in toxicological research: focus on lysine acylation. *Toxicol. Res.* **29**, 81–86 (2013).
48. Trefely, S., Doan, M. T. & Snyder, N. W. *Crosstalk between cellular metabolism and histone acetylation*. *Methods in Enzymology* vol. 626 (Elsevier Inc., 2019).
49. Olp, M. D., Zhu, N. & Smith, B. C. Metabolic-derived lysine acylations and neighboring modifications tune BET bromodomain to histone H4. *Biochemistry* **56**, 5485–5495 (2017).
50. Simithy, J. *et al.* Characterization of histone acylations links chromatin modifications with metabolism. *Nat. Commun.* **8**, 1–13 (2017).
51. Rousseaux, S. & Khochbin, S. Histone acylation beyond acetylation: terra incognita in chromatin biology. *Cell J.* **17**, 1–6 (2015).
52. Zhang, R., Erler, J. & Langowski, J. Histone acetylation regulates chromatin accessibility: role of H4K16 in inter-nucleosome interaction. *Biophys. J.* **112**, 450–459 (2017).
53. Tropberger, P. & Schneider, R. Going global: novel histone modifications in the globular domain of H3. *Epigenetics* **5**, 112–117 (2010).

54. Hassan, A. H. *et al.* Selective recognition of acetylated histones by bromodomains in transcriptional co-activators. *Biochem. J.* **402**, 125–133 (2007).

55. Josling, G. A., Selvarajah, S. A., Petter, M. & Duffy, M. F. The role of bromodomain proteins in regulating gene expression. *Genes.* **3**, 320–343 (2012).

56. Di Cerbo, V. & Schneider, R. Cancers with wrong HATs: the impact of acetylation. *Brief. Funct. Genomics* **12**, 231–243 (2013).

57. Parthun, M. R., Widom, J. & Gottschling, D. E. The major cytoplasmic histone acetyltransferase in yeast: Links to chromatin replication and histone metabolism. *Cell* **87**, 85–94 (1996).

58. Marmorstein, R. & Zhou, M. M. Writers and readers of histone acetylation: Structure, mechanism, and inhibition. *Cold Spring Harb. Perspect. Biol.* **6**, 1–25 (2014).

59. Lee, K. K. & Workman, J. L. Histone acetyltransferase complexes: one size doesn't fit all. *Nat. Rev. Mol. Cell Biol.* **8**, 284–295 (2007).

60. Alhamwe, A. *et al.* Histone modifications and their role in epigenetics of atopy and allergic diseases. *Allergy, Asthma Clin. Immunol.* **14**, 1–16 (2018).

61. Seto, E. & Yoshida, M. Erasers of histone acetylation: the histone deacetylase enzymes. *Cold Spring Harb. Perspect. Biol.* **6**, 1–26 (2014).

62. Zhang, Z. *et al.* Identification of lysine succinylation as a new post-translational modification. *Nat. Chem. Biol.* **7**, 58–63 (2011).

63. Xie, Z. *et al.* Lysine succinylation and lysine malonylation in histones. *Mol. Cell. Proteomics* **11**, 100–107 (2012).

64. Park, J. *et al.* SIRT5-mediated lysine desuccinylation impacts diverse metabolic pathways. *Mol. Cell* **50**, 910–930 (2013).

65. Hirschey, M. D. & Zhao, Y. Metabolic regulation by lysine malonylation, succinylation and glutarylation. *Mol. Cell. Proteomics* **13**, 1–22 (2015).

66. Li, L. *et al.* SIRT7 is a histone desuccinylase that functionally links to chromatin compaction and genome stability. *Nat. Commun.* **7**, 1–17 (2016).

67. Schneider, R. *et al.* Histone H3 lysine 4 methylation patterns in higher eukaryotic genes. *Nat. Cell Biol.* **6**, 73–77 (2004).

68. Karmodiya, K., Krebs, A. R., Oulad-Abdelghani, M., Kimura, H. & Tora, L. H3K9 and H3K14 acetylation co-occur at many gene regulatory elements, while H3K14ac marks a subset of inactive inducible promoters in mouse embryonic stem cells. *BMC Genomics* **13**, 1–18 (2012).

69. Edmunds, J. W., Mahadevan, L. C. & Clayton, A. L. Dynamic histone H3 methylation during gene induction: HYPB/Setd2 mediates all H3K36 trimethylation. *EMBO J.* **27**, 406–420 (2008).

70. Heintzman, N. D. *et al.* Distinct and predictive chromatin signatures of transcriptional promoters and enhancers in the human genome. *Nat. Genet.* **39**, 311–318 (2007).

71. Creyghton, M. P. *et al.* Histone H3K27ac separates active from poised

enhancers and predicts developmental state. *Proc. Natl. Acad. Sci. U. S. A.* **107**, 21931–21936 (2010).

72. Tie, F. *et al.* CBP-mediated acetylation of histone H3 lysine 27 antagonizes Drosophila Polycomb silencing. *Development* **136**, 3131–3141 (2009).
73. Nguyen, M. L. T., Jones, S. A., Prier, J. E. & Russ, B. E. Transcriptional enhancers in the regulation of T cell differentiation. *Front. Immunol.* **6**, 1–12 (2015).
74. Masumoto, H., Hawke, D., Kobayashi, R. & Verreault, A. A role for cell-cycle-regulated histone H3 lysine 56 acetylation in the DNA damage response. *Nature* **436**, 1–5 (2005).
75. Chakravarthy, S., Patel, A. & Bowman, G. D. The basic linker of macroH2A stabilizes DNA at the entry/exit site of the nucleosome. *Nucleic Acids Res.* **40**, 8285–8295 (2012).
76. Celic, I. *et al.* The sirtuins Hst3 and Hst4p preserve genome integrity by controlling Histone H3 lysine 56 deacetylation. *Curr. Biol.* **16**, 1280–1289 (2006).
77. Yuan, J., Pu, M., Zhang, Z. & Luo, Z. Histone H3-K56 acetylation is important for genomic stability in mammals. *Cell Cycle* **8**, 1747–1753 (2010).
78. Topal, S., Vasseur, P., Radman-Livaja, M. & Peterson, C. L. Distinct transcriptional roles for Histone H3-K56 acetylation during the cell cycle in Yeast. *Nat. Commun.* **10**, 1–13 (2019).
79. Xu, F., Zhang, K., Grunstein, M., Hall, B. & Angeles, L. Acetylation in histone H3 globular domain regulates gene expression in Yeast. **121**, 375–385 (2005).
80. Xie, W. *et al.* Histone H3 lysine 56 acetylation is linked to the core transcriptional network in human embryonic stem cells. **33**, 417–427 (2009).
81. Stejskal, S. *et al.* Cell cycle-dependent changes in H3K56ac in human cells. *Cell Cycle* **14**, 3851–3863 (2015).
82. Vempati, R. K. *et al.* p300-mediated acetylation of histone H3 lysine 56 functions in DNA damage response in mammals. *J. Biol. Chem.* **285**, 28553–28564 (2010).
83. Tan, Y., Xue, Y., Song, C. & Grunstein, M. Acetylated histone H3K56 interacts with Oct4 to promote mouse embryonic stem cell pluripotency. *Proc. Natl. Acad. Sci. U. S. A.* **110**, 11493–11498 (2013).
84. Davey, C. A., Sargent, D. F., Luger, K., Maeder, A. W. & Richmond, T. J. Solvent mediated interactions in the structure of the nucleosome core particle at 1.9 Å resolution. *J. Mol. Biol.* **319**, 1097–1113 (2002).
85. Pradeepa, M. M. *et al.* Histone H3 globular domain acetylation identifies a new class of enhancers. *Nat. Genet.* **48**, 681–688 (2016).
86. Luger, K., Rechsteiner, T. J. & Richmond, T. J. *Expression and purification of recombinant histones and nucleosome reconstitution*. *Chromatin Protocols* (Humana Press, 1999).

87. Iwasaki, W. *et al.* Comprehensive structural analysis of mutant nucleosomes containing lysine to glutamine (KQ) substitutions in the H3 and H4 histone-fold domains. *Biochemistry* **50**, 7822–7832 (2011).

88. Devaiah, B. N. *et al.* BRD4 is a histone acetyltransferase that evicts nucleosomes from chromatin. *Nat. Struct. Mol. Biol.* **23**, 540–548 (2016).

89. Tropberger, P. *et al.* Regulation of transcription through acetylation of H3K122 on the lateral surface of the histone octamer. *Cell* **152**, 859–872 (2013).

90. Lawrence, M., Daujat, S. & Schneider, R. Lateral thinking: how histone modifications regulate gene expression. *Trends Genet.* **32**, 42–56 (2016).

91. Di Cerbo, V. *et al.* Acetylation of histone H3 at lysine 64 regulates nucleosome dynamics and facilitates transcription. *Elife* **3**, 1–23 (2014).

92. Hake, S. B. & Allis, C. D. Histone H3 variants and their potential role in indexing mammalian genomes: The 'H3 barcode hypothesis'. *Proc. Natl. Acad. Sci. U. S. A.* **103**, 6428–6435 (2006).

93. Lai, W. K. M. & Pugh, B. F. Understanding nucleosome dynamics and their links to gene expression and DNA replication. *Physiol. Behav.* **18**, 548–562 (2017).

94. Giresi, P. G., Kim, J., McDaniell, R. M., Iyer, V. R. & Lieb, J. D. FAIRE (Formaldehyde-Assisted Isolation of Regulatory Elements) isolates active regulatory elements from human chromatin. *Genome Res.* **17**, 877–885 (2007).

95. Song, L. & Crawford, G. E. DNase-seq: a high-resolution technique for mapping active gene regulatory elements across the genome from mammalian cells Lingyun. *Cold Spring Harb. Protoc.* **2**, 1–13 (2010).

96. Wang, Y. *et al.* KAT2A coupled with the α-KGDH complex acts as a histone H3 succinyltransferase. *Nature* **552**, 273–277 (2017).

97. Liu, Y. *et al.* Two histone/protein acetyltransferases, CBP and p300, are indispensable for Foxp3+ T-regulatory cell development and function. *Mol. Cell. Biol.* **34**, 3993–4007 (2014).

98. Rardin, M. J. *et al.* SIRT5 regulates the mitochondrial lysine succinylome and metabolic networks Matthew. *Cell Metab.* **18**, 920–933 (2013).

99. Loyola, A., LeRoy, G., Wang, Y. H. & Reinberg, D. Reconstitution of recombinant chromatin establishes a requirement for histone-tail modifications during chromatin assembly and transcription. *Genes Dev.* **15**, 2837–2851 (2001).

100. Flaus, A. & Richmond, T. J. Positioning and stability of nucleosomes on MMTV 3'LTR sequences. *J. Mol. Biol.* **275**, 427–441 (1998).

101. Neumann, H., Peak-Chew, S. Y. & Chin, J. W. Genetically encoding Nε-acetyllysine in recombinant proteins. *Nat. Chem. Biol.* **4**, 232–234 (2008).

102. Elsässer, S. J., Ernst, R. J., Walker, O. S. & Chin, J. W. Genetic code expansion in stable cell lines enables encoded chromatin modification. *Nat. Methods* **13**, 158–164 (2016).

103. Baggett, N. E., Zhang, Y. & Gross, C. A. Global analysis of translation termination in E. coli. *PLoS Genet.* **13**, 1–27 (2017).

104. Petropoulos, A. D., McDonald, M. E., Green, R. & Zaher, H. S. Distinct roles for release factor 1 and release factor 2 in translational quality control. *J. Biol. Chem.* **289**, 17589–17596 (2014).

105. Youngman, E. M., McDonald, M. E. & Green, R. Peptide release on the ribosome: mechanism and implications for translational Control. *Annu. Rev. Microbiol.* **62**, 353–373 (2008).

106. Johnson, D. B. F. *et al.* RF1 knockout allows ribosomal incorportion of unnatural amino acids at multiple sites. *Nat. Chem. Biol.* **7**, 779–786 (2011).

107. Lajoie, M. J. *et al.* Genomically recoded organisms expand biological functions. *Science.* **342**, 357–360 (2013).

108. Schwark, D. G., Schmitt, M. A. & Fisk, J. D. Dissecting the contribution of release factor interactions to amber stop codon reassignment efficiencies of the Methanocaldococcus jannaschii orthogonal pair. *Genes.* **9**, (2018).

109. Huang, Y. *et al.* A convenient method for genetic incorporation of multiple noncanonical amino acids into one protein in Escherichia coli. *Mol. Biosyst.* **6**, 683–686 (2010).

110. Fan, C., Xiong, H., Reynolds, N. M. & Söll, D. Rationally evolving tRNAPyl for efficient incorporation of noncanonical amino acids. *Nucleic Acids Res.* **43**, 1–10 (2015).

111. Johnson, D. B. F. *et al.* RF1 knockout allows ribosomal incorporation of unnatural amino acids at multiple sites. *Nat. Chem. Biol.* **7**, 779–786 (2011).

112. Freeman, L., Kurumizaka, H. & Wolffe, A. P. Functional domains for assembly of histones H3 and H4 into the chromatin of Xenopus embryos. *Proc. Natl. Acad. Sci. U. S. A.* **93**, 12780–12785 (1996).

113. Howard, C. J., Yu, R. R., Gardner, M. L., Shimko, J. C. & Ottesen, J. J. Chemical and biological tools for the preparation of modified histone proteins. *Top. Curr. Chem.* **363**, 193–226 (2015).

114. Marzluff, W. F., Gongidi, P., Woods, K. R., Jin, J. & Maltais, L. J. The human and mouse replication-dependent histone genes. *Genomics* **80**, 487–498 (2002).

115. Forrest, A. R., Kawaji, H., Rehli, M., Baillie, J. K. & et al. A promoter-level mammalian expression atlas. *Nature* **507**, 462–470 (2014).

116. Yamamoto, Y. Y., Yoshioka, Y., Hyakumachi, M. & Obokata, J. Characteristics of core promoter types with respect to gene structure and expression in arabidopsis thaliana. *DNA Res.* **18**, 333–342 (2011).

117. Deaton, A. M. & Bird, A. CpG islands and the regulation of transcription. *Genes Dev.* **25**, 1010–1022 (2011).

118. Yokomori, R. *et al.* Genome-wide identification and characterization of transcription start sites and promoters in the tunicate Ciona intestinalis. *Genome Res.* **26**, 140–150 (2016).

119. Kim, D.-W., Cheriyath, V., Roy, A. L. & Cochran, B. H. TFII-I Enhances Activation of the c- fos Promoter through Interactions with Upstream Elements . *Mol. Cell. Biol.* **18**, 3310–3320 (1998).

120. Geltinger, C., Hörtnagel, K. & Polack, A. TATA box and Sp1 sites mediate the activation of c-myc promoter P1 by immunoglobulin kappa enhancers. *Gene Expr.* **6**, 113–127 (1996).

121. Buchheim, J. I. & Deindl, E. Early growth response 1- A transcription factor in the crossfire of signal transduction cascades. *Indian J. Biochem. Biophys.* **48**, 226–235 (2011).

122. Loyola, A., Bonaldi, T., Roche, D., Imhof, A. & Almouzni, G. PTMs on H3 variants before chromatin assembly potentiate their final epigenetic state. *Mol. Cell* **24**, 309–316 (2006).

123. Gates, L. A. *et al.* Acetylation on histone H3 lysine 9 mediates a switch from transcription initiation to elongation. *J. Biol. Chem.* **292**, 14456–14472 (2017).

124. Dong, X. & Weng, Z. The correlation between his tone modifications and gene expression. *Epigenomics* **5**, 113–116 (2013).

125. Stillman, B. Histone modifications: insights into their influence on gene expression. *Cell* **175**, 6–9 (2018).

126. Henry, R. A., Kuo, Y. M. & Andrews, A. J. Differences in specificity and selectivity between CBP and p300 acetylation of histone H3 and H3/H4. *Biochemistry* **52**, 5746–5759 (2013).

127. An, W., Palhan, V. B., Karymov, M. A., Leuba, S. H. & Roeder, R. G. Selective requirements for histone H3 and H4 N termini in p300-dependent transcriptional activation from chromatin. *Mol. Cell* **9**, 811–821 (2002).

128. Smestad, J., Erber, L., Chen, Y. & Maher, L. J. Chromatin succinylation correlates with active gene expression and is perturbed by defective TCA cycle metabolism. *iScience* **2**, 63–75 (2018).

129. Kaczmarska, Z. *et al.* Structure of p300 in complex with acyl-CoA variants. *Nat. Chem. Biol.* **13**, 21–29 (2017).

130. Kumar, S. & Lombard, D. B. Mitochondrial sirtuins and their relationships with metabolic disease and cancer. *Antioxidants Redox Signal.* **22**, 1060–1077 (2015).

131. Du, J. *et al.* Sirt5 is a NAD-dependent protein lysine demalonylase and desuccinylase. *Science* **334**, 806–809 (2011).

132. Sterner, D. E. & Berger, S. L. Acetylation of Histones and Transcription-Related Factors. *Microbiol. Mol. Biol. Rev.* **64**, 435–459 (2000).

133. Das, C. & Kundu, T. K. Transcriptional regulation by the acetylation of nonhistone proteins in humans - A new target for therapeutics. *IUBMB Life* **57**, 137–148 (2005).

134. Georges, S. A., Kraus, W. L., Luger, K., Nyborg, J. K. & Laybourn, P. J. p300-mediated tax transactivation from recombinant chromatin: histone tail deletion mimics coactivator function. *Mol. Cell. Biol.* **22**, 127–137 (2002).

135. Bao, X. *et al.* Glutarylation of histone H4 Lysine 91 regulates chromatin dynamics. *Mol. Cell* **76**, 1–16 (2019).

136. Lee, J.-S., Smith, E. & Shilatifard, A. The language of histone crosstalk.

Cell **142**, 682–685 (2010).

137. Zhang, Z. *et al.* Crosstalk between histone modifications indicates that inhibition of arginine methyltransferase CARM1 activity reverses HIV latency. *Nucleic Acids Res.* **45**, 9348–9360 (2017).
138. Suganuma, T. & Workman, J. L. Crosstalk among histone modifications. *Cell* **135**, 604–607 (2008).
139. Concino, M. F., Lee, R. F., Merryweather, J. P. & Weinmann, R. The adenovirus major late promoter TATA box and initiation site are both necessary for transcription in vitro. *Nucleic Acids Res.* **12**, 7423–7433 (1984).
140. Kraus, W. L. & Kadonaga, J. T. p300 and estrogen receptor cooperatively activate transcription via differential enhancement of initiation and reinitiation. *Genes Dev.* **12**, 331–342 (1998).
141. Fyodorov, D. V. & Kadonaga, J. T. Chromatin assembly in vitro with purified recombinant ACF and NAP-1. in *Methods in Enzymology* vol. 371 499–515 (Academic Press, 2003).
142. Gibson, D. G. *et al.* Enzymatic assembly of DNA molecules up to several hundred kilobases. *Nat. Methods* **6**, 343–345 (2009).
143. Peterson, C. L. Purification of recombinant Drosophila NAP1. *Cold Spring Harb. Protoc.* **4**, 1–4 (2009).
144. Peterson, C. L. Purification of recombinant Drosophila ACF. *Cold Spring Harb. Protoc.* **4**, 1–4 (2009).
145. Ito, T., Bulger, M., Pazin, M. J., Kobayashi, R. & Kadonaga, J. T. ACF, an ISWI-containing and ATP-utilizing chromatin assembly and remodeling factor. *Cell* **90**, 145–155 (1997).
146. Dignam, J. D., Martin, P. L., Shastry, B. S. & Roeder, R. G. Eukaryotic gene transcription with purified components. *Methods Enzymol.* **101**, 582–598 (1983).
147. Margueron, R. *et al.* Ezh1 and Ezh2 maintain repressive chromatin through different mechanisms. *Mol. Cell* **32**, 503–518 (2008).